ENGINEERING SYSTEMS TO STUDY THE MECHANICS OF CILIA- AND AIRFLOW-MEDIATED MUCUS CLEARANCE

Siddharth Kaup Shenoy

A dissertation submitted to the faculty at the University of North Carolina at Chapel Hill in partial fulfillment of the requirements for the degree of Doctor of Philosophy in the Department of Biomedical Engineering in the School of Medicine.

Chapel Hill
2015

Approved by:

Brian M. Button

Robert G. Dennis

Kenneth Donnelly

Johnny Carson

C. William Davis

Jeffrey MacDonald

ABSTRACT

Siddharth Kaup Shenoy: Engineering Systems to Study the Mechanics of Cilia- and Airflow-mediated Mucus Clearance
(Under the direction of Brian M. Button and Robert G. Dennis)

The pulmonary airway surface liquid layer is comprised of two components: 1) inhaled pathogens that are stuck to a mucus layer and 2) a periciliary layer (PCL) that provides an environment for mucociliary clearance (MCC) out of the lungs. The mechanisms of how the beating of cilia from adjacent ciliated cells is coordinated are poorly understood. In Chapter 2, the perfusion of fluid flow along the apical surface of airway cells was hypothesized to yield airway cultures that transported mucus uni-directionally. To test this hypothesis, perfusion protocols were performed during ciliogenesis and post-ciliation phase of *in vitro* human bronchial epithelial (HBE) airway models. The length of exposure of fluid shear stress on the apical surface of airway epithelial cultures yielded transient or permanent unidirectional mucus transport in the direction of fluid flow cue. These characteristics matched *in vivo* biology and remained unseen in standard tissue culturing protocols.

In addition to MCC, two other modes of mucus clearance have been studied namely cough clearance (CC) and proposed here, a third mechanism: cilia-independent "gas-liquid transport" (GLT). In Chapter 3, a system was engineered to deliver laminar, humidified airflow across the surface of HBE cultures, which emulated peak expiratory

flow rates associated with exhalation. In the GLT models, three conditions of mucosal hydration were tested to represent a variety of clearance models between health and disease: from well-hydrated, normal-like mucus, *in situ* mucus, to dehydrated mucus, which represented severe Cystic Fibrosis (CF) mucus. At healthy mucus concentrations (2-4%), GLT rate was much faster at clearing mucus than MCC. In contrast, under conditions of severe dehydration, CF-like, GLT failed to produce significant mucus transport, as observed with MCC. In Chapter 4, the effect of mucus clearance with air velocities associated with cough was investigated and captured using high-speed photography. CC was also observed to decrease as mucus concentration increased.

Together, the methods developed in this dissertation will help researchers to culture HBE cells with transport characteristics similar to *in vivo* behavior and help clinicians to better evaluate drug therapeutics on airway clearance for treating muco-obstructive diseases like CF.

HARE KRSNA

I dedicate this dissertation to following individuals
who have made a tremendous difference in my life:

My mentors: Brian, Bob, Kenny, Johnny, Bill and Jeff
My dad, Muralidhar, mom, Sudha, sister, Shivany, brother-in-law, Suraj and my adventurous nephew, Naren
My grandparents: Mamama (Tara) and Ajja (B. G Kamath)
My lab friends: Henry Paul Goodell, John Minges, Dominick Partlow, Elijah Lackey, Amy Ly, Jennifer Goralski, Zack Cashion, Devin Hubbard, Alex Mastro,
My students: Ayushi Deshwal, Stephanie Kim, Xuelan Wu, Nathan Shenkute
My BFFs: Jeremy and Amina Ford, Yolanda Fair, Sean Pollock, Joe Ketchum and Calvin Johnson
Other mentors: Steve Emmanuel, Michael Chua, Silvia Kreda, and David Hill

Thank you all for your support along the way

ACKNOWLEDGEMENTS

I am grateful for the amount of help I have received over the past six years.

First and foremost, I want to thank, my mentor, Dr. Brian Button for his gracious help in providing support, enthusiasm, guidance, offer critiques to my work and provide freedom to test my unique ideas. His breadth in airway physiology, cell and pathophysiology, engineering techniques has helped garner my thoughts on how biomedical engineering can help progress research at the Cystic Fibrosis research center. He has an off-hands type of approach that I like where I can explore other avenues to improve the research and to come up with my own non-standard protocols for culturing cells, creating environmental chambers, or building analysis software. I like his openness to freely discuss data and problems about the research and most often he provides a solution or a guide to meet challenges to the project. I also want to thank him for providing an atmosphere of learning at the lab by allowing undergraduate and high school students to work in the lab and by holding workshops to local high school students and his Boy Scout troop.

I want to also thank my BME adviser, Dr. Robert G Dennis who has given me invaluable help and guidance to attack challenging problems within each project in my graduate career. When I was faced with an insurmountable challenge, Bob had a unique solution from his expertise. I am grateful for him to let me use resources in his

machine shop. Also, I like to thank his collaborators, Steve Emmanuel and Dr. Kenneth Donnelly for their guidance in the fabrication phase of my projects. I want to extend a warm thanks to his graduate students as well: Dr. Jon Williams, Alex Mastro, MS., Dr. Devin Hubbard, Dr. Avery Cashion and Dr. Henry Goodell. I like to thank Dr. Henry P. Goodell for his brilliance, experience and extraordinary depth in biomedical engineering techniques. They have been the utmost help in providing electronics knowledge as well as broadening my horizons in reading science fiction, Carl Sagan, and in mastering culinary arts.

I want to thank Dr. Johnny Carson for being available for discussing projects and ways to progress research about ciliogenesis. I like to thank Dr. C. William Davis for giving me special insights in to physiology part of my research and for pushing me to think and pursue passions beyond graduate school. I want to thank Dr. Jeffrey MacDonald for his support and his guidance on the tubular project. I thank Dr. Richard Boucher for his guidance in my research and in my career as a research scientist.

I want to thank Dr. Paul Dayton and his lab for letting me use resources and Fastcam equipment for progressing on the cough clearance experiment. I want to extend a warm thanks to Dr. Eszter Vladar at Stanford University for her patience and effort in researching planar cell polarity expressions in the ciliogenesis project. I thank Dr. Peter Koenig for his assistance in analyzing cilia beat frequency in my assays.

Lastly, I want to thank my family for their immeasurable support and guidance in my life. I would not be where I am in my life without their love, dedication and happiness.

PREFACE

Symposium Abstracts:

Shenoy, S.K., Partlow, D., Kim, S., Goodell, H., Deshwal, A. Hill, DB, Rubenstein, MR., Boucher, RC., Dennis, RG., and Button, BM. “Increased mucus concentration reduces airflow-mediated clearance in an in vitro model of cough clearance.” Poster Session. Visiting Pulmonary Scholars Symposium. April 15, 2015. Chapel Hill

Shenoy, S.K, Goodell HP, Carson, JL, Davis CW, Dennis RG, and Button, B. “A SYSTEM TO ENTRAIN AIRWAY CILIA BEATING IN VITRO USING LAMINAR FLUID FLOW.” Poster Session Abstracts. Pediatric Pulmonology, 48: 207–453.

Shenoy, S.K., Goodell HP, Carson, JL, Mitran, S, Dennis RG, and Button, B. “AIRFLOW-MEDIATED MUCUS TRANSPORT: A NOVEL FORM OF CLEARANCE.” Poster Session Abstracts. Pediatric Pulmonology, 48: 207–453.

Oral Presentations:

Shenoy. S. “Up the Airway Escalator.” Amgen, Inc. July 21, 2015. Thousand Oaks, Ca.

Shenoy. S. “Up the Airway Escalator: Studies in Cilia Entrainment and Airflow-mediated mucus transport.” UNC/NCSU Department of Biomedical Engineering. February 22, 2013

Manuscripts in preparation:

Shenoy, S. *et al*. “Planar, linear coordination of mucus transport in an *in vitro* airway epithelial culture model.”

Shenoy, S. *et al*. “Third form of clearance: Gas-Liquid Transport *in vivo* and *in vitro*.”

Shenoy, S. *et al*. “Increased mucus concentration reduces airflow-mediated clearance in an in vitro model of cough clearance."

TABLE OF CONTENTS

LIST OF TABLES

LIST OF FIGURES

LIST OF ABBREVIATIONS AND SYMBOLS

ASL	Airway Surface Liquid (layer)
ATP	Adenosine Triphosphate
CBF	Cilia Beat Frequency
CC	Cough Clearance
cP	centipoise, unit of viscosity
CF	Cystic Fibrosis
CFD	Computational Fluid Dynamics
CO_2	Carbon Dioxide
COPD	Chronic Obstructive Pulmonary Disease
DNA	Deoxyribonucleic acid
DTT	Dithiothreitol
FPS	Frames per second
GLT	Gas Liquid Transport
GUI	Graphical User Interface
HBE	Human Bronchial Epithelial
HS	Hypertonic Saline
KRB	Kreb’s Ringer Solution
LFSS	Laminar Fluid Shear Stress
LPM	Liters per minute
MCC	Mucociliary Clearance
MCT	Mucociliary Transport
mM	milliMolar (moles per Liter)

mN	milliNewton, unit of force
ms	millisecond
MSD	Mean Squared Displacement
O_2	Oxygen
Pa	Pascal, unit of pressure
PBS	Phosphate Buffered Saline
PIV	Particle Image Velocimetry
PTV	Particle Tracking Velocimetry
PCD	Primary Ciliary Dyskinesia
PCL	Periciliary Layer
PFC	Perfluorocarbon
Re	Reynold's Number
RH	Relative Humidity
SS	Shear Stress
UPP	Ultrasonic Piezoresistive Pump
vs.	Versus
α	Alpha
Θ	Theta, angle
τ	Tau, stress
‖ ‖	Absolute value
°C	Degrees Celsius

CHAPTER 1: MECHANOTRANSDUCTION IN THE AIRWAY EPITHELIUM

Introduction

A key step in vertebrate evolution began with the transition from water to land,[1] and the lung became both a physical and chemical barrier between the surrounding environment and the body.[2,3] The air for respiration contained harmful pathogens such as small organisms, bacteria, viruses, and other particulates that posed threats against the body. Anatomically, in humans, the lung is divided into two regions: 1) proximal airways, which are responsible for conduction of air and 2) distal respiratory regions, which are responsible for gas exchange. In the proximal airways, health is maintained because particulates and pathogens are trapped in sticky mucus layers, which are swept from the lung by ciliary beating- this mechanism is called mucociliary clearance (MCC). In fact, MCC in healthy individuals has established an innate immunity against infections; however, environmental and genetic abnormalities of this system have compromised lung function that could be fatal namely in diseases like Cystic Fibrosis (CF).[4]

Airway Epithelium

The airway epithelium of proximal airways consists of eight principle types of cells including: ciliated cells, basal cells, neuroendocrine cells, mucus goblet cells, Clara cells, serous cells, small mucus granule cells, and brush cells.[5] The airway epithelium, *in situ*, secrets mucin from goblet cells[6] and from glands[7], which swells to form mucus. Mucus in healthy individuals is a viscoelastic material comprised of about 98% water, 0.9% salt, and 0.5% mucin polymers, a small amount of DNA[8], and 0.5% protein complexes.[5,9] Mucus is a sticky, viscoelastic, polymeric gel network that protects and lubricates the airway epithelium.

In mucus, a single mucin structure is an acidic composition of a string of polysaccharide chains which have "sticky" groups that allows for crosslinking or adhering to pathogens, proteins and other mucins.[10] The viscoelastic properties mainly come from the polymeric network of different gel-forming mucins, for example, mucus *in vitro* consists of mainly Muc5AC and Muc5B mucins.[11–14] Interestingly, glands have been shown to secrete mucus in an *in vivo* model of CF pig.[7] Goblet cells contain mucin granules, which are exocytosed to release mucins-- these mucins then swell and untangle to add to the mucin polymer network.[6]

Other cells also secrete mucin, but their roles are still being explored. Serous cells secrete Muc7, a non-polymeric mucin, which have not been found to be exocytosed by granules. In mice, Clara cells are found to primarily secrete mucin; however, in humans, Clara cells are expressed in the lower airways and have not been found to play a major role in mucus secretion (communication with Dr. CW Davis).[15]

In the lung, ciliated cells attach to basal cells and extend to the luminal surface.[16] In normal conducting airways, ciliated cells do not divide so they are terminally differentiated; unless they are perturbed during injury or wound healing.[17] The epithelium's cilia propel the mucus axially by incessant, asymmetric beating, called metachronal waves.[18–21] Ciliated cells have been found to widely populate in the proximal conductive airways and they are rarely found near alveolar cells.[5] The asymmetric, percussion (6~20 Hz) of bundles of motile cilia (200 ~300 cilia per cell) propel mucus in a specific direction toward the pharynx to be swallowed or expectorated thus promoting airway sterility.[21,22]

Effective mucus clearance depends on a variety of conditions including optimal viscoelasticity,[9] hydration,[23] and oncotic pressure balance between PCL and mucus layer.[24] In CF, a genetic defect of the cystic fibrosis transmembrane conductance regulator affects the ionic composition and lubrication of ASL, which have been found to result in dry, thick mucus.[25–27] Excessive mucus concentration of the mucus gel was found *in vitro* to increase oncotic pressure of mucus layer on the PCL layer and thus contributed to failure in mucus clearance.[24] Excessive mucus facilitates harmful pathogens to multiply and accumulates to form plaques plugging conductive airways.[28] This hypoxic environment is suitable for bacterial infections such as *Pseudomonas aeruginosa*,[29] which is found in 80% of adult patients with CF.[30]

Ciliogenesis

Ciliogenesis is the process by which cells developed the antennae-like sensory organelle called the cilium that is involved in numerous activities including fluid

clearance, cell signaling, shuttling proteins,[31] mechanosensing and direct fluid[32] or mucus flow.[33–36] Cilia develop into two main modes: immotile, which are involved in sensory roles, and motile, which are involved in providing motility in single-celled organisms such as alga or in propelling mucus over mucosal surfaces. In the ear canal, retina, and kidneys, cilia are immotile and serve as mechanosensors.[16] In the airway, cilia both motile and sensory immotile cilia are present.

On a cell body, a cilium, pictured in Figure 1.1, is an organelle formed as a slender protuberance of the plasma membrane that is enclosed by a microtubule-based assembly called an axoneme. The axoneme of primary and secondary cilia differ in that motile cilia have one additional pair of microtubules in the middle pictured in micrograph in Figure 1.1 and primary cilia lack the central pair.[37] Also, the axonemal cytoskeleton connects with the ciliary necklace which forms a scaffolding to connect with the plasma membrane and cytoskeletal network.[17,38] In the outer doublets of microtubules, a specific protein dynein, a high molecular weight ATPase, drives motility by a microtubule sliding mechanism.[39]

Figure 1.1. Anatomy of Cilium[1]

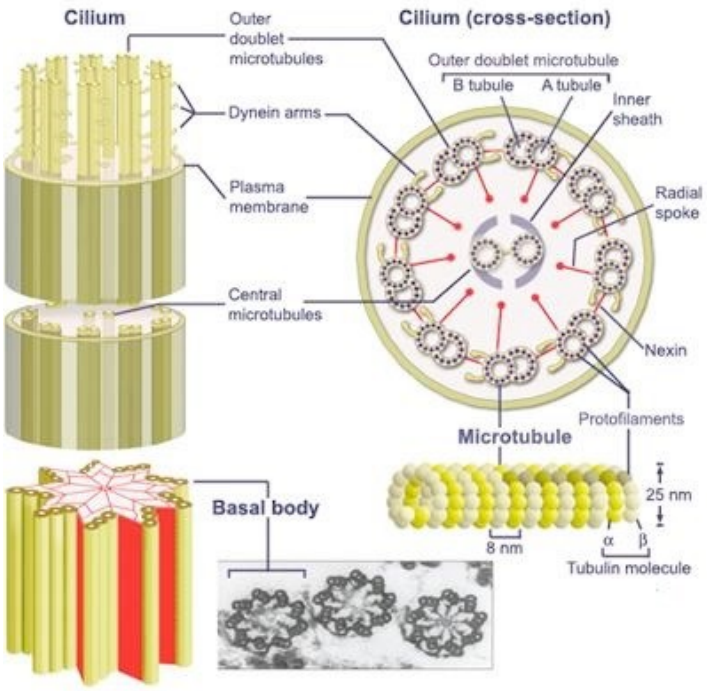

The primary cilium is appreciated for a critical role in chemical sensation, signal transduction, control of cell growth and mobility of stem cells.[40] Primary cilia play an important role in diseases involving dysfunction of cilia such as in polycystic kidney disease, congenital heart disease and genetic ciliopathies. Within the kidneys, the ducts that carry urine to the bladder are lined with cuboidal epithelial cells with immotile cilia to sense both concentration of urea and direction of urine fluid flow.[41–43] Primary cilia are "sensory cellular antennae that coordinate a large number of cellular signaling pathways, sometimes coupling the signaling to ciliary motility or to cell division and differentiation."[16] Primary cilia play a role in mechanosensing; however, there is little known regarding the role of primary cilia in airway epithelium during development.

[1] http://scienceblogs.com/transcript/2006/08/24/whats-inside-of-a-microtubule/

Sorokin *et al*. uncovered in a scanning electron microscopy (SEM) study that airway physiology development of motile cilia involved two stages: 1) a brief period of a primary, immotile cilia stage and 2) the resorption of primary cilia to form daughter cilia.[44] In an *in vitro* mouse tracheal epithelial culture model, a crossover period was discovered when primary cilia transformed into secondary motile cilia. During the crossover, on Day ALI 4, from primary to secondary cilia, the expression of a transcription factor called *foxJ1* decreased by 40% within two days.[45] Recent techniques do not permit assessment of crossover period from primary to motile cilia in HBE cultures; thus, the role of primary cilia in lung physiology still remains unknown.

Alternatively, motile cilia of the airway cells have been found to be both chemosensory [46] and mechanosensory.[47] According to immunohistochemical staining of ciliary tubulin, Morle, T. *et al*. showed that motile cilia began to develop three weeks after cell seeding of *in vitro* HBE cultures.[48] From the *in vitro* HBE model,[49] motile cilia of the human airways have been found to have bitter taste receptors which sensed noxious substances in the apical environment and responded by increasing cilia beat frequency (CBF).[46] Additionally, Button, B. *et al*. demonstrated that when different concentrations of low-melt agarose (LMA) gel solutions with different viscoelastic moduli were placed on the apical surface, the airway epithelial cells responded by regulating ATP concentration and fluid hydration, which allowed for efficient mucus clearance.[50]

Laminar Fluid Shear Stress

In studies of normal tidal breathing, a pressure gradient is formed causing a multitude of shear stresses (SS) on the airway surface.[51] SS has multiple effects on cell

function including the regulated release of ATP into the extracellular environment and affecting hydration properties by regulating ion transporters.[50,52] The effects of SS on airway surface have been studied by monitoring the ASL height by confocal microscopy. The ASL of the airway epithelium was a critical metric for mucus hydration and an indication for rate of mucus clearance. Tarran, R. *et al*. have shown that a change in SS rather than absolute SS increased ASL volume height both in cultures from health and disease origins.[53]

Studies in fish and amphibian development indicated that ciliary orientation at the apical membrane of vertebrate ciliated cells is a two-step process beginning with 1) tissue patterning and 2) followed by the stroke of ciliary beating aligning tightly with the direction of fluid flow.[54] Physical cues such as proper cell-to-cell ciliary orientation are necessary for cell culture development such that neighboring groups of cilia from different ciliated cells beat together in a metachronal wave with minimal interference.[18] Sleigh, M. *et al*. reasoned that the viscosity of the surrounding medium has a profound influence on metachronal wave synchronicity and coordinated cilia beating.[18]

However, coordination of cilia beating could not be reversed by breathing as seen in an *in vivo* rabbit study where a portion of a trachea was excised and re-stitched in a way that the dorsal part points anteriorly and ventral part points posteriorly.[55] The direction of mucus clearance remained intact; breathing and mucus flow did not re-coordinate ciliary beating and mucus pooled at the bottom of the trachea. The researchers concluded that coordination of mucus transport remained permanent from *in utero* development.[55] Within *in utero* development, the flow of amniotic fluid from alveolar cells to proximal areas of the lung is hypothesized to coordinate ciliary

beating.[56,57] The mechanism of how fluid flow affects the direction of ciliary beating and how the beating of cilia from different ciliated cells is coordinated are not well understood.

Laminar fluid shear stress (LFSS) has been applied to both *in vivo* and *in vitro* endothelial culture models to show the effects on cytoskeleton remodeling[58], mechanoreception, ion transport[52], and protein kinase signaling.[59] Critical to lung function, the airway epithelial barrier was constantly exposed to shear stresses (SS) produced by tidal wave breathing.[60] Sidhaye, K. *et al*. reported that LFSS enhanced airway epithelial barrier function by the regulation of cell membrane permeability and water homeostasis— one of many critical attributes for maintaining MCC.[52]

Motivation and Hypothesis

A good experimental *in vitro* human bronchial epithelial (HBE) cell culture model with consistently entrained cilia that beat in a single planar orientation has been unavailable. Previous studies at UNC have observed that 10 to 25% of HBE cultures develop millimeter sized patches of coordinated mucus transport in a circular pattern— called rotational “mucus hurricanes". The circular mucus pattern was hypothesized to reflect the circular boundary conditions of the *in vitro* culture insert. Recently, Sears, P. *et al*. reported a probability of at least 30 percent of cultures to spontaneously and without external shear stress produce continuous circular transport in a doughnut-shaped culture well.[61] Although these probabilities of producing coordinated circular transport are considered low, the HBE model is capable of producing sufficient unidirectional, coordinated mucus transport.

The research goal was to provide a significant refinement in mucus coordination in HBE cell culture systems, so that the cultures *in vitro* closely reflected the human airways *in situ* and transported mucus in a unidirectional manner.

The proposed research rested on the following central hypothesis:

Perfusion of apical, laminar fluid flow would train cilia in the direction of flow and allow for an understanding of tissue patterning

The goals included: (a) developing mucus clearance assays based on well-differentiated cell cultures, (b) shifting the assay to a high throughput system and (c) evaluating clearance based on particle image velocimetry (PIV). The experiments aimed at technical and conceptual improvements *in vitro* HBE culturing methods so that the HBE cultures propelled mucus in a vectoral manner that was observable *in vivo*. Accordingly, this research established an *in vitro* MCC model, developed clearance assays based on well-differentiated and entrained cell cultures, and tested mucus clearance in the presence of laminar fluid transport.

Goals and Specific Aims:

The overall goals of this project were to design, fabricate, and optimize growth and flow chambers to produce cilia-entrained HBE cell cultures, and to use these cultures to further basic understanding of MCC. Three specific aims were formulated:

Specific Aim 1. Assess Biocompatibility of growth chamber

To determine if polydimethylsiloxane (PDMS) growth chamber produced confluent and viable HBE cells for entrainment. Rationale: PDMS was the primary material used in soft lithography to produce microfluidic, lab-on-chip models for biomedical applications. Cured silicone is biochemically inert and has not been shown to produce cytotoxic effects on a wide variety of cell types including endothelia [62] and epithelia.[63]

Specific Aim 2. Perfusion Chambers for HBE cells

To develop an airtight flow chamber with a channel depth of about 200 microns that would allow for laminar flow to entrain HBE cultures. Rationale: In order to entrain the airway epithelium, a thin film (laminar) of fluid flowed across the epithelium. The airway surface liquid (ASL; mucus and PCL) height typically measured between 70 to 100 microns according to confocal microscopy studies.[64]

Specific Aim 3. Perfusion Systems for HBE cells

To determine a suitable perfusion system to entrain HBE cultures during shear stress. Rationale: Shear stress was directly proportional to the dynamic viscosity of the Newtonian fluid, flow rate and channel height. Therefore, the magnitude of the shear stress yielded more entrainment of mucus transport along a direction. Thus perfusion with perfluorocarbon (PFC) would yield cultures with linear transport than perfusion with buffer solution or no buffer solution. According to fluid dynamics, the amount of shear stress invoked on the surface of the channel has a direct relationship with viscosity of

the fluid. The viscosity of PFC (FC-3823, Fluorinert™, 3M) is 1.1 centipoise (cP) compared to viscosity of water: 1.002 cP at 37°C.

In biomedical applications, PFCs are used as oxygen carriers during liquid ventilation and for direct administration of drugs to diseased lung.[65,66] Also, as an immiscible layer, PFC does not mix with endogenous mucus[24]; thus PFC prevents any dilution or swelling of mucus,[67] which may perturb endogenous protein regulators, prevent normal growth of cultures and promote an undesired reabsorption of excess fluids. [68]

Fabrication and Optimization Proposal

Specific Aim 1. Growth Chamber Fabrication and Optimization

Fulcher, L. *et al*. recommended that primary airway epithelial cells extracted from conductive airways required both a collagen-based, permeable substrate and an air interface at the apical aspect of the epithelium, i.e., the so-called air-liquid interface (ALI) culture system.[49] This air-liquid interface culturing protocol allowed primary cells to proliferate within the first two weeks as a part of a wound-healing mechanism (verbal communication with Dr. Scott Randell), and to differentiate into a patent airway epithelium two weeks later. Gaillard, D. *et al*. discovered from dissection of fetuses that 6 to 7 weeks from week 12 of gestation were required for tracheal epithelial cells to be fully ciliated and differentiated *in utero.*[69] Remarkably, this development is accelerated in the standard HBE culture protocol. Within four weeks, primary cells are conditioned to develop in to well-differentiated airway epithelium *in vitro* to recapitulate *in vivo* biology.

This protocol used human placental Type IV collagen that was necessary for the development of a proper epithelial polarity, and further, collagen acted as the permeable support that allowed nutrients and regulatory factors access to the epithelium.[49] HBE cells could grow without the extra collagen because research has shown that cells lay down their own matrix to develop in to well-differentiated and well-ciliated cultures (unpublished research by Amy Ly, Button lab). In this system, a growth chamber for HBE cell culture's needs, minimally, incorporated an air-liquid interface for cellular development and a sterile environment for at least for four weeks.

Experimental phase of growth chamber design and fabrication. The chamber was fabricated from polydimethylsiloxane (PDMS) and incorporated the epithelial cell culture support (Corning Costar # 3801). The supports separated a bottom half-chamber for housing culture media (air-liquid interface media) for periodic nutrient exchange, and an upper half-chamber exposed to the surrounding air needed for growth. These modular supports were reproducibly incorporated in sterile, standard six-well plate and were used to investigate growth requirements necessary to allow a high degree of confluence and organization of cultures.

Optimization of chamber design and fabrication. The design of the chamber involved repeated optimization to arrive at a proper method of growing cultures to confluence and of transferring to flow chamber for entrainment. Because airway epithelial cells were very sensitive to exogenous agents, histological studies to assessed potential cytotoxic effects of PDMS and other agents (adhesives, tubing, etc.) on culture growth and differentiation. The thickness of PDMS determined permeability of oxygen[70] and carbon dioxide diffusion[71], which was pertinent to buffering the ALI culture

medium. ALI media contains sodium bicarbonate which is buffered by 5% CO_2 in the incubator such that pH is maintained at about 6.5 for proper growth of HBE cells.[49]

Specific Aim 2. Flow Chamber fabrication and optimization.

To entrain cilia in our flow studies, a chamber was fabricated from PDMS and incorporated with the Costar Snapwell epithelial cell support described above. Typically, cell culture on filters with supports incorporated cells above the filter and culture medium below the filter. In this project, the cell cultures were grown such that this relationship was flipped where the culture was exposed to constant perfusion of fluid below the filter without walls and the other side exposed for culture media exchange (see Figure 6.2). This initial chamber was used to investigate the flow requirements necessary to allow a high degree of ciliary entrainment and mucociliary differentiation.

Optimization phase of chamber design and fabrication. Design of the experiment was perfected by a continuous iterative process to generate required degree of ciliary entrainment in HBE cultures. About 4-5 weeks were required for mucociliary differentiation of HBE cultures.

Specific Aim 3. Initial study of mucociliary transport.

When the cell-to-cell beat orientation was mostly unidirectional, ciliary beating drove mucus transport. Mucus transport was studied in cilia-entrained HBE cell cultures by tracking the movement of fluorescent microspheres across their luminal surfaces by low/high power video microscopy. The effects of shear stress were compared between luminal flows of 1) standard phosphate-buffered saline (PBS), 2) perfluorocarbon (PFC) liquid, and 3) humidified air. The effects of continuous flooding of PBS or PFC

(hydrophobic mixture) on to the airway surface ("liquid bathing") was unknown; although, PFC was used acutely for maintaining hydration of airway surface during confocal studies.[72] Readout measures of the cultures included the quantification of percent ciliation, cilia beat frequency, and direction of ciliary-mediated mucus transport. With the help of circular statistics, mucus transport directionality was quantified in a compass plot in MATLAB. The quality of coordinated mucus transport was evaluated by calculating the deviation from fluid flow direction. Together, these aims helped produce reproducible cultures that transported mucus linearly *in vitro*, which reflected *in vivo* biology and which were not seen in standard culturing procedures.

CHAPTER 2: ENTRAINMENT OF MUCUS TRANSPORT BY LAMINAR FLUID FLOW

The mechanisms by which ciliary beating is coordinated by differentiated ciliated cells are poorly understood. The direction of the mucus transport was controlled by the direction of the coordinated ciliary beating, which is thought to be entrained *in utero* by fluid shear stress. Novel culturing protocols were developed to create confluent human airway cultures on membrane substrates. These cultures were encased in macrofluidic flow chambers and in a perfusion system while maintaining an air-liquid interface. The coordination of mucus transport was derived from particle velocimetry analyses (PIV). Cultures were perfused during ciliogenesis from Day ALI 7[2] to Day ALI 21 and on more mature cultures from Day ALI 30+. Perfusion during ciliogenesis stage resulted in entrained mucus transport after several weeks of exposure to fluid shear stress. Also, short-term exposure of shear stress on the luminal surface of well-differentiated cultures with uncoordinated cilia beating yielded coordination of mucus transport in the direction of fluid flow. We found that this coordination could persist for several hours after removal from the fluid flow. However, the planar coordination was inevitably transient and mucus transport returned to their pre-shear, uncoordinated state. There was little or no correlation between percent ciliation and entrainment. Together, these results supported the hypothesis that motile ciliated cells in the lung biology are mechanosensory, that coordination is fine-tuned later on in development, and that *in*

[2] Day ALI 7 is two weeks after cells are seeded on to a substrate.

vitro airway cells were coaxed to coordinate mucus transport along a particular direction by fluid flow.

Materials and Methods.

Materials and Reagents

Snapwell inserts (Costar 3810, 0.4 micron, 12-mm diameter) were purchased from Fisher Scientific (Cat# 07-200-708, Pittsburgh, Pa). Millicell inserts (PICM01250, 0.4 micron, 12-mm diameter) and Millipore Biopore membrane sheets (BGCM00010, 0.4 micron, 40 micron thick) were purchased from Millipore (Billerica, MA). Polycarbonate sheets (Cat# 8574K281), O-rings, tubing, and other hardware were purchased from McMaster- Carr (Atlanta, GA) and electronics for circuit boards from Digikey (Thief River Falls, MN). Sylgard 184 or polydimethylsiloxane (PDMS) was purchased from Dow Corning (Midland, MI). The oxygen plasma cleaner was purchased from Harrick Plasma (Ithaca, NY). Micropumps (Bartels mikrotechnik, mp6-oem) were purchased from Servoflo (Lexington, MA). Servo motors (Hitec 32645S) were purchased from Hitec RCD, INC (Poway, CA). Microprocessor units utilized here were purchased from Arduino, LLC (arduino.cc). Perfluorocarbon (Fluorinert 3823) was purchased from 3M (Maplewood, MI). Fluorescent carboxylated polystyrene microparticles (FluoSpheres) were purchased from Molecular Probes (Life Technologies, Inc). Low melt agarose (LMA, A9414), pig gastric mucin (PGM, M1778) and human placental collagen (C7521, type IV collagen) were purchased from Sigma-Aldrich (St. Louis, MO). One-micron yellow-green (Excitation/Emission: 505 nm/515 nm) microspheres were used in the mucus transport experiments (Life Technologies, Inc).

Other equipment, chemicals, reagents, and receptacles were standard laboratory grade unless otherwise noted.

Culture Protocols.

Human bronchial epithelial cells were procured from the University of North Carolina Cystic Fibrosis Center Tissue Procurement and Cell Culture Core with protocols approved by the University of North Carolina Department Of Medicine's Institutional Review Board. The protocols for procurement, culture media preparation, and basic cell culture procedures have been published.[49] In this study, cell cultures were utilized from different donors coming from different passages: P0 (primary), P1 (1st passage), and P2 (2nd passage). The airway culture cells were re-suspended in air-liquid interface (ALI) media at a cell density of 3000 cells per microliter and plating density of 300,000 cells per square centimeter.

Inverted Snapwell Perfusion Chamber

The number of manipulations during seeding and plating of the cells were kept to a minimum to reduce risk of infection. We chose Snapwell™ (Corning Costar 3801) geometry as our initial filter support membrane for entraining HBE cells by fluid shear shown in Figure 2.1.

Figure 2.1. Snapwell™ filter support dimensions (inches)

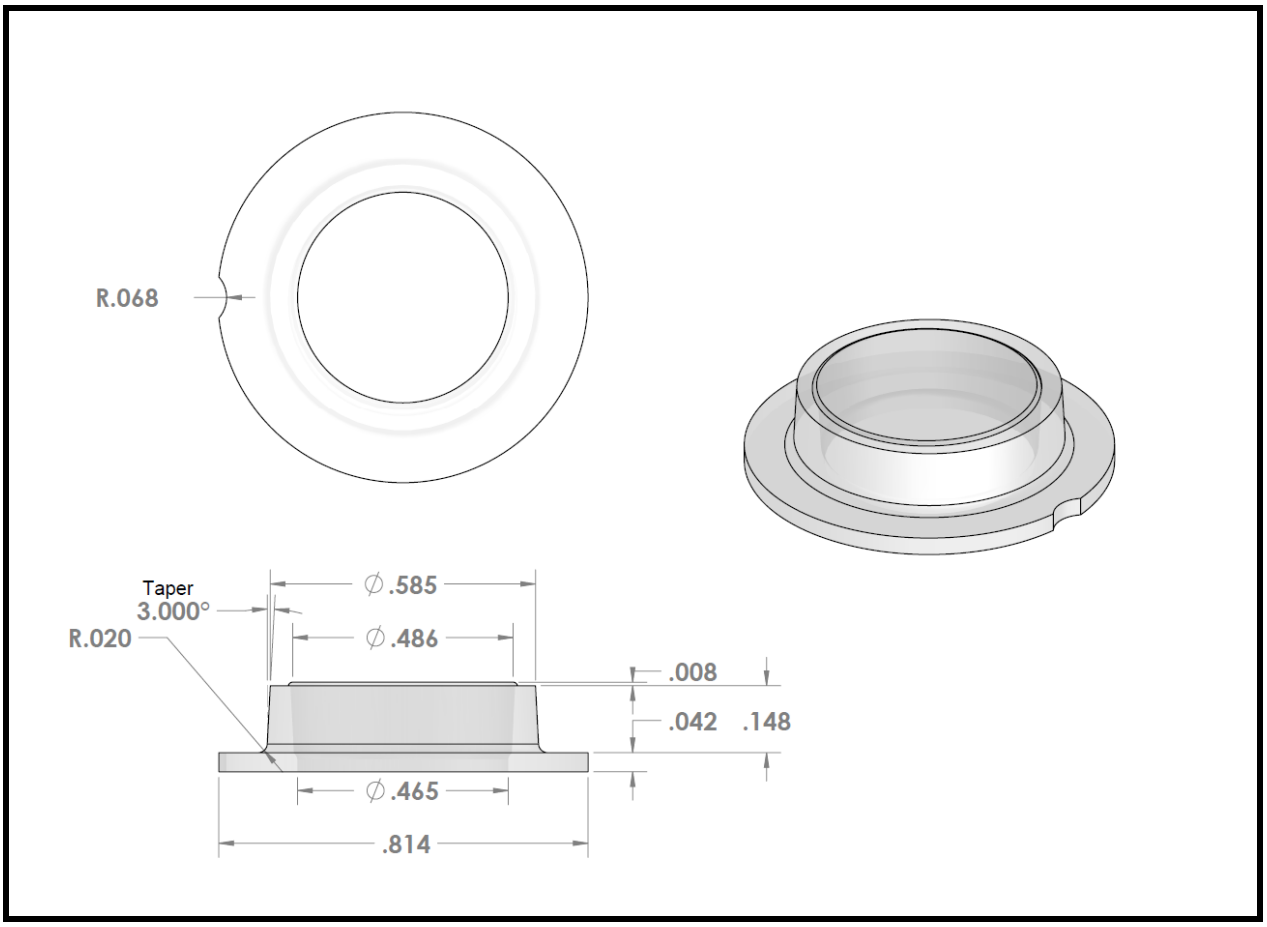

Conventionally, the HBE cells were grown within the Snapwells, which was surrounded by a wall to maintain hydration; however, in the experiment cells were seeded on the underneath surface of the Snapwell filter membrane, without walls, to expose the cells to fluid flow. This technique was named as an “inverted culture,” pictured in Figure 2.2. In the “inverted” method, rubber tubing was placed around the Snapwell as a wall for protection during culturing procedures and for supplying an artificial meniscus of fluid for extra hydration. Without this artificial wall, the cultures did not become viable over three weeks due to rapid dehydration. A photograph of culture model is pictured in Figure 3.5.

Figure 2.2. Conventional vs. unconventional (inverted) HBE culturing method

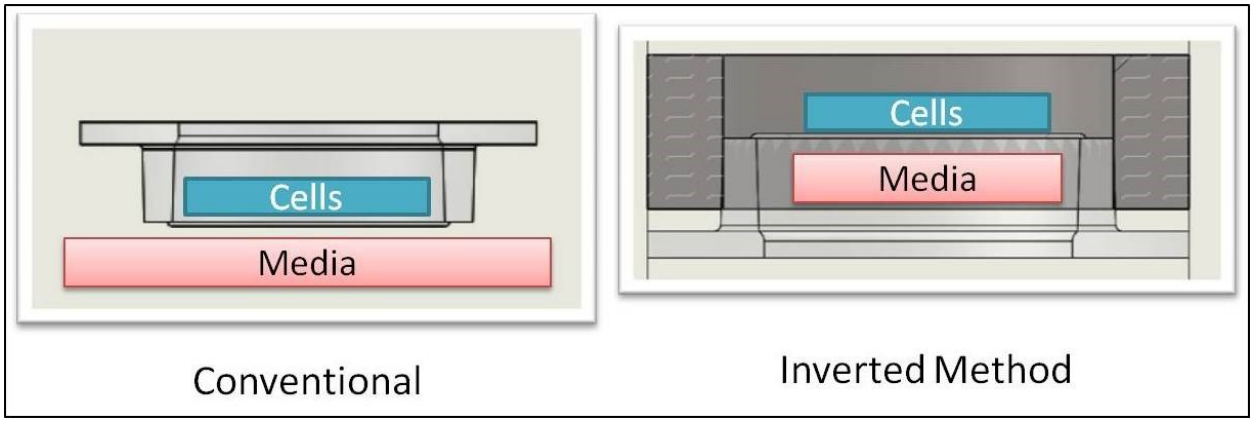

The media was “suspended” on the underside of the inverted Snapwell insert. The technique incorporated low-melt agarose to form a semi-solid based culture media to feed the cells. This media was termed as “AgALI” (Agarose-based Air-Liquid Interface) media. This semi-solid culture media was sterilized by autoclaving a stock solution of 5% agarose and then diluted to 0.5%, which was filtered through a 0.22 micron filter prior to feeding (see Chapter 5 for further details). This semi-solid based culturing protocol proved worthwhile as it reduced the number of manipulations to the cultures, maintained minimal hydrostatic pressure, allowed ease of replenishing media, and allowed use of autoclaving techniques to reduce risk of infections. The oncotic pressure of the 0.5% AgALI was measured to be near isotonic buffer at this reduced concentration (measured by Dr. Henry P. Goodell), which meant there was no difference in oncotic pressures between using 0.5% AgALI and liquid ALI media. We also achieved satisfactory oxygenation by using this semi-solid technique. Additionally, potentially, any type of media along with antifungal or antibacterial agents can be prepared with this method of growing inverted cultures. Histological sections showed no difference between conventional and inverted methods of growing HBE cells. A disadvantage to the technique was that careful consideration of temperature of agarose

gel was needed for effective use of this method since the sol-gel transition time at room temperature was 20 minutes. This AgALI method was used to feed and maintain inverted cultures for several months.

Inverted Snapwell Flow Chamber

The flow chamber was engineered using microfluidic techniques bonding a PDMS chamber mold to a glass substrate by surface treatment by ionized oxygen gas - O_2 plasma treatment (shown in Figure 2.3). The PDMS chamber was a custom-made injection mold that carries a specific geometry that encapsulated the following:

- fully developed laminar flow across several cultures
- vertical pre-load mechanism to ensure each culture receives same shear stress as they rest flush against the inner wall of the flow channel (Dr. Robert Dennis)
- radial pre-load mechanisms to hamper leaks around 3° tapered wall of Snapwell™ (Dr. Robert Dennis)
- a soft press fit of Snapwell™ in to silicone-based chamber eliminates leaks during experiment and cultures can be removed for analysis (Dr. Robert Dennis)

Figure 2.3. Macrofluidic Chamber

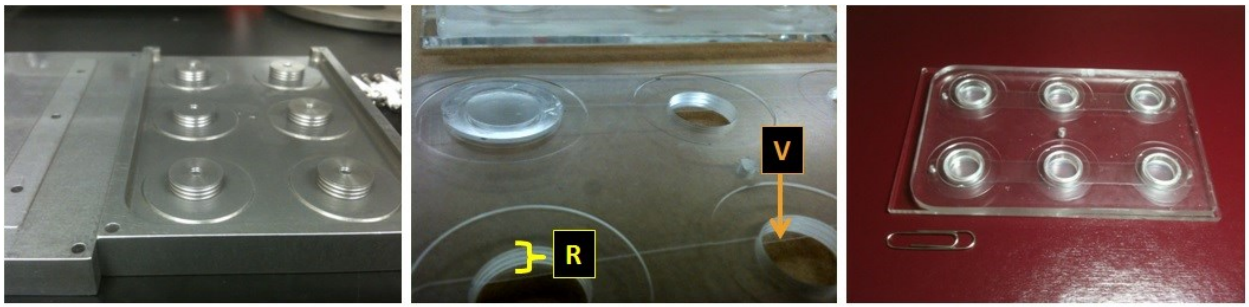

A. Aluminum Master B. PDMS Injection Mold C. Macrofluidic Chamber

Laminar Fluid Flow Chamber Design. A. Machined multi-part aluminum master, B. Injection-molded PDMS Chamber with vertical, small flap, pre-load mechanism (V) and radial, multi-ring pre-load mechanism (R), C. Plasma treated, silicone and glass flow chamber.

Because of the narrow channel and high resistance to flow, this rendition of the flow chamber was used with low flow rates of up to 1 mL/min and low shear stress (0.1 - 20 dyne*cm^{-2}). The glass substrate and very shallow channel depth (150 ~ 200 microns) allowed for the use of DIC, bright-field and epi-fluorescence microscopy. A laminar, parallel flow stream was modeled in a fluid dynamics simulation in Solidworks[3] (Figure 2.4). In Tarran, R. *et al*., phasic shear stress experiments were conducted to impart a shear stress of 0.5 dyne*cm^{-2} because this is the shear stress presumably imparted on to airway epithelial cells during tidal breathing.[60] With an initial condition of a flow rate of 125 µL/min for PBS fluid perfusion, the fluid simulation model and equation (1) predicted about 0.5 dyne*cm^{-2} shear stress along the inner surface of the channel area, where the cultures resided, highlighted in blue, in Figure 2.4.[73]

[3] This simulation assumed an adiabatic wall condition of 0 (walls did not bend with pressure) and environment temperature was at a constant 37°C.

Figure 2.4. Laminar Fluid Flow Soldiworks Simulation Model

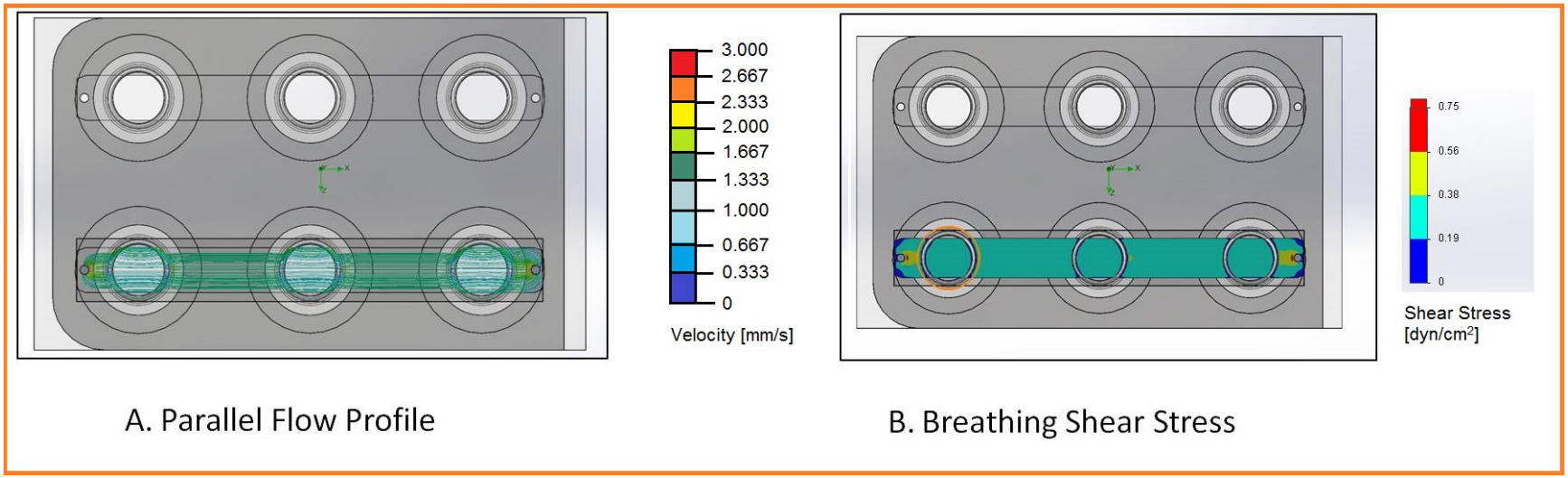

$$\boldsymbol{WallShearStress}, \tau_{wall}(Q) = \frac{6\mu}{\boldsymbol{width}_{channel}(\boldsymbol{height}_{channel})^2} Q \quad (1)$$

Q: Shear Fluid flow rate, $\frac{Liters}{min}$

μ: Dynamic Viscosity, centipoise

Microfluidic Perfusion Chambers

In a second set of experiments, small flow channel microfluidic chips were made by adhering plasma treated Millipore Biopore membrane to plastic flow cells (Ibidi, Sticky Luer I 0.8, 4 mm wide, 50 mm long, and 0.8 mm deep, #80198, sterile) – see Figure 2.5. The plasma or UV treatment of the ePTFE membrane enhanced the bonding of the 3M VHB adhesive to the ePTFE membrane material on which cells were cultured (verbal communication with 3M). The VHB adhesive tape created a hermetic seal around the flow channel to prevent leaks during perfusion. The tape was tested by 3M to last in a salt-water environment for more than 10 years with minor change to the adhesive strength (verbal communication with 3M). Cells were seeded in the flow channel by the use of negative pressure hand regulated by a slip tip syringe (BD, 1 mL slip tip syringe, Cat#309659). The flow cell chip was kept offset from the surface by attaching two O-rings (McMaster #9396K21) to the outer edges such that media could be maintained underneath the cultures.

The main key principles to properly seed the cells in to these flow cells were 1) to slowly fill the channel with cell suspension such that the flow profile is straight rather than parabolic,[74] 2) to allow cells to settle on to the membrane for at least 30 minutes in the laminar flow hood prior to incubation, 3) to reduce hydrostatic pressure by feeding the basolateral part with 0.5% AgALI and 4) to provide ample humidity to the flow cell to prevent evaporation by enclosing the flow cell in two petri dishes - a “moat”- (main – 100 mm, secondary – 1000 mm) with about 50 mL of distilled water surrounding the smaller dish with the flow cell, and 5) by adding PFC to the apical surface to reduce

dehydration.[75] Cells were cultured at 37.5 °C, 5% CO_2, and 95% RH, supplemented with fresh medium every other day, and they were imaged at 37.5 degrees C, 5% CO2 and 60% RH in an environmental chamber at daily or weekly time points unless otherwise noted.

Figure 2.5. Ibidi Linear Perfusion Chamber

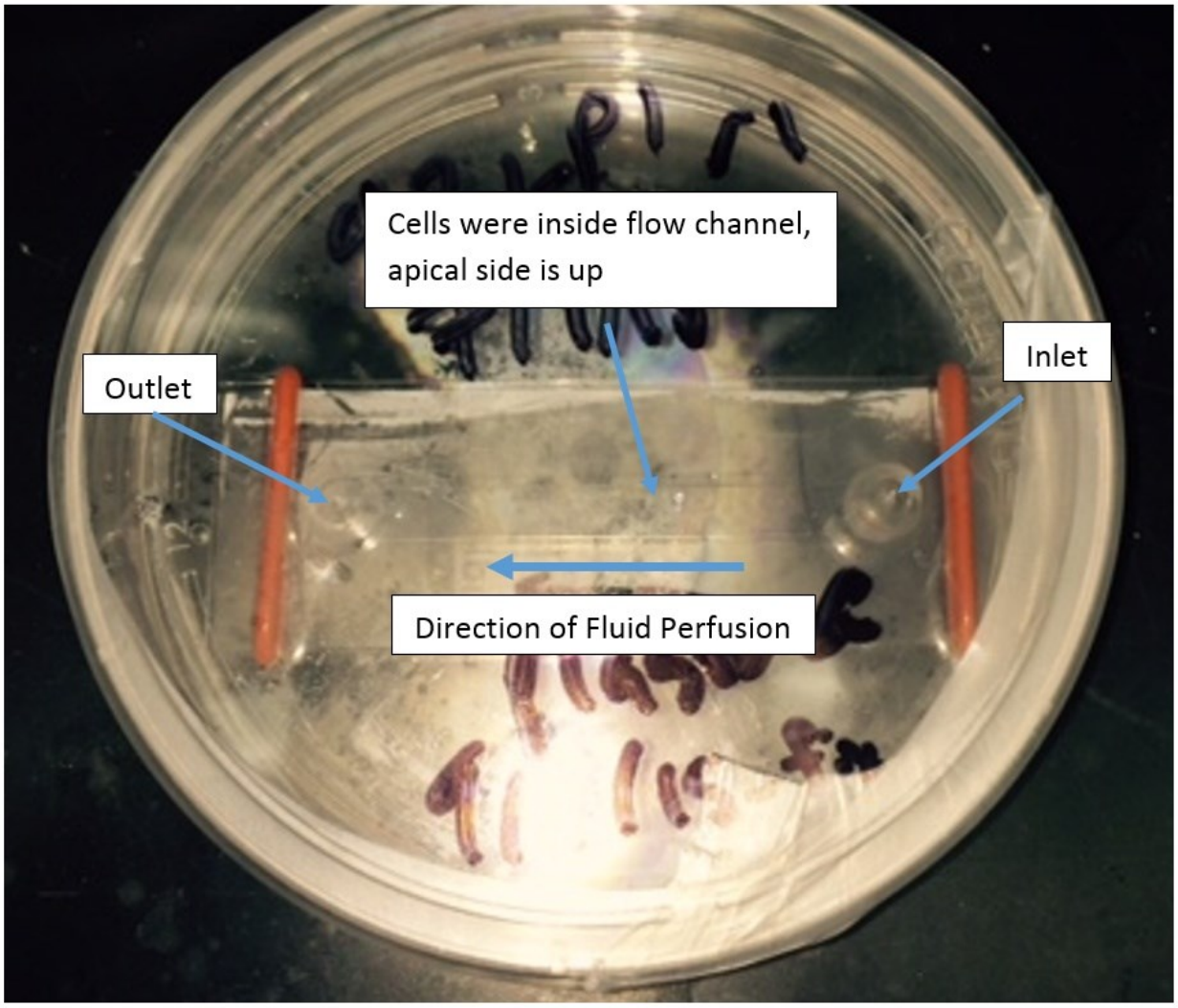

An IBIDI single channel culture slide was kept in a petri dish during the perfusion studies. Two silicone O-rings helped offset the culture to supplant 0.5% AgALI to fee the cultures. The perfusion method used was oscillatory in nature (2 % duty cycle) yet achieved net volumetric flow of 1 mL /min.

Figure 2.6. Ibidi Chamber Fluid Flow Simulation Model

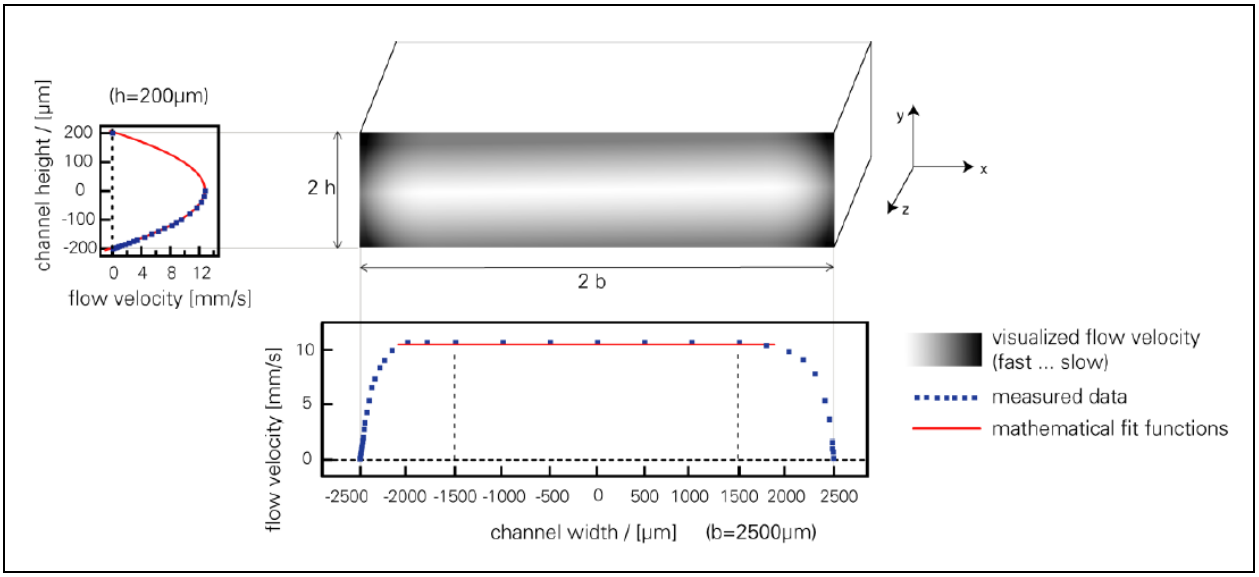

This flow simulation model of the flow profile in the y-direction was adapted from the specification sheet for the chamber.[76] The flow profile is a parabolic curve where the majority of the shear stress was evoked through the middle of the chamber.

The wall shear stress and shear rate calculations were derived below according to the equations provided by the company (in Figure 2.6).[76] According to these empirical equations, at a net flow rate of ~1 mL/min and a dynamic viscosity of 1.1 cP for PFC, the shear stress for the experiment was maintained at around 0.5 dynes*cm^{-2} and the shear rate was estimated to be 34.7 s^{-1}.

Asymmetric Shearing Chambers.

Cells were sheared apically and basolaterally with an asymmetric shearing profile. In Figure 2.7, cells were seeded either in a custom PDMS-polycarbonate-Biopore palette (PC-tilt) with multiple wells (~0.8 cm^2) or in a parallel 6-channel enclosed flow cell (6-tilt) (Ibidi, Cat# 80608, sterile, Sticky Luer IV 0.4, 4 mm wide, 20 mm long, and 0.4 mm deep channels). Cells were plated with standard culturing

procedures for the PC-tilt flow chip.[49] For the Ibidi 6-channel flow chip, HBE cells were cultured with the same protocol mentioned in the previous section.

Figure 2.7. Asymmetric Polycarbonate Perfusion Chip

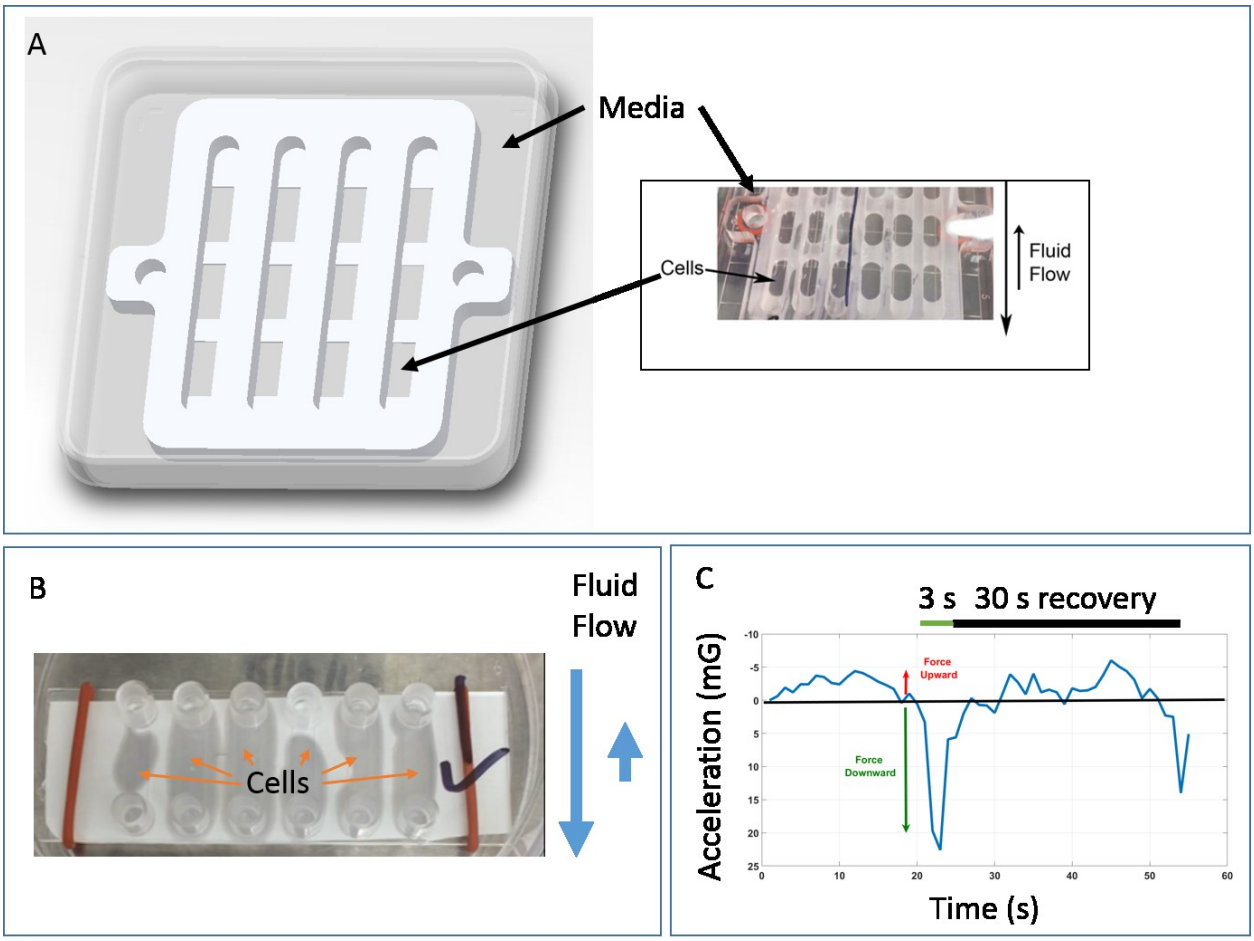

A. Polycarbonate palette model incorporated a large, rectangular, open channel with 3 replicate culture wells. The channels were loaded with 500 microliters of PFC such that the cultures were flooded with PFC. Cultures were fed with 12 mL of ALI media.
B. An Ibidi 6-channel, parallel culture slide contained Luer ports to add 50 microliters of PFC such that the cultures were flooded with fluid. The cultures were fed with 6 mL of ALI media.
C. The fluid flow was asymmetric where the downward force (about 20x force due to gravity) is greater in magnitude than the upward force (about 5x force due to gravity). The duty cycle was maintained at around 10% with 3 s duration of the peak force and 30 second duration of the smaller force. The acceleration was recorded by TI Sensor Tag Bluetooth sensor.

The wall shear stress for the asymmetric perfusion model was derived with the following equation (2) for a tilted, channel geometry.[77]

$$\tau_w = \frac{1}{2} \rho g R \sin \beta \quad (2)$$

ρ, density of the fluid – 1789 kg/m^3 (37°C)
g, gravity – 9.8m/s^2
R, effective radius of the fluid
B, angle of the tilt – 22°

The peak wall shear stress evoked on the cells was derived to be 104 dyne/cm^2 for the polycarbonate palette (R = 0.125 inches) and 13 dyne/cm^2 for the Ibidi culture chip (R = channel height of 0.4 mm). The shear stress in the polycarbonate palette was not desired, and this protocol provided an avenue to study mucus entrainment under extreme loads, which are thought to occur in turbulent flows in the bifurcations of the lung.[78,79]

Drip perfusion chambers

Cultures were plated in an open rectangular channel (40 mm by 6 mm) machined from polycarbonate, the cells seeded on Millipore™ Biopore™ membrane, and a compartment underneath was made to enclose AgALI media to feed cells and to maintain an air-liquid interface (see Figure 2.8). The drip chip was adhered to a microscope glass slide (75 mm by 25 mm), and the adhesion between the layers of PC, membrane and glass was held by PDMS. The moat idea was also used to maintain humidity for the cultures during culturing window. For the perfusion setup, the drip chip was designed to fit snugly in a 50-mL conical tube for the experiment where about 50

microliters of PFC dripped across the surface of the airway cultures and recirculated inside the conical tube. The drip chips were laid down horizontally while they were imaged on an epifluorescence microscope.

Figure 2.8. Gravity-fed Perfusion Chamber

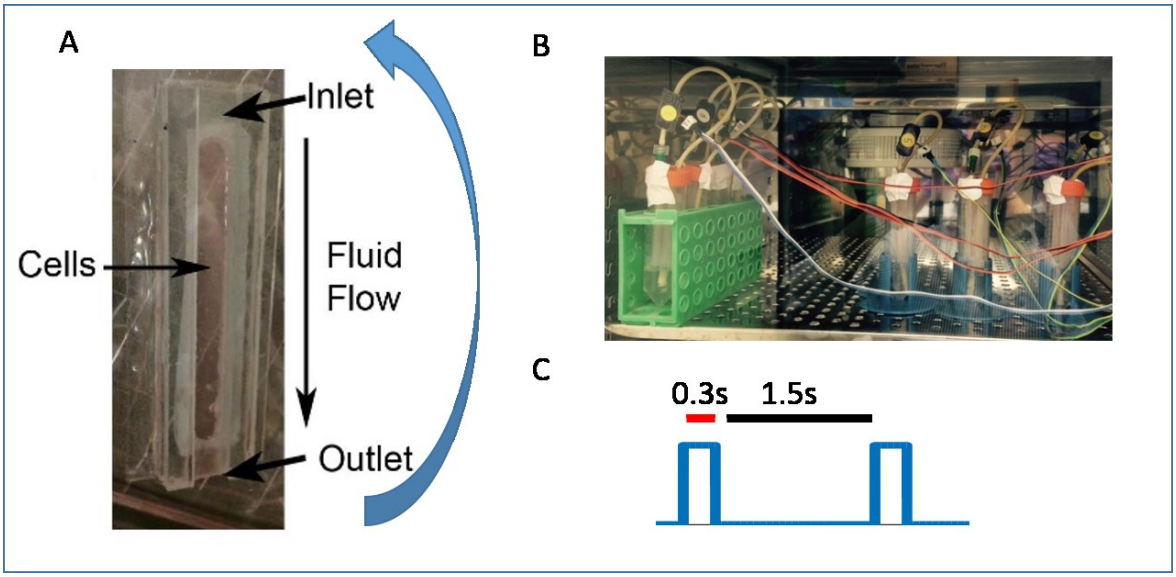

A. Drip chamber showed that the cells are kept vertical in the conical tube. The cells were fed with 0.5% AgALI to reduce hydrostatic pressure while being upright. A piezo pump sucks fluid from the bottom reservoir. The inlet was where fluid drips PFC from an oval shaped syringe needle (Gauge 15) on to the culture. The outlet was where the PFC fluid drips on to a reservoir of fluid mixture (PFC saturated with PBS) and the PFC re-circulated.
B. Picture of the perfusion setup showed 12 parallel experiments
C. The perfusion was oscillatory in nature with a 15% duty cycle. The net flow rate was measured to be about 1.5 mL/min

The wall shear stress was derived to be 17.5 dyne/cm^2 for the open channel geometry using a film thickness of 200 microns (50 microliters / 2.5 cm^2 surface area) and equation 2 with an angle of 90 degrees.

Table 2.1. Summary of peak fluid shear stress on airway cultures

Perfusion Chamber	Fluid Shear Stress	Perfusion Type	Perfusion Time	Duty Cycle
Snapwell Flow Channel	~0.5 dyne/cm^2	Laminar, continuous	Post-cilia	100%
Ibidi Flow 1 Channel	~0.5 dyne/cm^2	Laminar, oscillatory	Pre-cilia	2 %
12 –well PC palette	~104 dynes/cm^2	Asymmetric, oscillatory	Pre-cilia	10 %
6-ch Ibidi slide	~13 dynes/cm^2	Asymmetric, oscillatory	Pre-cilia	10 %
Drip Flow	~18 dynes/cm^2	Laminar, oscillatory	Pre-cilia	15 %

Perfusion Systems

Several perfusion systems were developed to deliver fluid shear across cultures for six hours to one month while maintaining an "air"-liquid interface including a syringe pump perfusion and an ultrasonic piezoresistive pump (UPP) perfusion system (see Perfusion Protocols in Appendix 1). The challenge was that this system needed to be compact so that it could fit in an incubator for maintaining physiologic conditions during the treatment. Each system had its own setbacks – such as leak problems that were resolved in the final system incorporating UPP. The perfusion system was designed to be a closed-loop fluid perfusion system with minimal maintenance requirements such as re-feeding cells and replenishing shear fluid in case of evaporative loss. A dedicated microcontroller (Microchip PIC18f4550, PIC18f1320, or Atmega16U2) was central to each version of the perfusion system which managed fluid flow rate and acquired pressure readings. In the fluid flow system, to maintain an "air"-liquid interface, the software bubbled incubator air and 5% CO_2 in the shear fluid reservoirs at timed intervals.

Experimental Timelines

Figure 2.9. Experimental Timeline for Short-Term Perfusion Studies

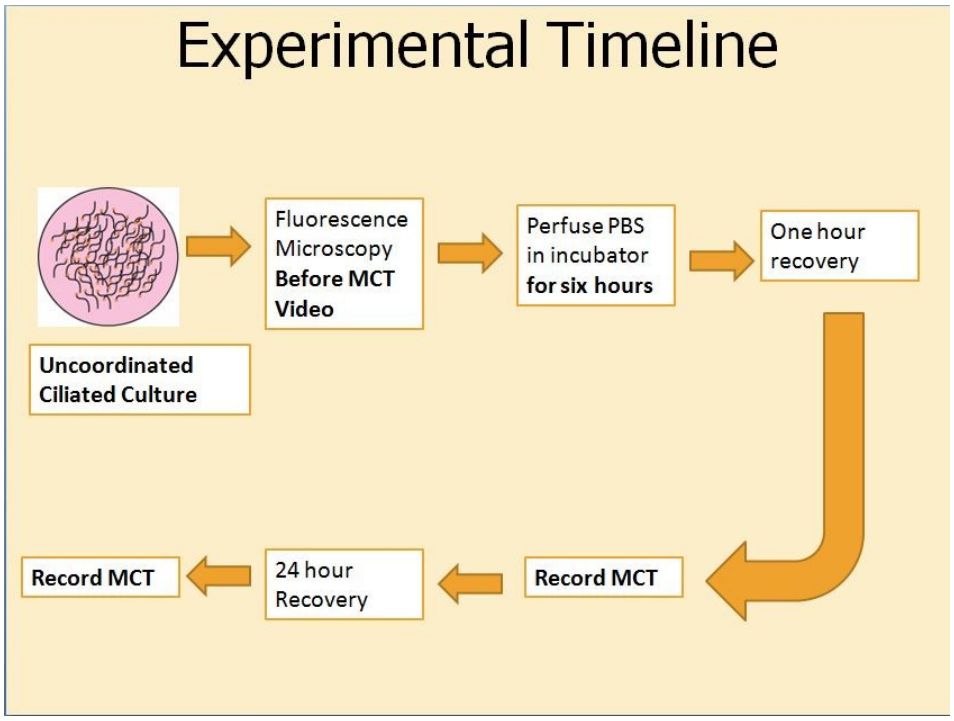

Figure 2.10. Long-term perfusion protocol and imaging during ciliogenesis

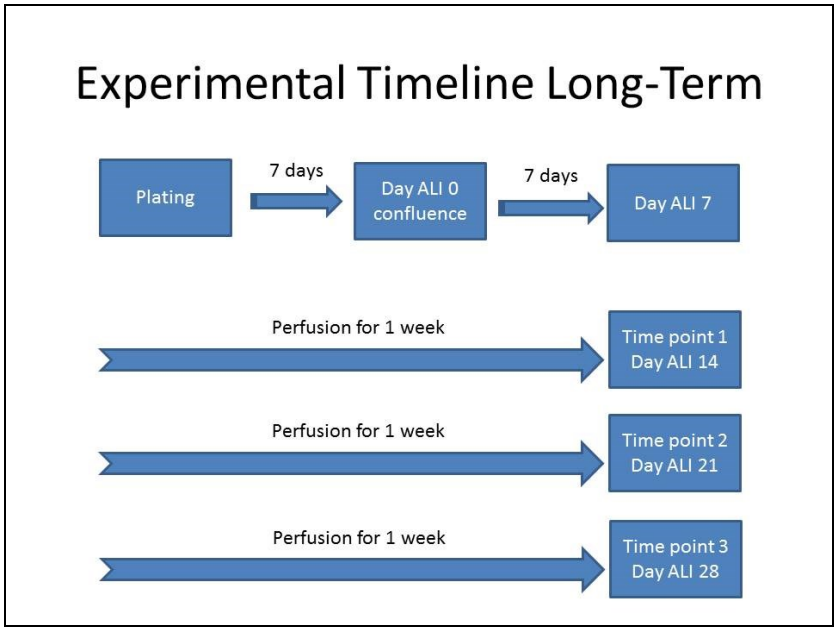

Figure 2.11. Long-term perfusion protocol and imaging post ciliogenesis

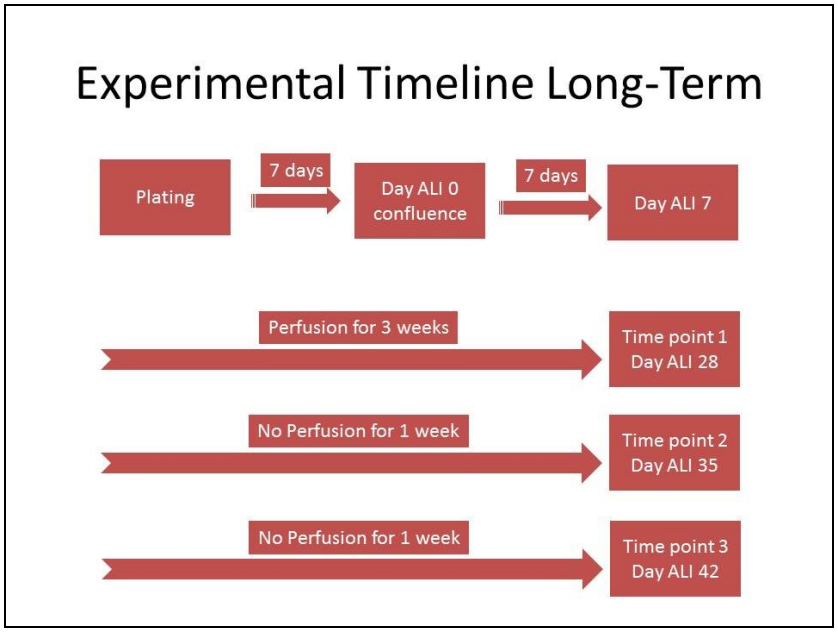

The figures above outlined three different protocols that were used to study the dynamics of mucus transport in airway cultures. For short-term perfusion on well-differentiated cultures, in Figure 2.9, which lasted for several hours to several days,

mucus transport in three to four pre-selected regions of interests (ROIs) was monitored before and after perfusion challenge. An automated stage or a gridded cover glass was used to ensure the same ROI (x, y) was observed on each time point with an accuracy of 10 to 100 microns. Fiducials on the culture helped to orient the culture on the microscope. For long-term perfusion experiments on differentiating cultures, which lasted for several weeks, mucus transport, cilia beat frequency, and percent ciliation in two to five ROIs were captured at weekly time points during ciliogenesis and after ciliogenesis (see Figure 2.10 and Figure 2.11). The perfusion experiment lasted for approximately one month and then the cultures were taken off the system to determine if entrainment remained during the next month.

Labeling

Cells were quickly washed with PBS to remove nascent mucus within 30 seconds. Then, 10 microliters of yellow-green fluorescent, carboxylated microspheres (0.02% v/v) in PBS were deposited on to the culture. After a brief incubation of 5 minutes, the cultures were imaged for mucus transport and/or for percent ciliation. A similar methodology has been shown to describe mucus transport in the absence of mucus.[80] For the Ibidi slides, however, the mucus was removed through a 5 min wash with Dithiothreitol (DTT, 10 mM or 0.1 mM final concentration) and incubated over night before imaging the next day.[68] The channels were flooded with a PBS solution of the microspheres prior to imaging near the PCL layer.

Figure 2.12. Mucus Transport Entrainment Metric

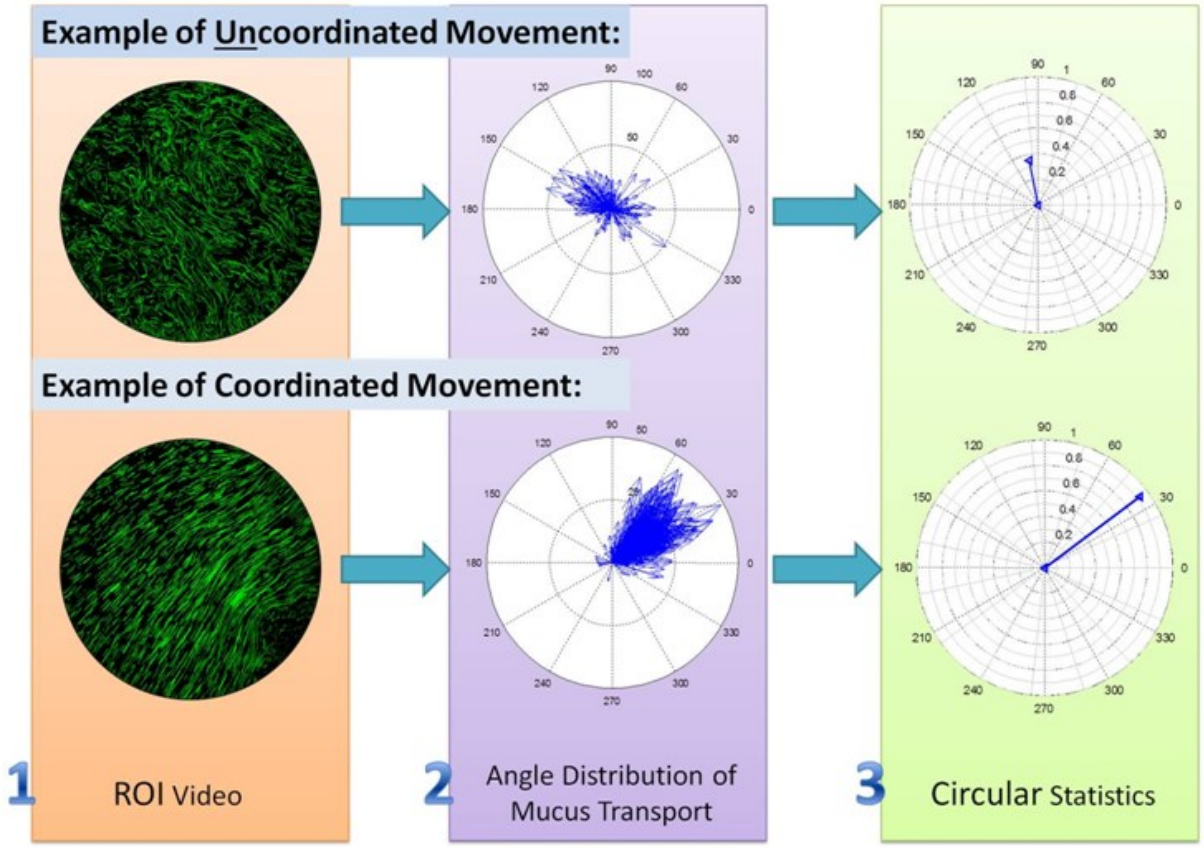

Three steps were involved to analyze mucus transport in areas that showed uncoordinated and coordinated mucus transport.

Mucus Entrainment Metric

As shown in Figure 2.12, at each region of interest (ROI), a 30 second video captured movement of fluorescent tracers, added by a five microliter bolus, which were used as surrogates for describing mucus transport. The video data was processed by particle tracking software, Video Spot Tracker, and the trajectories are analyzed in MATLAB (Mathworks, Inc). For each resulting video, the compass plot and angle distributions of the tracer movements were tabulated. In the third step, a single arrow in the compass plot represented the net displacement from start position (0, 0) and end position (x, y) at 30 seconds from the video. Circular statistics were performed to find

the mean angle or coordination direction of angle distribution (N=100+ tracers). The resulting length of the arrow is between 0 and 1 represented whether the distribution was non-uniform (uncoordinated, high variability) or uniform (coordinated, low variability).

In the perfusion experiments during ciliogenesis, there was much more variance in mucus transport where a) beads were stuck to surfaces and showed little transport, b) beads were driven by diffusion if the area was poorly ciliated, c) beads were driven in circular, d) beads were driven in a linear fashion by MCC. A more in-depth particle tracking algorithm was developed to only focus on the driven transport (see pg.114).

Results:

Perfusion during ciliogenesis: Linear Mucus Transport

Cells obtained from a total of 10 patient codes were sheared using the Ibidi microfluidic single channel and the drip perfusion assay to yield vectoral mucus transport (see video supplemental “drip shear.avi”). The best alignment along the fluid flow cue was reached between culture age of day 22 to day 70 (day ALI 14 to day ALI 56). The level of entrainment or resultant was between 0.3 (70% variance, uncoordinated) and 0.8 (20% variance, highly coordinated) among the replicates. In Figure 2.13, an example of a single experiment from a grand mean of 5 ROIs depicted mucus entrainment on Day 70 with 40% ciliation. On day 14 for all of the codes, cilia were absent and thus the cultures were not imaged on that day. The percent ciliation plateaued around 40% for the drip perfusion cultures and 60 to 80 % for the cultures in the microfluidic chamber. The discrepancy in percent ciliation between the two

experiments may have been due to substrate modification (e.g. plasma treatment of the microfluidic chamber prior to cell seeding), or by a difference of 30 fold in shear stress (see Table 2.1). The Ibidi long channel also had a shorter period, ~10% less duty cycle, of shear than the drip flow, which may have allowed for cell regeneration.[56] For both experiments, ciliated cells preferentially populated along the edges or boundaries of the chamber instead of the middle of the channel (experimental observation).

Figure 2.13. Example linear perfusion during ciliogenesis experiment

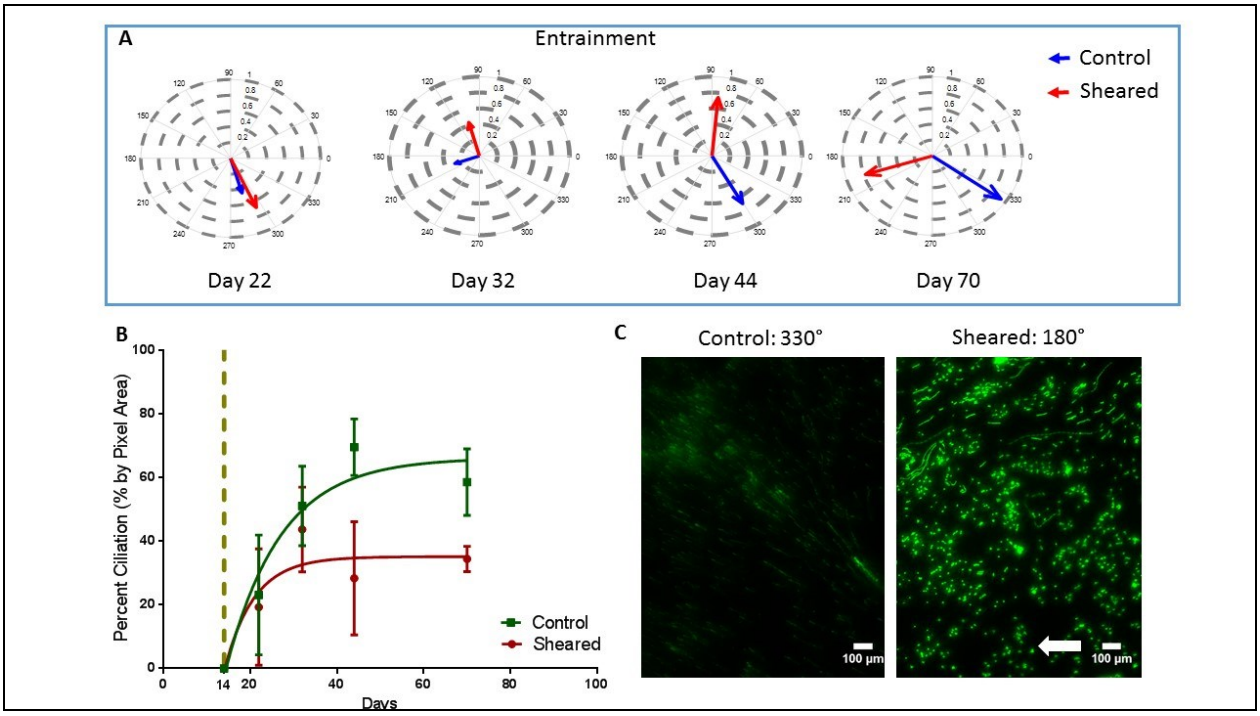

A. A series of compass plots illustrated the variance of driven mucus transport from the average of 4 to 5 ROIs between control and sheared sample. Above 0.5 indicated coordination along a mean direction. By the end of about 70 days of perfusion, the cultures yielded net mucus transport along the fluid flow direction of 180 degrees.
B. The sheared culture reached a plateau of about 40 percent ciliation compared to 60 percent for the non-sheared controls.
C. Image representative of the ROIs on day 70 showed the difference in magnitude of entrainment between sheared and control. Scale bar =100 microns. The arrow in the sheared picture indicated the fluid flow direction.

Perfusion during ciliogenesis: Asymmetric Perfusion

Cells from a total of 6 patient codes were experimented with a replicate count (# of wells) of 6 to 12. The best entrainment along a vertical axis was reached between days 22 to day 68 in the experiment. Individual replicates were selected for entrainment along 90- or -90-degree direction that had above 0.5 resultant. Majority of the replicates showed entrained mucus transport along the downward or -90 degree direction (an example shown in Figure 2.14). The percent ciliation also matched well with the control from the initial onset of the experiment; however, the cultures had stayed at 40% ciliation throughout the experiment.

Figure 2.14. Example asymmetric perfusion during ciliogenesis experiment

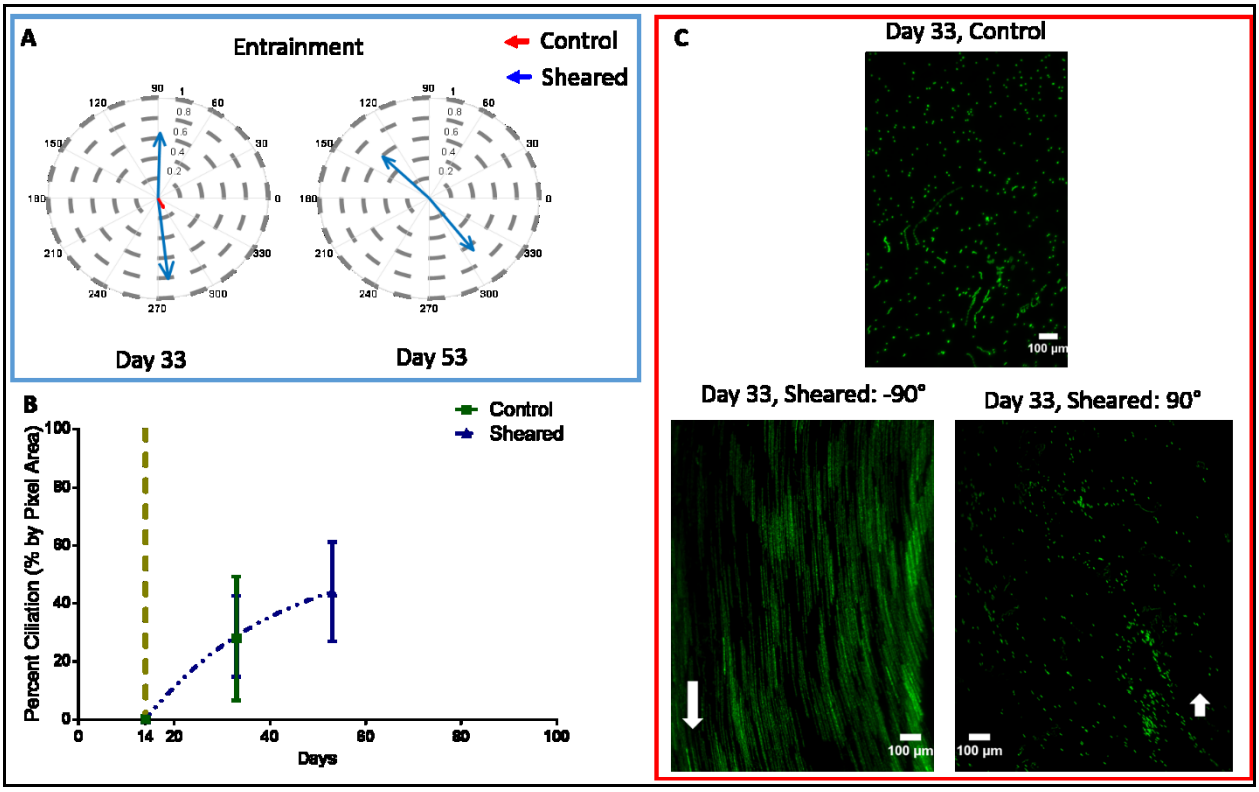

A. A series of compass plots illustrated the variance of driven mucus transport from the average of 4 to 12 ROIs between controls and sheared wells in a polycarbonate palette sample. Above 0.5 indicates coordination along a mean direction. The controls were uncoordinated with a resultant of less than 0.1 or highly uncoordinated or showing no linear transport across multiple ROIs. Whereas, the sheared samples showed coordination with 70% of the distribution of mucus transporting in the direction of fluid shear. By the end of about 20 days of perfusion, the cultures yielded net mucus transport along the fluid flow axial direction of 90 to -90 degrees. About 50 percent of the culture wells showed net transport downward and 40 percent of the culture wells showed net transport upward. The controls were not viable to make another measurement on day 53.
B. The sheared cultures reached a plateau of about 40 to 50 percent ciliation.
C. Representative images for day 33 (Day ALI 19) where the controls showed random mucus transport and the sheared sampled showed bidirectional entrainment. The magnitude or lengths of streaks/displacements were three times as large in the sheared (downward) vs. non-sheared sample. Scale bar =100 microns.

Figure 2.15. Histogram plot of succsessful entrainment of transport

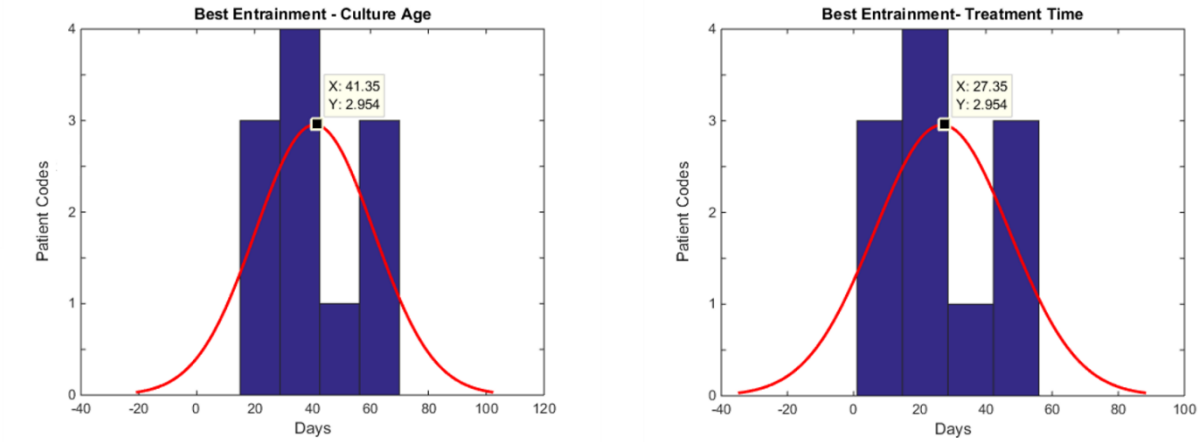

The average culture age for an entrained culture was about 42 days[4] and the treatment time of 28 days for the perfusion during ciliogenesis experiment. About three codes responded well to the treatment immediately, and three codes needed at least 40 days of treatment. Two of the three codes that needed more than 40 days of treatment came from patients with smoking history. The median codes were all from patients without smoking history.

Table 2.2. Grand summary of the perfusion during ciliogenesis experiment

	Non-sheared control	Linear	Asymmetric	
Ideal Angle (Deg)	180	180	90	-90
Mean Transport angle (Deg)	-10	-177	94	-81.4
Entrainment	0.2	0.6	0.5	0.6
Standard deviation (Deg)	65	74	61	47.5

Both the linear and asymmetric techniques showed about 50 to 60 percent success at creating coordinated cultures along a particular direction. However, the standard deviation was pretty large compared to the individual standard deviations between codes. The mean coordination direction did meet the ideal coordination direction by less than 0.1% error. The non-sheared controls showed as much deviation between codes and with 80 percent variation in coordination between codes. N = 10 codes, n = 1 to 12 replicates.

[4] 42 is the answer to the ultimate question of life, the universe, and everything.[118]

Post-ciliogenesis: UPP Perfusion

Short-Term. Cell cultures were grown to maturity (Day ALI 30+) and transferred to the Snapwell laminar perfusion system on Day 0 (see pg. 82) using continuous fluid flow while maintaining constant shear stress of 0.5 dyne*cm^{-2}. Three culture wells were sheared by PBS perfusion continuously for three days and a fourth culture non-sheared control dish was kept separate in the incubator for comparison. The flow direction and reference was at 90-degrees (see example video supplemental “center-af.avi”). From day 3 onwards, cultures that were sheared were kept in the incubator for observing recovery stage following transient entrainment (Figure 2.16 and Figure 2.17).

Figure 2.16. Short-Term (3 days) Temporary Entrainment

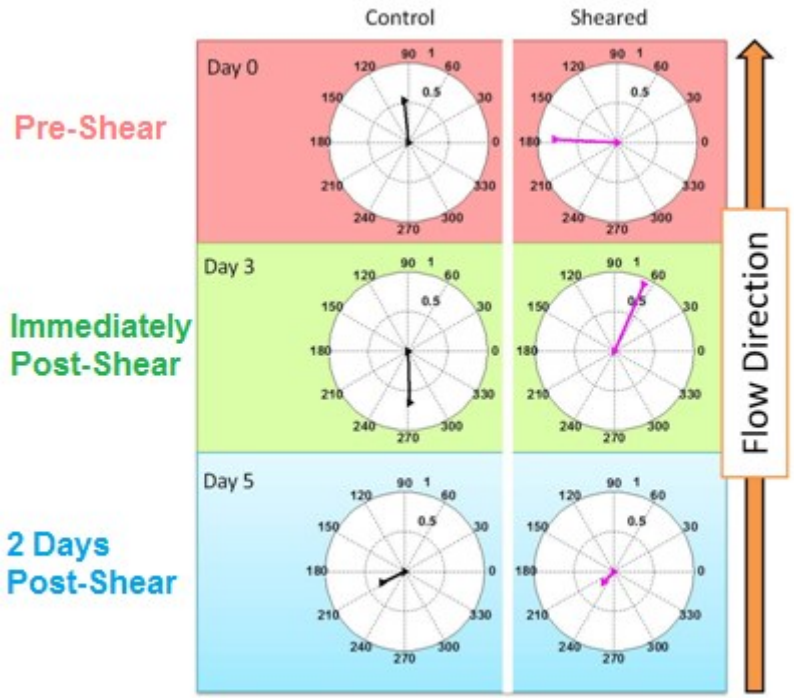

Mean distribution and angle of transport over three separate ROIs from a triplicate sample were shown. The sheared culture showed that if mucus transport was not well defined in the beginning it could be improved by laminar perfusion.

Figure 2.17. Short-Term Entainment: Representative Images

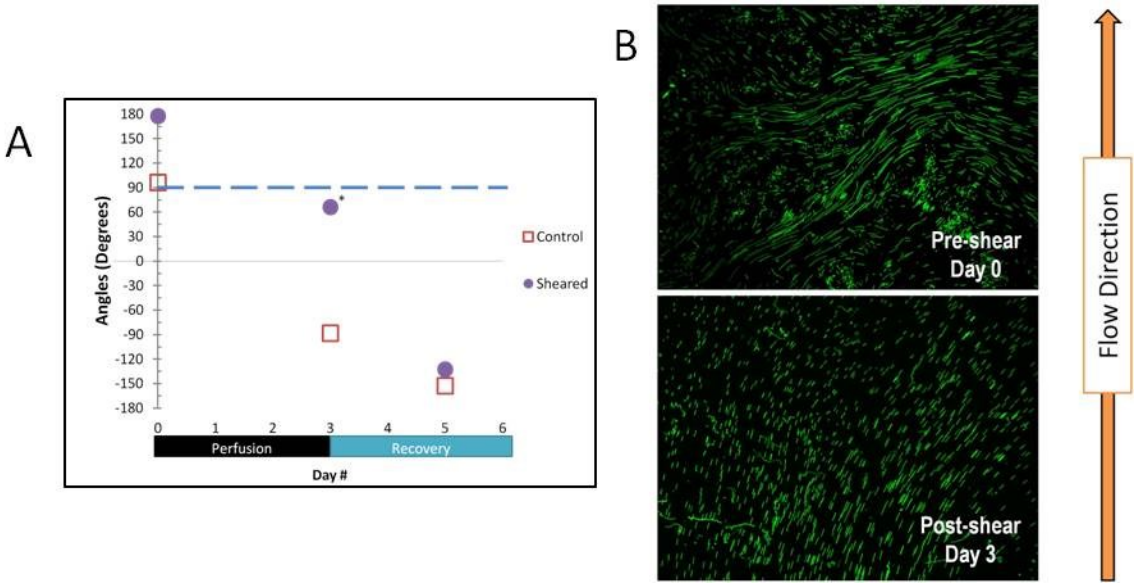

A.) ROIs showed significant coordination along 90line (flow direction) ($p<0.05$ V-Test significance). B.) Time-lapse projection showed linear mucus transport along the flow direction in Post-shear Day 3 from sheared culture.

Long-Term. Three culture wells were sheared by PBS perfusion continuously for seven days and a fourth culture non-sheared control dish was kept separate in the incubator for comparison. The flow direction/reference was at a 90 degree angle. From Day 7 onwards, cultures that were sheared were kept in the incubator for observing recovery behavior (Figure 2.18 and Figure 2.19). On Day 22 (not shown), sheared cultures returned to an uncoordinated, pre-shear state.

Figure 2.18. Long-Term (7 days) Entrainment

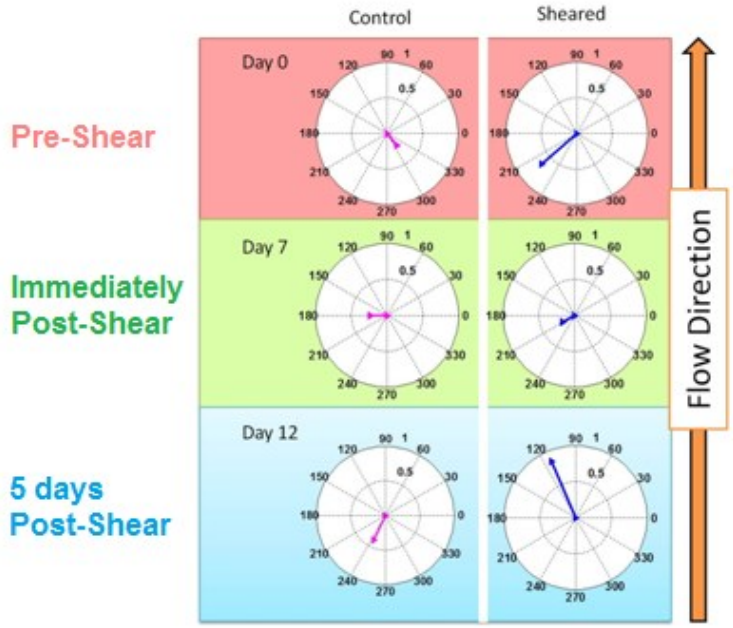

Entrainment of mucus transport from long-term perfusion in sheared culture was seen to be effective in the recovery stages on Day 12. Interestingly, mucus entrainment remained uncoordinated on Day 7 immediately after shear stress, which did not correlate with Figure 2.16.

Figure 2.19. Long-Term (7 days) Entrainment: Representative Images

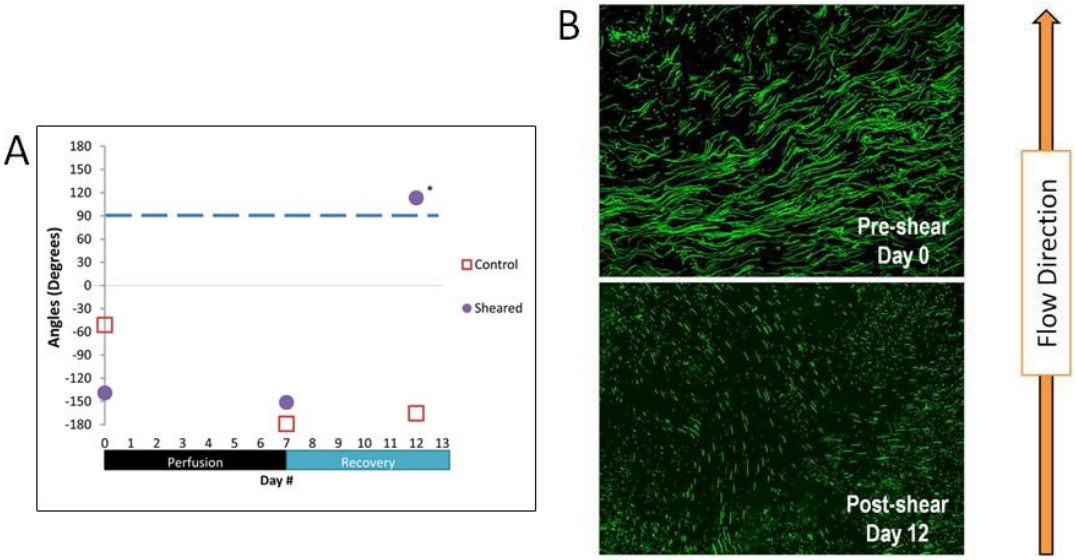

A.) ROIs showed significant coordination along 90line (flow direction) ($p<0.05$ V-Test significance). B.) Time-lapse projection showed linear transport on Day 12 from sheared culture.

Discussion

The ability to guide vectoral mucus transport and the time in which the ciliated cells polarize to maintain linear transport were not known before these perfusion studies. For the perfusion assay during differentiation, cultures were entrained on average about 42 days after the onset of perfusion on day ALI 7 (day 14 after seeding cells) (see Figure 2.15). The most effective method for entraining the cells in a linear direction was the gravity drip perfusion and IBIDI slide linear perfusion experiments with a 50 to 60 % success rate. The asymmetric tilt shear assay yielded cultures with entrainment mucus transport within one week of perfusion after day ALI 7. The tilt assay also produced cultures that would transport both directions along the axis of the tilt where the transport that was fast aligned with the peak downward force cue and where the transport that was slow aligned with the peak upward force cue. These findings suggested that level of entrainment of mucus transport correlated with the magnitude of the shear stress evoked on the cell culture. Assays that emulated breathing with stress associated with breathing (0.5 dyne/cm^2) took on average 30 to 60 days to yield entrainment of mucus transport along a linear path; thus, fine tuning occurred at a later stage after ciliogenesis. Our experimental findings also correlated with the fetal trachea studies by Gaillard, *et al*., who found that ciliated cells took up to 6 weeks during gestation to develop in to a mature epithelium *in utero.*[81] Also, we found that percent ciliation did not correlate with linear mucus transport in the single channel experiments against controls *in vitro*. However, a code by code variation in the percent ciliation metric was present and the level of ciliation, overall did not reach past 80 %.

The post differentiation perfusion assay showed that short-term and long-term exposure of shear stress on the luminal surface of well-differentiated cultures with uncoordinated cilia beating caused coordination of mucus transport in the direction of fluid flow. In the short-term experiment, coordination persisted for several days after removal from the fluid flow; however, the planar coordination was inevitably transient and ciliary beating eventually returned to their pre-shear, uncoordinated state. The success rate for short-term treatment was found to be 50% effective post-shear and 25% effective in recovery stages. In the long-term experiment, the cultures became entrained to transport mucus in the direction of fluid flow during recovery stages. Long-term treatment was found to be 50% successful in the recovery stages. This treatment was not 100% effective as some cultures did not respond to the shear treatment. A summary of the pre-ciliogenesis experiments and post-ciliogenesis experiments is provided in Table 2.2 and Table 7.1 (see Chapter 7) respectively.

Conclusion

HBE cultures in both pre- and post-ciliation stages were entrained *in vitro* by controlling shear stress and by regulating the direction, interval and fluid pressure, thus providing an *in vitro* system that can partially mimic human airway physiology. Together, these methods would allow researchers to not only culture HBE cells with coordinated ciliary, but also to understand the signals and parameters which facilitate cilia coordination and mucus transport. A novel high throughput, automated bioreactor system was developed to be set in an incubator that maintained a) an "air"-liquid interface necessary for growth and b) continuous laminar fluid shear to produce cultures that showed vectoral transport.

Future Directions

Interestingly, though unexpected, the perfusion of Kreb's Ringer solution (KRB) with the post differentiation perfusion assay did not entrain mucus transport in the direction of fluid flow but perpendicular to the fluid flow. Dr. Eszter Vladar at Stanford University helped to identify how the perfusion assay affected cell morphology and distribution of protein complexes by staining for planar cell polarity proteins, which localized to different parts of the ciliated cells in polarized epithelia.

Figure 2.20. Example of PCP staining on post-ciliogensis entrained vs. non-sheared control culture

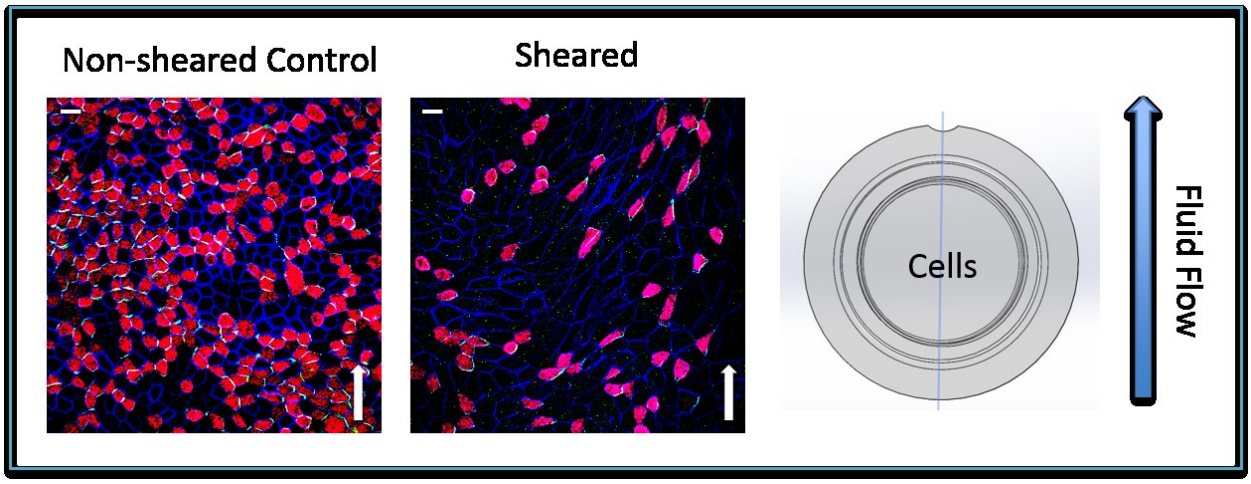

This panel showed the results of an immunohistochemical staining of planar cell polarity proteins on HBE cells that were perfused by KRB for several days. The protein expressions in green showed location of Vangl1, the blue color looked at e-cadherin which stained for the cell to cell junctions, and the red represented ciliated cells stained by α-tubulin. The white arrows indicated direction of fluid perfusion. Scale bars are 10 microns.

Planar cell polarity proteins were a set of biological markers or proteins that were expressed in the cytoskeletal network within the plasma membrane of cells. Dr. Eszter Vladar has researched a set of PCP proteins involved in development of ciliated cells *in vivo* and *in vitro* using a Drosophila model.[82–84] Her hypothesis was that this set of proteins was expressed throughout the ciliated cell as a global pre-cursor and that

during ciliogenesis, the localization of the protein shifted to form an asymmetric pattern around the cilia: Van-gogh-like1 (Vangl1) and Prickle stayed behind cilia, and Disheveled (Dsh) and Frizzled (Fz) stayed in the front. However, the fine tuning process was unknown and her assertions were that hydrodynamic forces such as fluid flow or airflow may impart some signaling cues towards global PCP localizations. An experiment of applying phasic shear stress onto cerebral cultures with motile cilia revealed that Vangl1 expression aligned with the direction of fluid flow.[85]

Vladar's initial findings for the KRB experiment revealed that airway cells do change shape under continuous shear compared to intermittent shear (control examples). Ciliated cells appeared to turn along with the cells or they may slough off giving sparse regions compared to control cultures. Ciliogenesis took weeks to develop in an airway epithelial model. The short-term experiments of temporal entrained mucus transport went against research that showed ciliated cells could not turn and change direction in the rabbit trachea model.[55] The current hypothesis for the possibility of short-term entrainment was that some cilia stood together as they beat along direction of fluid flow currents within the channel and that other cilia sloughed off or disappeared during remodeling of the tissue.

Byproducts from PFC Perfusion

Figure 2.21. Interesting byproducts from PFC perfusion experiment

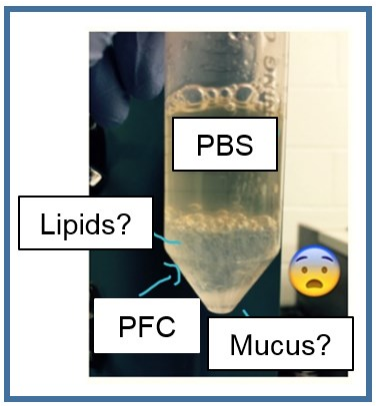

An example picture of byproducts procured from a PFC perfusion experiment. There were two distinct layers that separated PBS and PFC from each other. Interestingly, mucus, protein, or cell debris accumulated in the hydrophobic PFC phase than the PBS phase.

A perfusion experiment with PFC was carried out by UPP perfusion system; however, the results were inconclusive due to mucus plugs, which developed during the experiment. This outcome was the result of two properties: 1) airway cells produced mucus in response to shear stress owing to increase in ASL height[53,72], and 2) PFC was immiscible in water[65] including mucus. Thus, a continual perfusion of PFC boded well for overproduction of mucus (about 500μL/day), plugged the chamber channel (about 150 μm). Interestingly, the mucus produced by the cultures had an opaque white phase transition compared to control cultures which did not have PFC and had a clear film of mucus. The mucin polymers within mucus may have formed micelles such that hydrophobic domains interacted with the hydrophobic PFC solvent (verbal discussion with C.W. Davis). Future experimental analyses with mass spectrometry or dynamic light scattering techniques will help in determining whether the micelle hypothesis was valid.

CHAPTER 3: GAS-LIQUID TRANSPORT

Cilia- and cough-mediated clearances of mucus are the primary mechanisms to remove mucus from the lungs. However, a third mechanism of mucus clearance, cilia-independent two-phase co-current flow or “gas-liquid transport ”(GLT), has been proposed to occur as a result of the entrainment of the mucus layer due to airflow shear forces during tidal breathing. One of the first experiments that demonstrated the existence of GLT was in a mouse model lacking functional cilia, where mucus clearance persisted in the absence of both cilia beating and coughing (Figure 3.1A).[86] The overarching goal of this project was to investigate the relationship between GLT associated airflow rates, mucus concentration and mucus film height, which could not be controlled in the *in vivo* models. An *in vitro* approach was developed to help elucidate the dynamics of this gas-liquid transport (GLT) effect on well-differentiated human bronchial epithelial (HBE) cells.

This system simulated a deep exhalation that lasted for a few seconds on airway epithelial cells. A range of airflow rates known to occur during peak expiratory phase of tidal wave breathing was investigated over a range of mucus concentrations. The tested airflow rates were shown to be physiologically relevant. According to a Poiseuille viscous pressure drop mathematical model developed by Schroter, RC. *et al*., the linear air velocities used in GLT experiment of rest (1 m/s) and exercise (5 m/s) represented velocities that are associated with 4th and 10th generation of tracheobronchial tree.[87]

Dr. Adrian Kendrick predicted that these airflow rates likely represented velocities in the 6th generation of bronchial tree for both rest and exercise (Figure 3.1B).[88]

To understand the dynamics of GLT, a system was created to deliver laminar, humid airflow across the surface of human bronchial epithelial (HBE) cultures. After full differentiation of HBE cultures, the mucus concentration *in situ* from cultures was conditioned to a different mucus concentration. In these studies, three conditions of mucosal hydration represented a variety of clearance models between health and disease: 1) well-hydrated, normal mucus, 2) moderately dehydrated mucus representing mild CF-like mucus, and 3) *in situ* mucus, exhibiting high dehydration, a mimic of severe CF disease.[24] HBE cells were cultured on Snapwell substrates such that the cells were not surrounded by walls (see Figure 2.2) and transferred to a custom-designed macrofluidic chamber for perfusion with humidified air (Figure 3.2A).

Figure 3.1. *In vivo* GLT and Ventilation Map

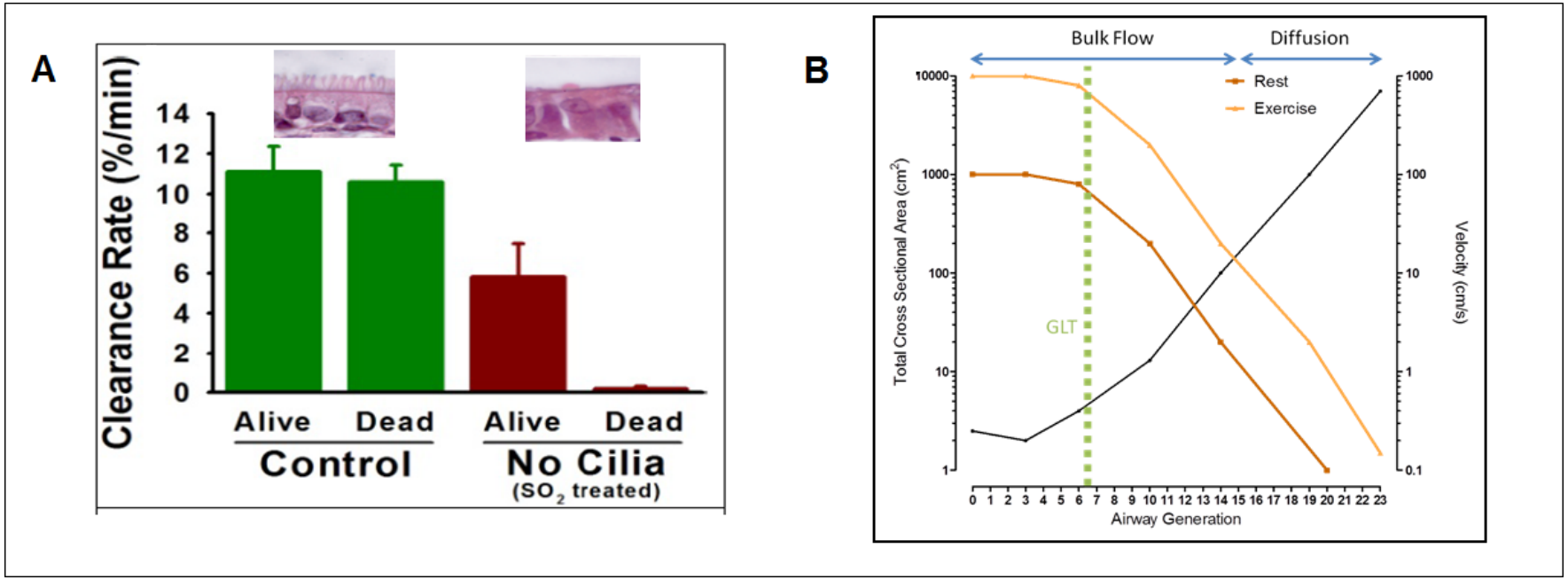

A) Radiotracer particle clearance *in vivo* animal model. Control had intact airways with cilia vs. experimental animal models were treated with sulfur dioxide to denude cilia from epithelium. B) Reproduced figure to show that GLT *in vitro* experiment may provide insight about airflow dynamics on airway cultures between the 6th and 7th airway generation for Rest and Exercise -associated flow rates.[88]

Experimental Methods

Labeling Mucus

To monitor mucus transport we aerosolized each culture with less than one microliter volume of fluorescent microspheres (diameter one micron) onto each culture. The mucus concentration of each culture was evaluated from a wet-to-dry ratio.[24] several metrics were measured throughout the mucus film thickness derived from our gas-liquid transport system model including: a) airflow clearance rate, b) overall net displacement of mucus due to airflow, c) percent recovery that represented the loss due to elastic recoil forces, and d) effective clearance direction.

Chamber and System Design

The chamber that housed the cultures during the gas liquid transport experiment had several features that allow for the following:

- modularity in creating new designs for different air flow patterns
- fluorescent particle imaging
- maintenance of air liquid interface
- a leak-proof chamber made of PDMS covalently bonded on to a glass coverslip by plasma treatment

To accommodate the majority of the cells on the Snapwell membrane, the chamber was designed to have a channel that was approximately 0.7 mm in height, 20 mm in length and a width of approximately 10 mm. The PDMS mold was injection molded into a custom made aluminum master at 1:10 ratio as per the manufacturer's manual (Corning, Sylgard™184). The gas liquid transport system was configured to produce low airflow rates related to breathing through the macro-fluidic chamber (see Figure

3.2A). The past observations demonstrated that HBE cultures did not tolerate large negative pressures; thus a solenoid opened briefly for a set duration during the capture sequence of the microscope. A vacuum pump with an inline flow meter (TSI) and a needle valve adjusted the flow rate from 0.1 to 3 L/min. On the other side, the PDMS chamber was placed in a heated chamber (Tokai Hit) that both humidity and regulated temperature for the objective and sample (Figure 3.2B). The GLT metrics were derived from 15-second videos at 60 frames per second (fps), acquired with Flea3 camera and controlled from custom MATLAB script code (Figure 3.2C). The vacuum/air pump operated on a separate table from the microscope to lessen any interference from vibrations.

Figure 3.2. Gas-Liquid Transport Experiment

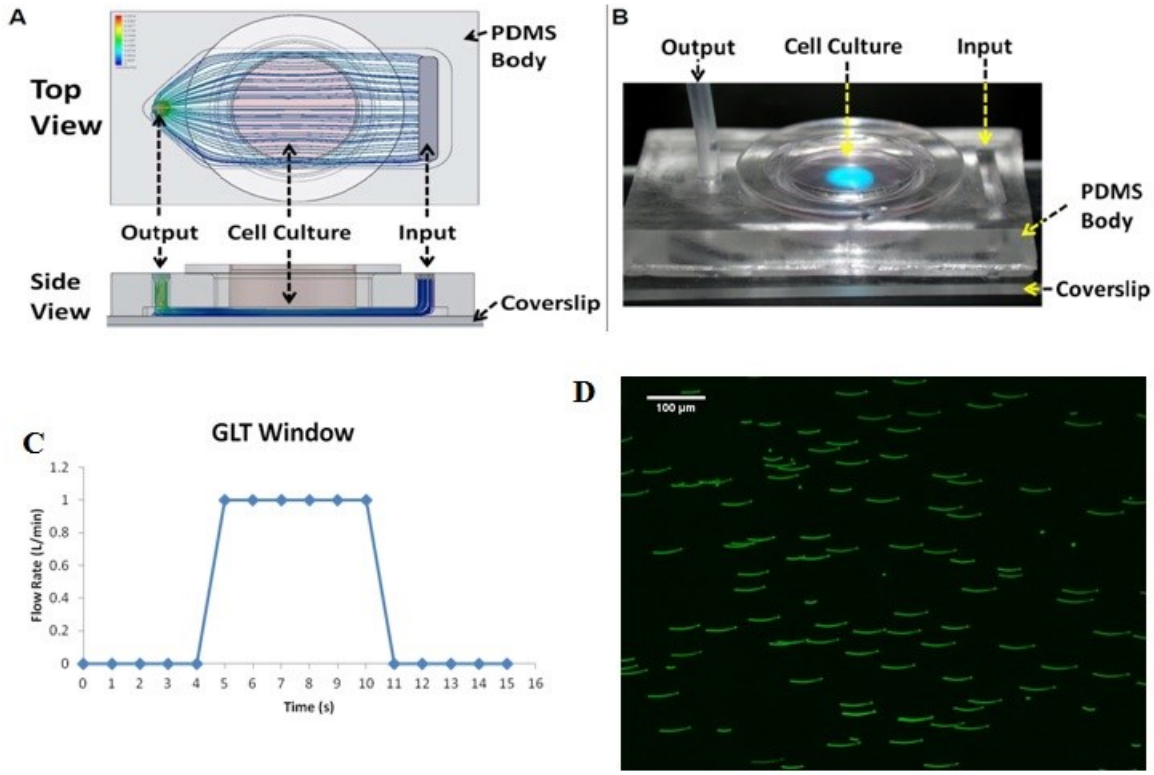

A) Computational Fluid Dynamic model showed laminar perfusion of air across culture. PDMS body dimensions are 20 x 40 mm. B) The PDMS chamber was covalently bonded to glass for a leak proof chamber. C) Example tracing showed flow rate across culture vs. time. D) Clearance rate was evaluated by particle tracking fluorescent tracers during video (3% mucus solids concentration, 5 second time-lapse). These streaks showed overall entrainment by airflow during GLT window.

Culturing

Cells for these studies were provided by the Tissue Core Facility at the CF Center. They were seeded on six-well Snapwell culture plates at a density of about 300,000 cells per well. The airway epithelial cultures in this experiment were from several codes and fed three times a week with Air liquid interface (ALI) media for four weeks at 37.5 °C, 95% humidity and 5% CO_2. Studies were initiated after four weeks, when the culture reached maturity with sufficient cilia and accumulated mucus.

Conditioning Mucus for GLT experiment.

Generating cultures with specific mucus solids in a specific range was challenging. According to Dr. LiHeng Cai's studies of mucus solids in Transwell cultures described in his dissertation, mucus solids increased within over a period of several weeks to reach a steady state of 15% mucus solids if cultures were unwashed (Figure 3.3).[89] Typical unconditioned cultures from an incubator maintained at 95% RH, 37.5 °C and 5% CO_2 yielded mucus solids between 8 and 20%. Airway diseases such as Cystic Fibrosis are characterized by having "dehydrated" mucus with mucus solids several times higher than normal mucus (2 % solids).[90]

Figure 3.3. Mucus Accumulation in Transwell HBE Cultures

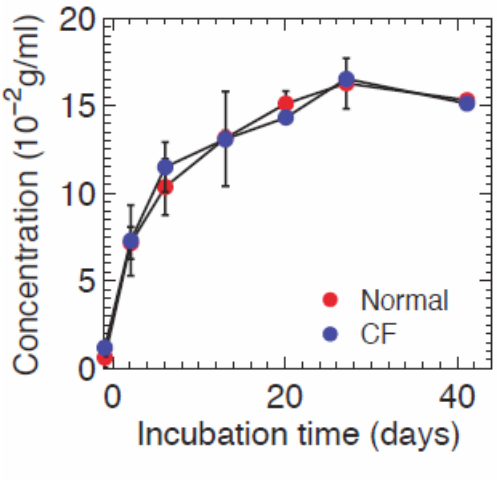

Dependence of incubation time on mucus concentration. Figure kindly provided by Dr. Liheng Cai and Dr. Brian Button.

By knowing the dependence of incubation time on mucus concentration, several methods were explored to hone in on specific mucus concentration ranges to test in the GLT system.

Several ways that adjusted mucus solids in HBE culture system model:

1. Add a known bolus, observe solids and volume absorption curves and predict a time where mucus solids are within a certain range.
2. Lavage off mucus and spin concentrate it to known percent solids and reapply to cell surface.
3. Add an osmotic gradient across epithelia such as adding dextran in basolateral media so that water may be transported to or from mucus.[91]

The first option was evaluated as shown in Figure 3.4, in which a known quantity of PBS was added to mucus layer, and the reabsorption of fluid and mucus solids were measured over time. The main idea here was to swell mucus to a certain mucus solids range and perform GLT during that period.

Figure 3.4. Prediction of Mucus Solids

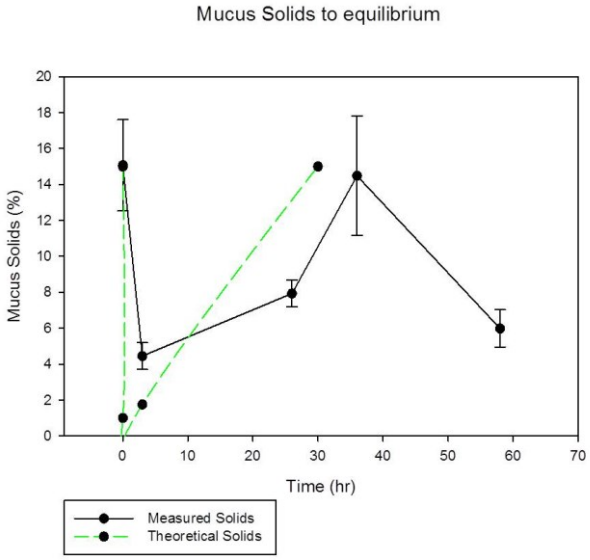

Solid black line indicates mucus solids (-0.9% salt content of PBS) by mesh integration method. Green dotted line shows theoretical mucus solids under assumption that there is 1 µL of mucus prior to bolus addition. The last measured solids at about 60 hours showed that the technique reproduced similar results as the first hour within a margin of error of 1% mucus solids. N = 1 patient code, n= 3 replicates.

Option 1 did not work very well and the resorption rates differed between replicates and different patient codes (not shown, 3 patient codes). Next, option 2 gave consistent mucus concentration results from spin concentrating lavaged or aspirated

samples of mucus. After a 20 minute spin cycle at 5000 x g of a 5 mL lavaged sample, the spin column yielded a gradient of mucus samples ranging from 2% to about 11% mucus solids depending on the code type. A protease inhibitor cocktail (cOmplete Mini EDTA-free, Roche Pharmaceuticals) was added at 0.1x concentration to prevent cleavage of mucins from proteases in the sample. For a GLT experiment, a known volume was added to the culture such that the height of the mucus film is kept relatively constant, which was a variable in the initial experiments. Samples were frozen at -20°C and thawed at the time of an experiment. A freeze-thaw cycle did offset the mucus solids metric by as little as 0.2% and as much as 1 %, which was within the measurement error. This technique yielded repeatable results so option 3 was not explored although it was previously published to control mucus concentration.[91]

Duplicate cultures were selected for three conditions: unconditioned (dehydrated) (>8% mucus solids), moderately-hydrated (3-6% mucus solids), and well-hydrated (<2% mucus solids). A day prior to the experiment, a sterile, damp cellulose mesh was placed on each culture and allowed to incubate overnight for measuring mucus solids as shown in Figure 3.5.

Figure 3.5. Incubated Cellulose Mesh

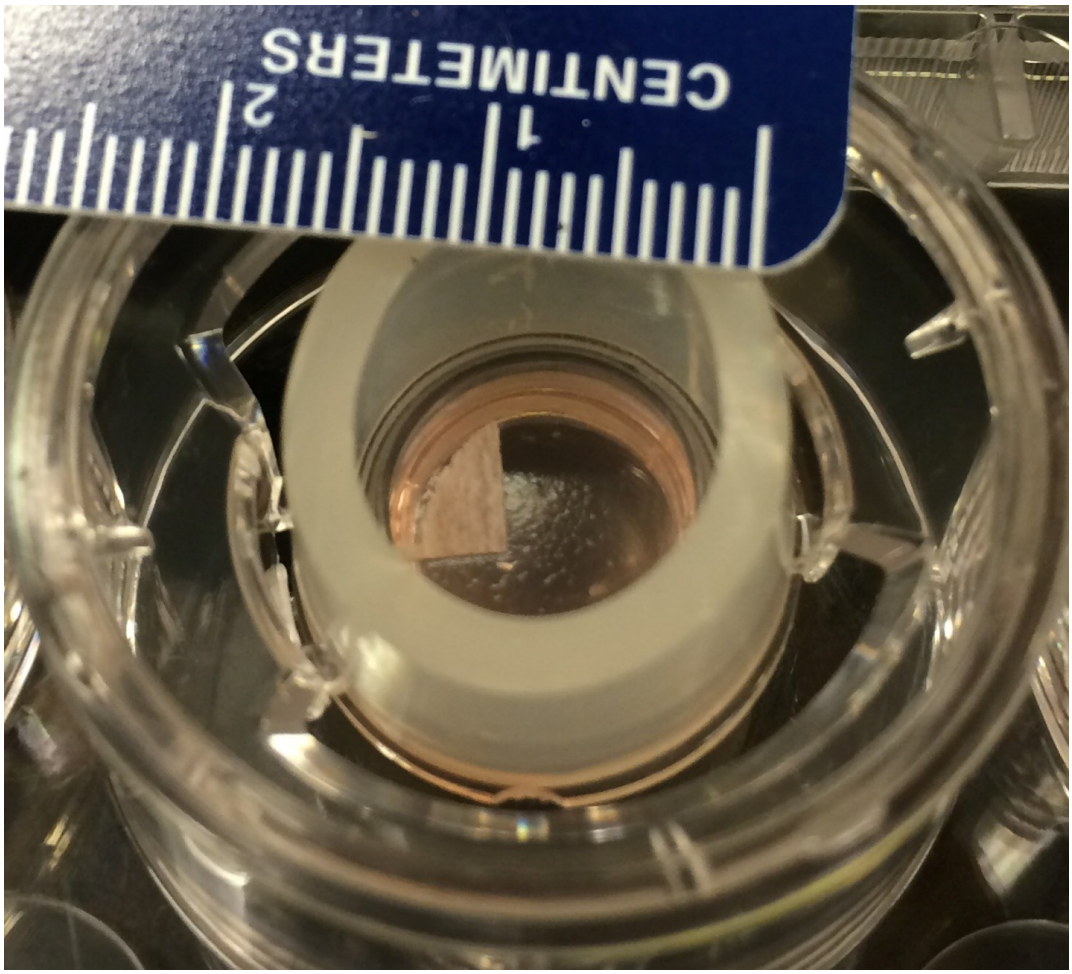

Here, an inverted culture was pre-incubated with a cellulose mesh on top to soak up mucus overnight to perform wet to dry analysis of mucus solids.

Because mucus concentrations varied between patient cultures, studies were designed such that a GLT and mucus solids measurements were derived from a single replicate culture. Normally, cultures were grown in a dehydrated condition (i.e. >12% solids) so these were used as unconditioned, "dehydrated" state. Cultures were then re-hydrated to a very dilute state by a quick bolus of PBS (20 µl) and aspirated quickly to leave approximately one microliter of volume on the apical surface. After the mucus was conditioned, a wet weight of the mucus was derived using the aforementioned

technique. Yellow-green carboxylated, fluorescent polystyrene beads in PBS (0.0004% v/v) were aerosolized (<1 microliter) on to the cultures prior to running GLT sequence.

GLT Pulse Sequence

Each culture was sheared by a range of volumetric flow rates: 0 (no flow control), 0.2, 0.5, 1, 2, and 3 liters of humidified (80% RH) air per minute (Lpm) (see Table 8.1 for more details). At each flow rate condition, videos were recorded at a specific z-height (4x or 10x Plan Fluor, Nikon Ti-Eclipse, Flea3 camera, MATLAB Image Acquisition). The rationale here was to derive mucus shear rate (mean velocity/film height) due to airflow, to empirically calculate the shear stress forces evoked across the epithelia, and to relate them to tidal wave breathing shear forces.[64]

Analyses. GLT clearance rates were derived by analyzing bead trajectories in recorded videos from Computer Integrated Systems for Microscopy and Manipulation's (CISMM) Video Spot Tracker (http://cismm.cs.unc.edu/downloads/). Data analyses were performed using custom MATLAB script code. The transport rates of the mucus were derived by linear regression models. The trajectories were also evaluated by vector algebra to account for assessing any pre-pulse trajectories due to endogenous cilia transport of the particles or drift (see pg. 121). In Figure 3.6, the particle did not travel in parallel with airflow direction likely due to boundary effects. The analysis reported a percentage of the particles that moved along direction of airflow within a range (120 to 240 degrees) since boundary effects dominated in some regions on the culture due to mucus plaques, edge effects or uneven mucus layer.

Figure 3.6. Airflow-Mediated Transport Vectors

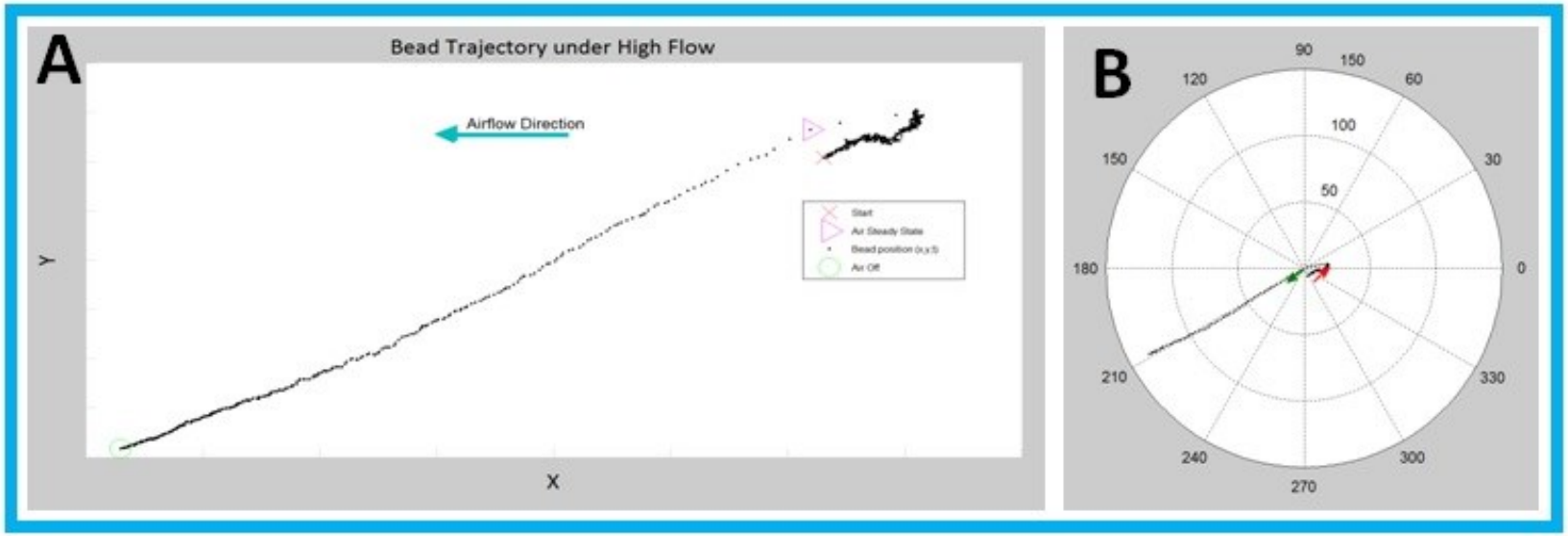

A) Example of time-lapse bead trajectory in relation to airflow direction. B) Polar (r, ɵ) plot of trajectory. Red arrow represented initial trajectory, and green arrow represents final trajectory. The origin of the polar plot was shifted from the starting position of the bead to the point at which the bead transport had constant velocity due to air pulse (purple triangle).

Gas-liquid Transport Experiment

Based on initial preliminary findings, we observed variability in GLT near the mucus/air boundary (Figure 3.7B) and near mucus/PCL layer boundary (Figure 3.7C). Our GLT flow rates are as follows: no air flow, middle range (1.1 m/s average linear air velocity) and high range (5.7 m/s average linear air velocity).

Figure 3.7. GLT Experiment

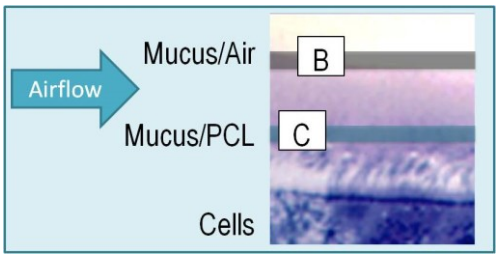

This image was adapted from Button, B. *et al.*, Science (2012). The different interfaces within the mucus layer were examined in GLT studies.

Single Breath.

A number of "test tube" models have been performed to show airflow-mediated transport to be beneficial to clearance of mucus and to be dependent upon mucus film height.[92,93] However, these studies did not show the relationship of endogenous mucus concentration with respect to GLT and show slip velocities along mucus and periciliary layer (PCL) interface. Airflow across the epithelial layer induced a plug flow of mucus, which meant that each layer of mucus was entrained by the air including the mucus-PCL layer (Figure 3.7C). This plug flow model demonstrated that the mucus-PCL layer was in fact a slip layer with non-zero mucus clearance velocities. The GLT rates were also dependent upon disease state measured as mucus concentration. In “No Breath” or control videos, a brief video was taken which showed muco-ciliary clearance (MCC) in poorly ciliated areas where the average velocity was about 1μm/sec and these areas

showed about 40 microns of net displacement (not shown). GLT improved mucus clearance in areas that were poorly-ciliated (“No Breath”) by 0.5 log-fold with rest rates and a log fold with exercise rates at the top mucus-air interface (Figure 3.7B, lower right panel). This data matched with the *in vivo* data that GLT cleared mucus in the absence of cilia or in poorly ciliated areas and that GLT rates were a small fraction of MCC rates which were about 60~100 μm/sec for healthy state. Furthermore, MCC rates dropped to 1 μm/sec in the case of CF severe states whereas it was 7 times higher with rest and exercise rates. Health and mild CF samples GLT clearance improved with increasing airflow rates by about 20 to 30 microns per second; however samples representing severe CF disease did not improve linearly with increasing rates used in GLT experiment.

Figure 3.8. Plug Flow Model.

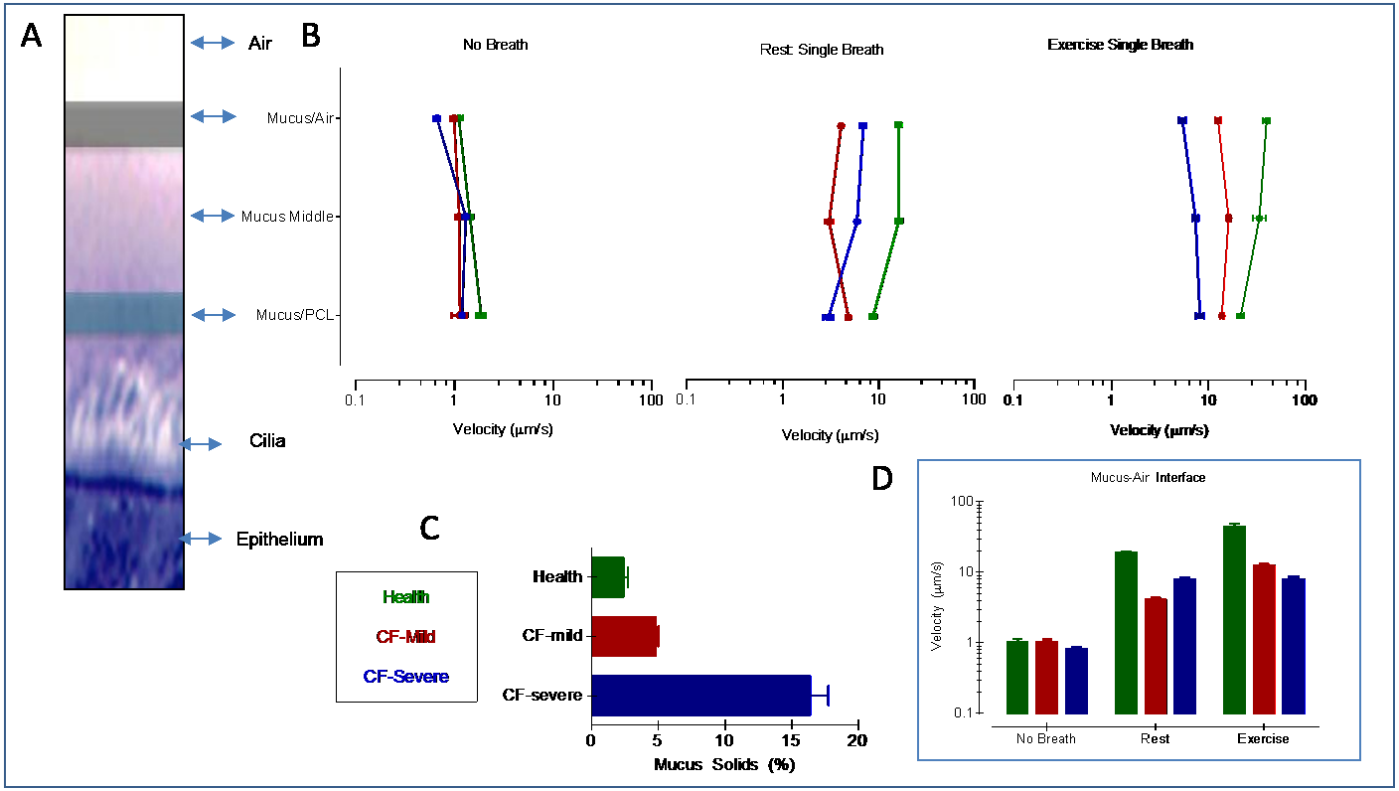

A) Mucus clearance was evaluated at different interfaces within the airway surface liquid: Mucus-Air, Mucus-middle and Mucus-PCL layers. B) A semi-log velocity profile across the mucus height at different z-stack height on epi-fluorescent microscope (standard error of mean, N=3 patient codes, n=6 replicates). The clearance rates were derived by linear regression models of particle tracer tracking data and by vector algebra to account for initial conditions of mucus transport prior to airflow. C) Legend and Mucus solids results from wet-to-dry mesh, D) Comparison of velocities at mucus/air interface alone from panel A.

61

Multiple Breaths.

The idea here was to explore the yielding property of mucus at different mucus concentrations.[94,95] Optimal GLT clearance rate was found at the mucus/air interface according to Figure 3.8D. The GLT pulse window lasted for 200 milliseconds and the interval between pulses lasted for 30 seconds. Mucus solids in health was 1.8 % ± 0.8 and in disease was 4.9 % ± 2 in the range of mild CF. The effect of multiple breaths on mucus clearance was predicted to have three different curves: a) "ideal" or no yielding or increase in GLT regardless of number of breaths, b) "yielding" curve, which showed an exponential growth in GLT after each breath, and c) "hardening" curve, which depicted the effects of dehydration with decreased GLT after each successive breath (Figure 3.9A).

GLT at low flow rates remained consistent and constant over time using this pulse train which suits the “ideal” hypothesis (Figure 3.9B). However, GLT rates at exercise provided enough shear force to yield mucus with a few pulses and then GLT rates become steady state after 7^{th} pulse (Figure 3.9C). Additionally, a minimum threshold of 5 m/s was needed to increase GLT within the first few pulses to reach a plateau and that mucus at low concentrations yielded exponentially for a very short period of time. After this yield stress was achieved, GLT reached a constant speed of 125 μm/s regardless of number of breaths. For the disease state at 5 m/s, GLT progressively decreased very slightly with each consecutive pulse, which likely meant that the mucus did not yield regardless of number of breaths with an interval of 30 seconds.

Figure 3.9. Multi-Breath Model

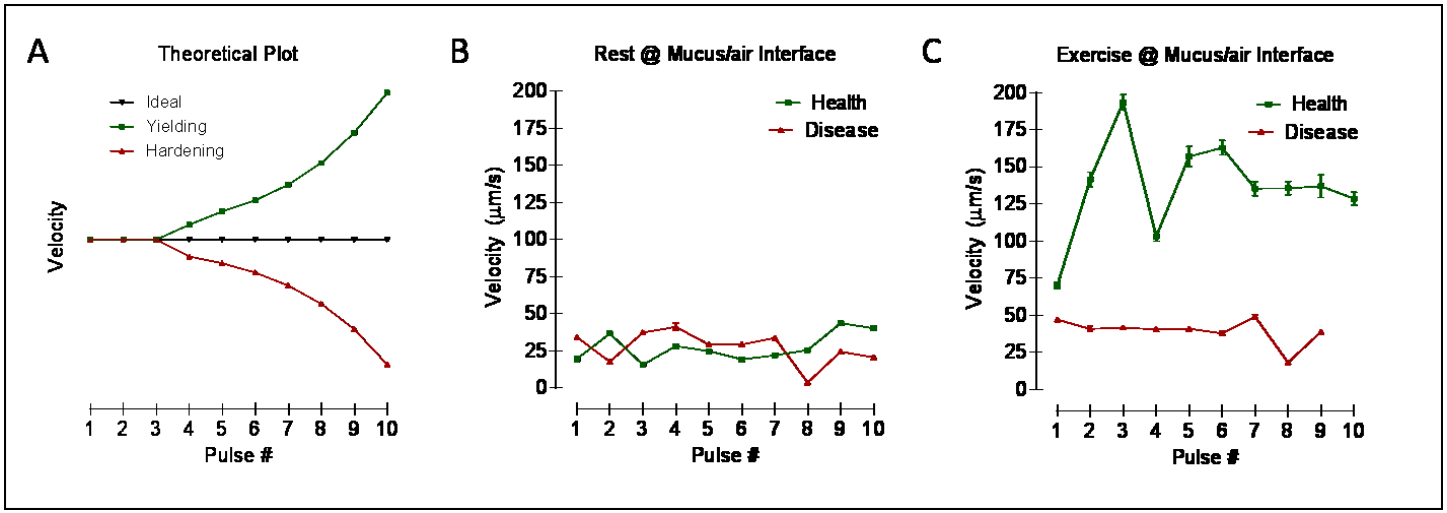

A) Theoretical plot detailed possible GLT rates with multiple pulse trains: ideal- very consistent GLT rates, yielding – GLT rates increased exponentially and hardening – GLT rates faltered exponentially due to viscoelastic properties of mucus. B) Evaluation of GLT in 200 ms time window per pulse with 30 second period of rest between pulses. Rest rate- linear air velocity of 1.1 m/s. n = 3 replicates. C) Similar to B, exercise flow rate was 5.5 m/s with n = 3 replicates for each condition. Error bars were standard error of mean. Mucus solids were tabulated before and after the experiment, and averaged for each condition. Videos were acquired by Flea3 (PointGrey, Inc) in MATLAB, 1 second video at 120 fps, with a rest time of 30s between each acquisition.

Interval between breaths.

The idea here was to explore whether GLT improves if the period between consecutive air breaths shortens (see Figure 3.10). Highly viscoelastic mucus gels have been hypothesized to take approximately 30 to 60 seconds to relax after being stressed (verbal communication with Dr. Michael Rubenstein). The control was to use 30 second interval with a flow rate of 5 m/s average linear air velocity. Mucus solids for health were 3 ± 0.5 % solids and for disease 4.6 ± 0.1 % solids. Increasing inter-breath period greatly improved clearance for both health and disease at very high airflow rates like that in exercise within ten breaths. Interestingly, the 15-second period improved GLT clearance in health by as much as four times; a 1 second period improved GLT rate of disease sample after the 10^{th} breath by as much as 3.5 times the initial velocity. After subsequent breaths, the viscoelastic properties have changed and thus become more flow-able at high rates and shorter inter breath periods were more beneficial for greater mucus solids. The improvement likely stemmed from breaking cohesive bonds at shorter intervals and not allowing mucus to relax to equilibrium as in the longer intervals (30 and 15 seconds).

Figure 3.10. Exercise: Varying Interval between Breaths.

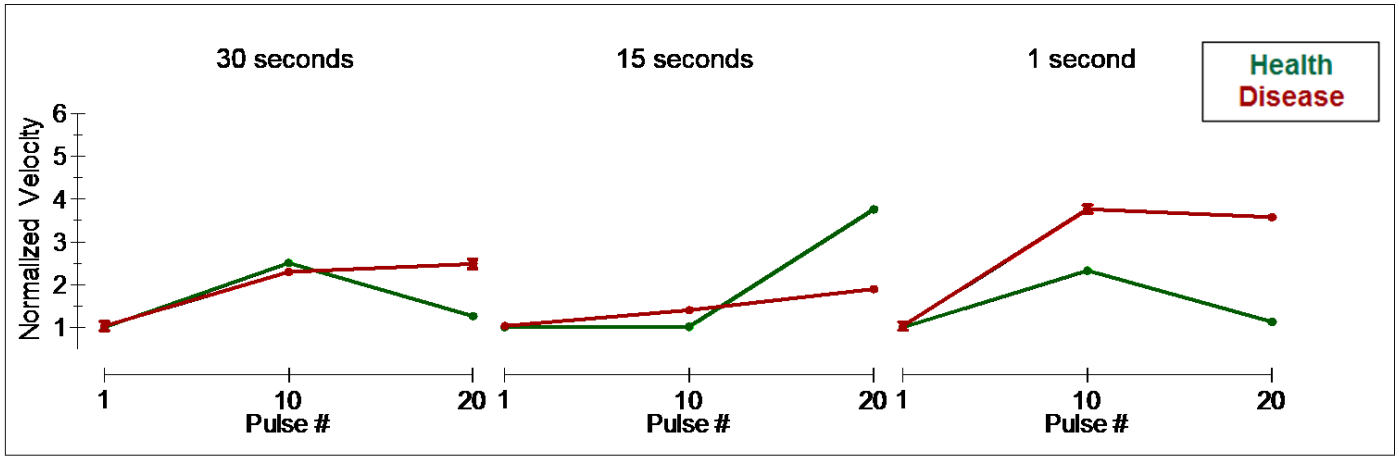

Velocities were normalized to the first GLT rate at pulse 1 in each experiment to show the effect of GLT over the course of pulses. Error bars were standard error of mean. N=2 codes, n = 2 replicates. A single culture was sheared by a train of 20 pulses with air pulse lasting for 200 ms and with a set interval between consecutive pulses. The set intervals were 30-, 15- and 1-second. Videos were acquired by Flea3 (PointGrey, Inc), 1 second video at 120 fps, with programmable rest time between each acquisition in MATLAB.

Conclusions

Like the previous observations with cilia-mediated clearance, these results demonstrated that airflow-mediated transport was very sensitive to an increase in mucus concentration. Here, GLT failed above 8 percent solids, as evidenced by a low velocity (<20 μm/s), displacement (10 to 20 μm) and mucus recoiling back fully. However, in cases of mild to moderate levels of dehydration, such as 4 to 6% solids, representing mild-CF-like mucus, the results indicated that GLT rates likely increased overall clearance velocity rates up 2 to 10 fold compared to MCC. It should be noted that the effectiveness of transport depended on mucus layer height.[96] In cases of increased hydration (<3% solids) GLT cleared mucus at even faster rates (60 μm/s) with high air flow rate (5.7 m/s) with greater displacement (>40 μm) than MCC. In conclusion, a system was engineered to explore rheological properties of mucus under humidified laminar airflow conditions associated with peak expiratory phase of tidal wave breathing on varying mucus concentrations. These *in vitro* studies validated the earlier animal studies and demonstrated that the airflow at levels below 25 m/s coughing velocities[97] could elicit clearance of mucus.

Future Directions

In the future, GLT mediated mucus transport will be studied in highly ciliated areas for comparison with this data set. The slopes of the velocity profiles will be used to determine the shear forces applied across epithelium and viscoelastic properties of mucus depending upon disease state. Also, velocities used in the experiment will be validated against clinical data and/or numerical models of ventilation maps during tidal

wave breathing.[51,98] The GLT experiment will help guide understanding of mucus clearance in the lung at different airway generations for use in mechanical ventilation techniques in the clinic.

Mucus Simulants on GLT. The main challenge that remained was attaining an optimal mucus concentration, which was complicated owing to cell line variability, absorption properties and environmental conditions. Mucus simulants such as agarose, dextran, sucrose and locust bean gum are being evaluated with GLT model. The gels have their own rheological properties that could be tuned to certain mucus-like solids ranges. Cultures are thoroughly washed off of mucus and these mucus simulants are applied on to the HBE cell surface or on to glass substrate. These findings will be compared with earlier studies of GLT clearance by Cheung, K. *et al*.[99]

Mucolytic Agents on GLT. Mucolytic agents will aid in breaking up mucus faster so that GLT rates can be improved for very thick and concentrated mucus. The effects of reducing agents such as n-acetylcysteine (NAC), and compounds from Parion Sciences, Inc. are being evaluated on GLT transport rates. The GLT model may be another way to screen the efficacy of these drugs on airway-mediated mucus clearance in a variety of peak expiratory flow rates.

CHAPTER 4: AN *IN VITRO* COUGH CLEARANCE MODEL

Cough clearance (CC) is known for its significance in diagnosing breathing ailments, in helping to clear blocked airways, and like cilia-mediated mucus clearance, in maintaining health. In patients with Cystic Fibrosis (CF), the high velocity airflow and shear forces associated with cough have helped to break away mucus from the lumen, and clear pathologic, concentrated and highly viscoelastic mucus. Many *in silico* computational models and "test tube" models have been utilized to determine how shear forces associated with high-speed airflow are able to effect a change in the biophysical properties of mucus or of other mucus-like fluids during cough clearance.[100–102] CC failed to be an effective mode of clearance in CF when compared to healthy controls in clinical studies (Figure 4.1A). To better understand why this occurred, an *in vitro* “cough machine” was developed to incorporate human bronchial epithelial (HBE) cell cultures with mucus over a range of mucus concentrations (spanning healthy to diseased states) to study effects of air flow rates on clearance of mucus.

In this study, a cough event was simulated by drawing humidified air across cultures. The cough clearance of mucus was analyzed by tracking contrast agents in mucus and by syncing a hi-speed camera during airflow pulses that lasted for a fraction of a second. These results correlated complex relationships between various mucus properties such as mucus concentration, oncotic pressure, and rheological properties. Our initial results showed that cough clearance *in vitro* was dependent upon mucus

concentration. There was efficacy of cough clearance for mild-CF like mucus concentrations where mucociliary clearance began to falter. However, cough clearance was significantly reduced when mucus concentration approached severe CF-like concentrations. Overall, this *in vitro* cough clearance model elucidated that cough clearance correlated with mucus solids concentration. Importantly, drug therapeutics that modify viscoelastic properties improved cough clearance rates for both mild and severe CF-like mucus concentrations.

Clinical Significance

In health, proper regulation of ions and water provided an environment for cilia to propel mucus at around 60 microns per second. In cystic fibrosis, the CFTR regulator that facilitated chloride was defective and thus salt and water were mainly absorbed which resulted in thick mucus plaques that hampered cilia-mediated flow. In health, it is twice as effective in clearing mucus compared to cilia-mediated clearance, as shown in Figure 4.1 in a clinical study with retention of radiotracer particles. In patients with Cystic Fibrosis (CF), the high velocity and shear forces associated with cough helped to break away mucus from the lumen, and clear pathologic, concentrated and highly viscoelastic mucus (Figure 4.1A, unpublished preliminary data from Dr. William Bennet, UNC EPA). Also, mucus concentration (solids) showed a linear relationship with the severity of disease as shown in mucus concentration data from sputum samples; mucus solids was used as a clinical biomarker.[90] In this study, a range of between 2~3% mucus solids was reported as health, 4~6% as mild-CF and above 8% solids as severe form of CF (Figure 4.1B, data provided by Dr. Brian Button).[9,90]

Figure 4.1. Clinical Significance of Cough Clearance

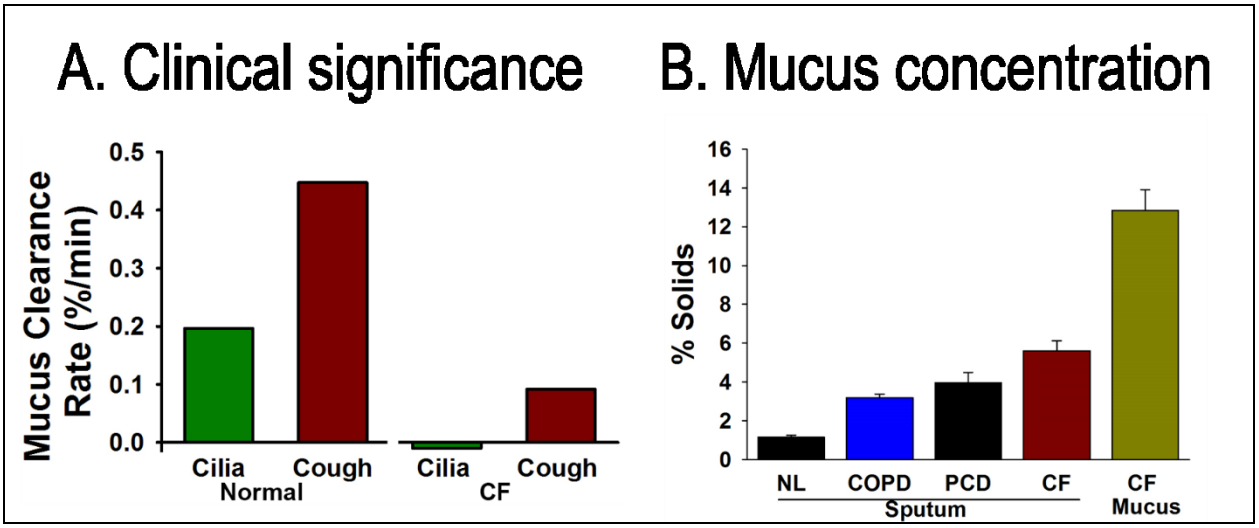

A) (Permission from Dr. William Bennet) Mucus clearance measured as percent of particles that moved away from a region in the lung per unit time. The data represented a set of healthy patients and patients with CF. A negative rate indicated recirculation of particles. B) Mucus concentration, a wet-to-dry ratio, were measured across disease spectrums from clearable mucus or sputum samples (mixed with saliva) and a mucus plug, a severe case of CF, within the smaller airways.

Cough Clearance model

After providing a foundation to study airflow mediated mucus transport, next clearance rates were investigated with airflow rates between 6 m/s to 30 m/s linear average velocities, which were related to peak cough velocities from PIV analysis of saliva droplets from the mouth during a cough.[97] This model was one of the first to experiment with air flow rates in the cough regime on the living airway epithelium.

The cough clearance experimental protocol was very similar to the gas-liquid transport system with minor adjustments. A larger capacity vacuum pump (Hi-Vac) pumped 11 to 12 liters per minute (Lpm) of air (open) and about 6 to 8 Lpm (closed). The sharp decrease in flow rate owed to the restriction of air through the macro-fluidic channel. The maximum pressure of a single pulse was equivalent to about 10 to 12 Pa

(1 mbar differential sensor, Digikey # 442-1011-ND) across the cultures at an average, linear velocity of 28 meters per second, which was comparable to a mid-range cough.[103] Additionally, a hi-speed camera (Fastcam SA 1.1, Dr. Paul Dayton and/or UX100, Motion Capture Technologies) captured mucus transport at about 1000 fps for several seconds. A poly-dispersed solution of graphite particles (0.005% v/v) was dispensed on top of the airway liquid surface to provide contrast in the video as well as a way to track mucus transport. The graphite particles acted similar to carboxylated polystyrene beads as they adhered to mucus and thus facilitating data acquisition and analysis. A z-stack analysis was not performed here because mucus ploughed over and mixed with layers of mucus at the higher velocities— this phenomenon made z-stack data interpretation difficult.

Figure 4.2. Cough Clearance Setup

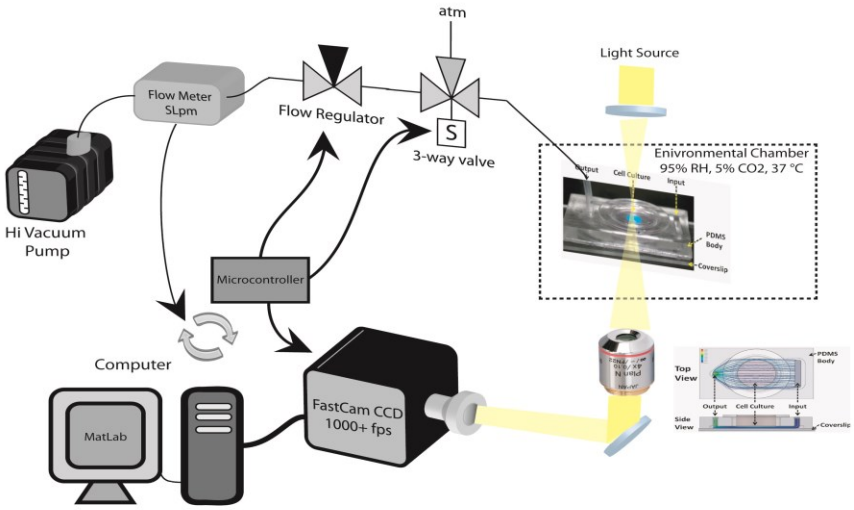

The cough clearance setup was very similar to the GLT setup. However, a higher volume vacuum pump was used for generating faster speeds of airflow. A faster camera was used to capture mucus traveling at 1000 frames per second. For the optics bright-field imaging was used instead of epi-fluorescence. Fluorescence was not preferred since background cells and debris interfered with analysis of mucus clearance due to

short pulse of air traveling at cough velocities. An Arduino microcontroller was used in conjunction with MATLAB to acquire video data and time the pulse of air.

In the supplemental video, CC.avi, of the cough clearance experiment, the dimensions of the field of view were 1 mm by 1 mm, the airflow rate was 13 m/s and the movement of graphite particles within mucus (about 3% mucus solids) lasted for a fraction of a second (0.2 s) to emulate the duration of a cough in the one second video (1000 fps, Fastcam SA 1.1). Interestingly, in the supplemental video, the movement of the graphite particles under cough velocities was not a single stream, and the flow had the characteristic of a stick-slip motion under high shear forces of air.[77,104,105] The ultimate goal of the *in vitro* cough clearance model was to elucidate cough clearance as a function of mucus solid concentration as seen in Figure 4.3. Also, in Figure 4.4, in a preliminary study, therapeutics were evaluated to improve cough clearance rates.

Figure 4.3. Airflow Mediated and Cilia-Mediated Mucus Transport

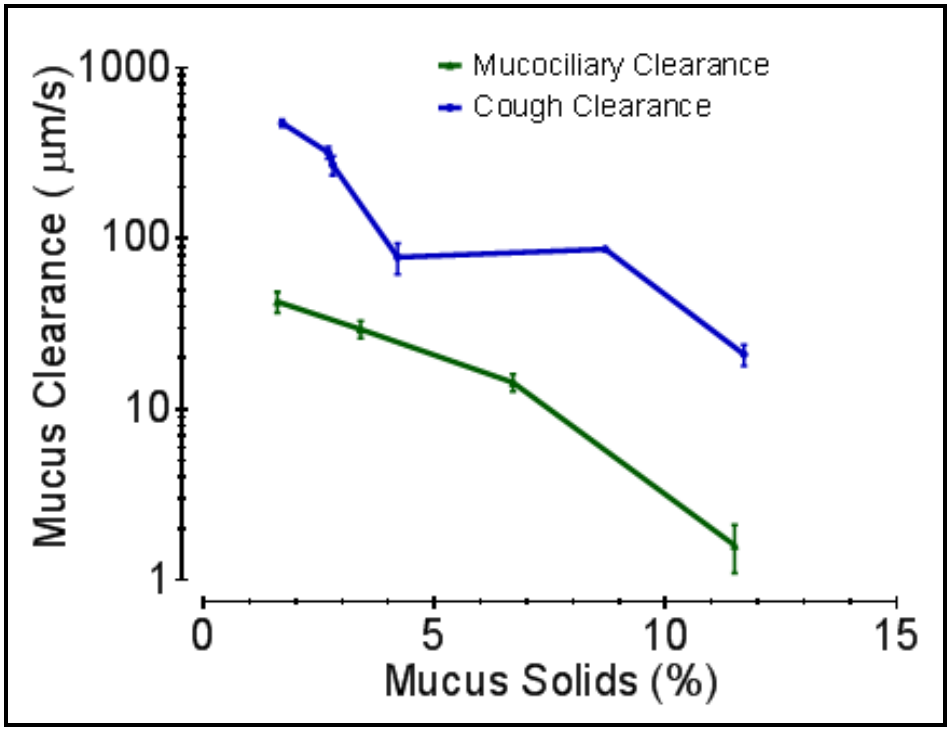

This figure showed a semi-log plot of the relationship of airflow-mediated clearance rates (GLT and CC) compared to mucociliary clearance rates across a wide spectrum of mucus solids. N = 3 patient codes, n = 2 replicates

Figure 4.4. Effect of Mucolytics on Cough Clearance

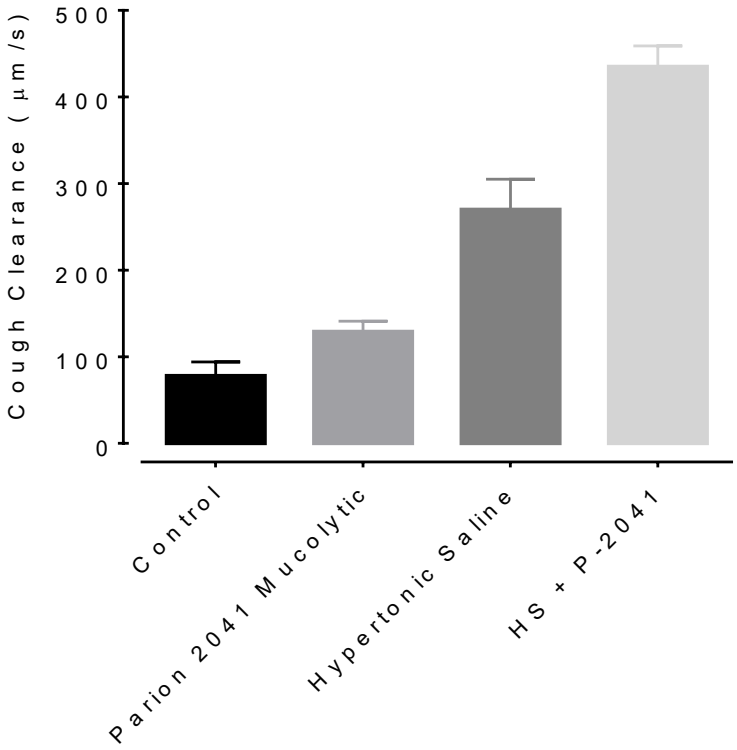

The efficacy of mucolytics with the cough clearance model yielded promising results. Cough clearance doubled with the addition of a mucolytic at 2 mM final concentration in comparison with control starting at 4.5 % mucus solids (80 microns per second +/- 16). An equivalent hydration protocol similar to using hypertonic saline yielded 2 % mucus solids and a CC of 270 microns per second +/- 35. The addition of the mucolytic along with the hydration protocol improved the clearance rate to 435 microns per second +/- 25. Overall, the addition of hydrators and mucolytics improved cough clearance of mild-CF like mucus. N = 1 patient code, n = 2 replicates

Discussion

This initial cough clearance model predicted that between 4% and 8% mucus solid concentration clearance rates between 600 and 900 µm/s were achieved which was a 10-fold increase in transport compared to mucociliary clearance in this range with a mucus film thickness of ~100 microns. These CC rates were comparable to previous studies using test tube models which quoted about 0.5 to 1.5 mm/s clearance rate with

a "mucus" film thickness of 1 mm.[100] Below 3% mucus solids, rates above 1000 μm/s were achieved at the mucus-air interface. These clearance rates were substantially greater by two log fold than mucociliary clearance rates within this range. Above 10% mucus solids, which represented CF-like mucus, cough clearance was over 90 μm/s while mucociliary clearance rates were negligible (1 to 10 μm/s) considering that the tracer particles measured 1 μm in diameter. Additionally, the adhesive properties of mucus affected cough clearance. Mucus had been documented to hold many adhesive bonds to ciliated cells which is integral to mucociliary clearance[18,24]. The video of a cough showed some evidence of breaking bonds within a short air pulse window of 200 milliseconds.

Conclusion

Overall, the *in vitro* cough clearance model elucidated that cough clearance decreased as mucus solids concentration increased as seen in the clinical assessment. Drug therapeutics that modified mucus properties improved cough clearance rates for both mild CF-like mucus concentrations. Together, this model-system provided an approach to understand the parameters mediating cough clearance in health and why it failed in disease. Additionally, this approach had the capability to identify novel drug targets, evaluate drug efficacy, and to test a variety of cough maneuvers used in the clinic setting.

Future Experiments

These findings can be improved by further validation of shear rates and stresses of known gels with documented rheological properties (i.e. Agarose, gelatin or alginate) by induced force with cough. Agarose is preferred since the viscoelastic properties are already available from Dr. David Hill and Dr. Brian Button.[50] Fluorescently tagged polymers can also be used to evaluate whether the mucins elongate and break in a cough event.

Cough Clearance and Shear Stress

The "stick and slip" motion under CC correlated with fracture toughness of mucus - the force necessary to break cohesive bonds of mucus and overcome friction of the PCL layer. Fracture toughness of mucus was measured by a peel adhesion machine engineered by Dr. Robert G. Dennis and Dr. Henry P. Goodell and technique developed by Dr. Brian Button. The wall shear stress may be calculated by experimental models of two-phase flow under turbulent conditions; however, the viscoelastic nature of mucus cannot be modeled with experimental parameters such as humidity and temperature. Thus, a novel method to bridge two techniques together is proposed to measure the shear forces imparted by air under cough velocities to move mucus at high velocities. Pictured in Figure 4.5, an average velocity of mucus clearance is derived from CC experiment, and then using the same velocity, an average friction force can be measured by dragging mucus across the culture using the peel machine (manuscript in preparation).

Figure 4.5. Measuring CC Stress Imparted on to Culture

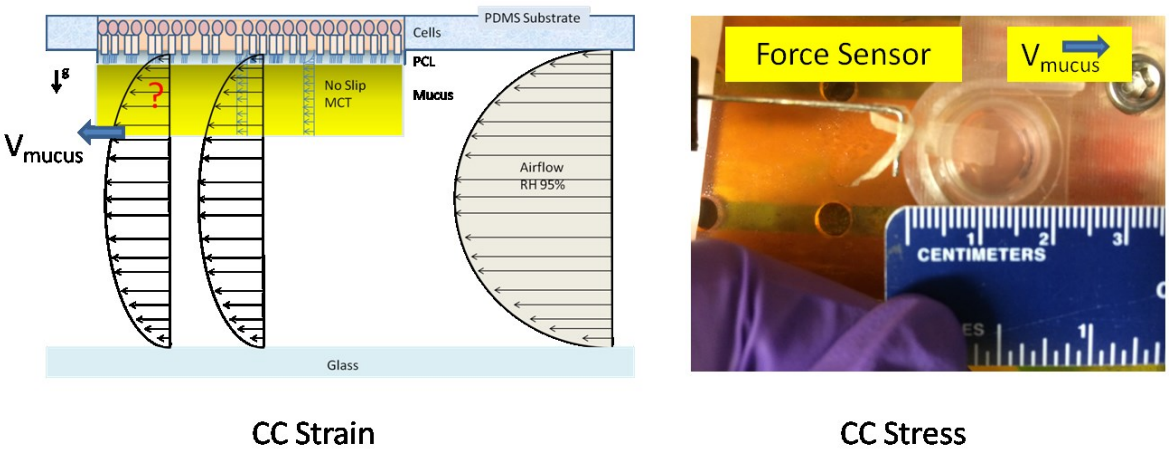

(Left) This pictorial depicts a CC pulse of air flowing through the chamber in the brief 0.2 s window. The average mucus velocities were gathered at the very top layer of the mucus film. (Right) The measurement of shear stress was the force acting on to the area of the mesh in contact with the mucus. The movement of the culture had a constant velocity by a 3D micrometer precision stage that matched the average cough clearance rate measured in the CC airflow experiment.

Cough Clearance and Mucus Plug Tearing

In health, the conductive airways naturally get plugged with mucus, and reopen by either breathing or by cough for proper ventilation.[94] In the case of CF, mucus is hypersecreted and likely hosts many pathogens that pose threats to the body.[106] Also, in CF, CC is inefficient at clearing mucus with high mucus concentration as shown previously. Studies on mucus plug rupture in smaller airways has shown that efficient clearance of the plug occurred if the stress was greater than the yield stress of mucus.[94] In these studies, the mucus acted as a Bingham fluid with shear-thinning properties under stresses associated with breathing.[94]

In this model (see Figure 4.6), mucus plug tearing or rupturing will be studied under cough velocities and high shear forces. The mucus will be adhered to a cellulose mesh substrate on two sides to emulate the surface interaction between mucus layer and the PCL.[24] Thus, mucus clearance is hypothesized to flow along the middle of the channel. The stress will be recorded with a pressure transducer before and after the mucus breaks apart in the middle of the channel. The viscous moduli will be determined by a rheometer. The strain will also be recorded by the clearance of mucus due to the cough. A Bingham number is a dimensionless number that shows the proportionality between yield stress and viscous stress.[107] Initially, different concentrations of mucus and sputum samples ranging from health to disease will be tested under cough velocities to estimate the Bingham number at each mucus concentration. Furthermore, once a protocol has been established, HBE cells will be incorporated in the model to test whether epithelial cells rupture along with the mucus under cough velocities.[94]

Figure 4.6. Concept for Cough Clearance and Mucus Plug Tearing

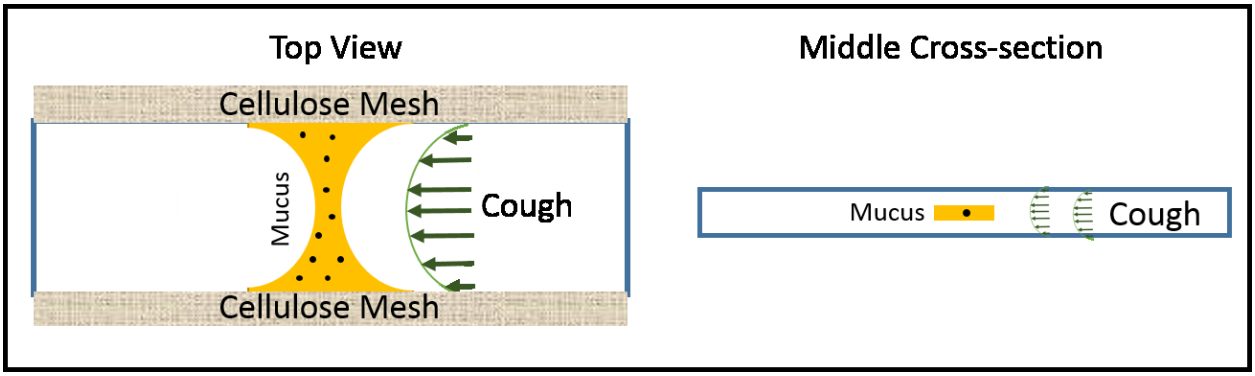

(Left) This cartoon shows a top-down view of a microfluidic channel with cellulose mesh substrates, which hold mucus as a plug in the channel. Black microspheres or graphite particles will be embedded to act as a surrogate to describe mucus clearance due to cough. (Right) A side view of the microfluidic channel shows that the mucus plug will likely have an air interface.

APPENDIX 1: PROTOCOLS AND SUPPLEMENTAL DATA

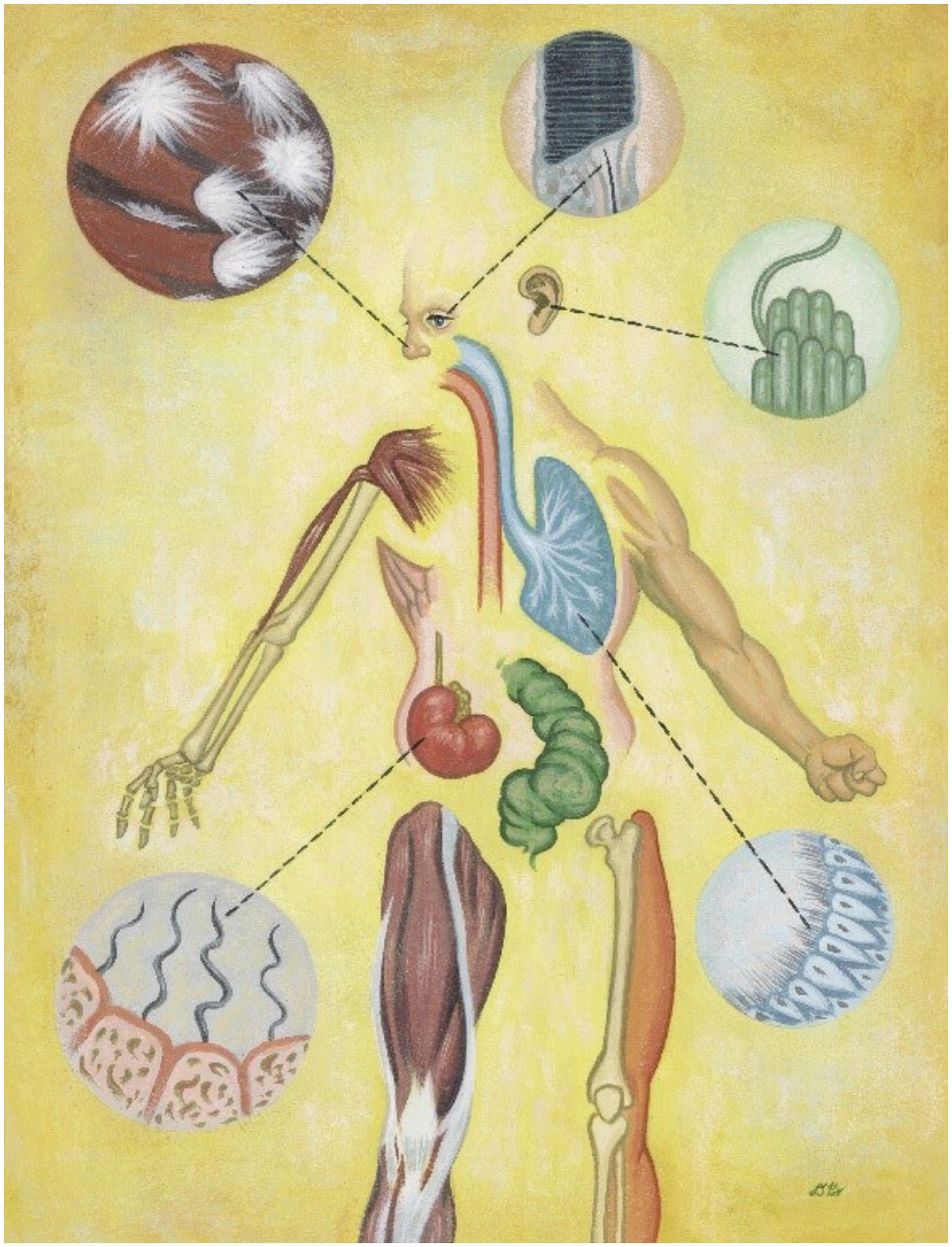

This artistic image portrays the different roles cilia play in the human anatomy. Adapted from *The Importance of Being Cilia* [16]

CHAPTER 5: CULTURING INVERTED AIRWAY EPITHELIAL CULTURES

Preparation of Silicone Rings

Make appropriate amount of silicone rings for the number of Snapwells to be utilized by cutting 0.25" lengths from PVC Tygon Tubing (McMaster Carr, #5554K82) from a PVC pipe cutter (Kobalt). Sterilize these links by treating them with ethanol in a tray under UV for 20 minutes. Air dry and attach each link to uncoated sterile Snapwell (Corning, #3801) by the following method:

1. Flip 6-well plate upside down so that the underside membrane is right-side up. Lift the bottom cover. This underside is the membrane upon which cells are seeded and grown.
2. with sterile hands, attach the link to the outer side of the Snapwell leaving a small hairline gap for later
3. Slide the Snapwell/link assembly away from the Snapwell support. Flip the assembly and slide it back in place. It may take some wiggling but the Snapwell should snap in to the support again. Then place the assembly back in to the tray and repeat steps 2 and 3 for the remaining Snapwells. There are several benefits to having a wall around the membrane; this wall keeps hydrostatic pressure in check. It supports a meniscus of fluid on the apical surface and prevents cells from drying out and it protects the membrane from damage.

Preparation of Snapwell coated Collagen supports

Once silicone walls are in place around the Snapwell membrane, flip the assembly right side up again and pipette 150 microliters of pre-prepared 1x collagen matrix in distilled water.[108] Place the plate on a rotator to evenly spread the collagen across the membrane for an additional six hours. Treat the plates under UV light for 30

minutes to crosslink collagen matrix. Aspirate any excess media and uncrosslinked monomers.

Preparation of Cell Culture Media Gel

The media will be supported by an agarose gel matrix mixed with cell culture media that is about 0.5% in concentration. A five percent agarose gel matrix is prepared by mixing 5 grams of low gelling temperature agarose (Sigma, A9045) in 100 mL sterile PBS and autoclaving the suspension using the liquid cycle. Autoclaving helps to reduce the chances of cross-contamination. Place the agarose in the fridge or keep the agarose at a working temperature of 45 °C. To reflow agarose, place the container in water and set to boil, once the agarose flows homogenously, place it in an oven at a working temperature of 45 °C. Agarose is an interesting gelling material as the gel is set by temperature so having a higher working temperature ensures that there is enough working time before it begins to gel. The agarose gel concentration used in this protocol is 0.5% which is a very low gel percentage and this allows cells easily absorb the media through the matrix. Prior to pipetting 0.5% BEGM/ABS media on to each culture insert, the media gel is prepared by the following method:

1. Pre-warm 45 mL of ALI media in the water bath at 37°C for 20 minutes
2. After a few minutes of heating the 5% agarose at 100°C, cool 5% agarose to 45 °C for 40 minutes
3. Pre-warm a Steri-Flip 0.22-µm filter for conical tubes to 45°C for 20 minutes
4. Bring all materials to the hood, using a 25-mL pipette, take up about 5.1 mL of 5% agarose, then take up the ALI in the pipette to thoroughly mix the gel and media together. After a few cycles, the AgALI mixture is ready to be sterile filtered. Use parafilm to seal the top and store in the water bath for up to 1 week.
5. For each inverted culture, 400 microliters of 0.5% AgALI is enough to last three to four days for nourishment.
6. Any antibiotic or antifungals must be added to the AgALI media only after filtration.

CHAPTER 6: PERFUSION PROTOCOLS

Syringe Pump Perfusion System

In the first iteration of the perfusion system, a closed loop syringe pump perfusion provided constant flow of fluid across cells for 30 minutes into a reservoir and refilled back for another 30 minutes to recycle shear fluid solution. This fluid flow system included an embedded microcontroller program that communicated to a Harvard Syringe Pump to dispense a set volume of fluid through the flow channel. Then the fluid was sterilized by an inline-ultraviolet lamp before being recycled back in to the original syringe. The fluid flow direction was controlled by a set of 24V solenoid pinch valves by adjusting the holding current by pulse-width modulation. A bubble trap was needed on the input side of the flow chamber as pinch valves are prone for making small bubbles in the tubes. A bubble within the channel occluded flow and affected shear invoked on to the cells. The disadvantage of this system was that it was very bulky, as the syringe mount and stand would take up majority of the space within the incubator. As a result, this system was not ideal for a high-throughput application. However, this syringe pump system showed promise as our initial results revealed that six hours was sufficient to re-train mucociliary transport in the direction of fluid flow. The main set-backs to this system were the following:

- Positive-pressure induced flow elicited more leaks around culture filters

- Normally closed solenoids would over-heat and fail in the incubator (i.e. humidity and additional heat)
- It was challenging to self-prime tubing after replacing syringes with new perfusate

Figure 6.1. Flow Diagram of Syringe Pump Perfusion System.

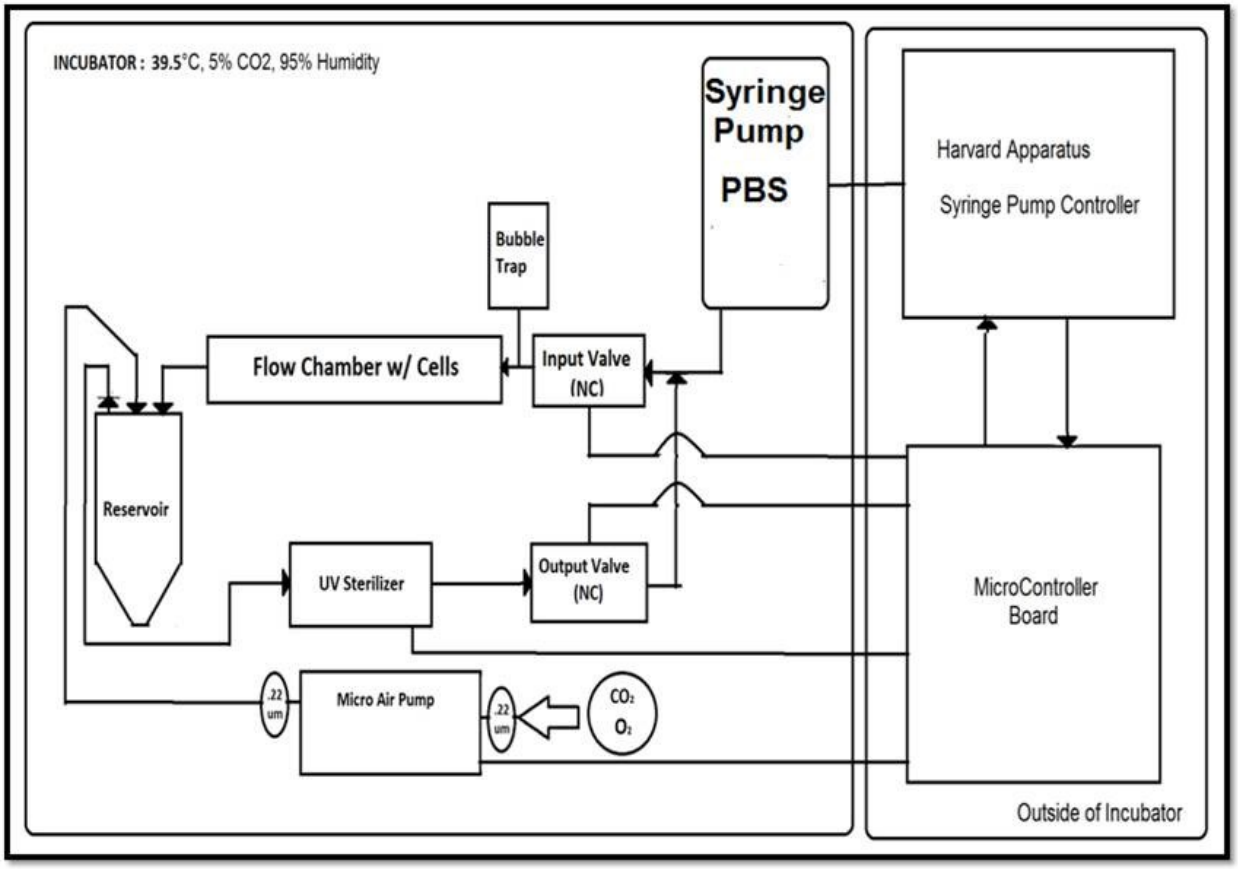

The addition of radial pre-load mechanisms was incorporated in the chamber which helped eliminate leaks around culture filters. This method was abandoned in favor of miniature (1 inch length) UPPs, which reduced the overall footprint of the perfusion system, sufficient to allow for high-throughput applications.

Syringe Pump Experimental Protocol

Materials. Phosphate buffered saline (1x) and perfluorocarbon were used in the initial studies of perfusion. Four inverted culture filters were selected from two different

codes for the experiment. Three culture filters were utilized in the perfusion experiment and a single culture filter was used as a non-sheared control for comparison.

Sterilization. The sterilization protocol was one of the many severe drawbacks to utilize this system in the laboratory setting due to a large number of components required in the system and the chance for infection with each component. While, great care was undertaken when sterilizing the system, the challenge was that the acrylic components of the system were incompatible with solvents such as 70% (v/v) ethanol. Ultraviolet sterilization was needed for the chamber and clear tubing. Pre-sterilization was needed before the components of the system were assembled in the laminar flow hood which includes dousing of ethanol where possible, air drying, and UV sterilization. An autoclavable steel pan was used to prevent any fluid spillage in the event of leak in the incubator. After pre-sterilization was complete and all the components are completely dried, the system is assembled under sterile conditions. Two syringe filters were needed, conical tubes are filled half way and 60-mL syringes are filled to the 45 mL mark with about 5 cc of dead space for trapping bubbles in the system.

Priming Sequence. The initial perfusion step of a completely assembled system posed technical difficulties, because fluid-filling of hydrophobic tubing with small rectangular slit channels create air pockets which had to be overcome to create uniform flow. Turning on the microcontroller program started infuse and refill sequence automatically after which the parameters of target volume and infusion rate were manipulated. The infusion and refill rate were entered in to the syringe pump controller. A set of blank Snapwells without cultures were used for priming before cells were introduced into the system, This step minimized the number of air pockets created in the

center of the flow channel and prevented laminar flow across cells downstream of the inlet. After 10 mL of shear fluid, namely perfluorocarbon (Fluorinert 3823, 3M), is perfused across the flow channel, the air pump oxygenates the fluid with the laminar flow hood air and the refill sequence commences and UV re-sterilizes the fluid. The UV sterilizer ensured that the shear fluid does not carry any infectious bacteria and fungus that may have escaped the pre-sterilization process.

Perfusion program. Once the cultures were in the system, the flow rate was changed to recommended 0.125 mL/min rate for a shear stress of 0.5 dyne/cm^2. The cell culture Snapwells with agarose based media (AgALI) were transferred to the system with 5 mL of shear fluid perfused. Subsequently, the program was temporarily stopped after several cycles. The connection tubing between the syringe and flow chamber are disconnected and protected by sterilized parafilm to reduce chance of contamination. Each component was transferred into the incubator, where it was reassembled utilizing proper sterile techniques and subsequently monitored for signs of leaks for several additional hours.

Maintenance. The agarose based media was highly recommended for use with perfusion system as this mode of feeding cultures not only prevents the chance of shear fluid from leaking through porous membranes (experiment observation). Under shearing conditions, the airway cells burned through the culture media, typically, 500 microliters of ALI media a day. Therefore, media was replenished daily using a pipette connected to a flask and vacuum. Additionally, the syringes had to be replaced on a daily basis as a consequence of the wearing of rubber plunger under constant strain and high temperature environment. Because the system was engineered to be utilized for an

entire month, it was necessary to ensure that the components were easy to disassemble and reassemble.

Ultrasonic Piezo Pump Perfusion

The final laminar fluid flow shear system replaced the syringe pump component with a set of small ultrasonic piezoelectric pumps (OEM pump) driven by PIC microcontroller unit (MCU) (18f1320) and a piezo controller. The MCU code provided the ability to drive an unlimited number of piezo pumps. Piezo pumps were advantageous to use because they could self-prime by themselves and be optimized by adjusting the back pressure and driving frequency. They pumped a maximum flow rate of 7 ml/min with a back pressure of 600 cm H_2O. Each piezo pump functioned as a syringe pump combined with a check valve in one small component. These piezo pumps actuated bulk fluid flow by acting in a pull-push method in one direction similar to heart valves. Each piezo pump was calibrated to 125 $\mu L*min^{-1}$ ± 1% by mass to deliver a wall shear stress of 0.5 $dyne*cm^{-2}$. This calibration also included the tolerances within each channel's geometry. Additionally, each channel now had a dedicated pump that could be adjusted during the course of the experiment. Differential pressure sensors were used to provide additional feedback towards monitoring and controlling fluid flow rate. The results showed promise with this method of perfusion and an interesting relationship between the duration of fluid flow and degree of entrainment.

UPP Experimental Protocol

Sterilization The sterilization protocol was one of the many severe drawbacks to utilize the laminar perfusion system in the laboratory setting due to the numerous

amounts of components required in the system and with every component there was a chance for contamination. The following table highlighted each component and method of sterilization:

Table 6.1. Ultrasonic Piezo Pump Perfusion Sterilization Methods

Component	Use	Sterilization Method
Piezo Pumps	Source for Unidirectional Oscillatory Flow	Isopropyl Alcohol
PTFE Tube Sleeving	Transfer Fluid	Autoclaving
Bubble Trap (PC)	Trap Bubbles during perfusion	Autoclaving
Fluid Reservoir (PC)	Store perfusate and provide oxygenation	Autoclaving
PDMS Chamber	Bioreactor to house cells	Ethylene Oxide
System Tray	Ease of maintenance	Autoclaving

Ultraviolet sterilization was needed for the chamber and clear tubing. Pre-sterilization was needed before the components of the system were put together in the laminar flow hood which included dousing of ethanol where possible, air drying and UV sterilization. An autoclavable steel pan was used in the event of leak in the incubator. All the other components could not be autoclaved. After pre-sterilization was complete and all the components were completely dried, the system was assembled in a laminar flow hood.

Pre-priming: The piezo pump system was initially primed manually by activating pumps and drawing in liquid downstream of chamber such that bubbles were removed from the system. The advantage of the piezo pumps were that they are inherently self-priming so the maintenance was very minimal in this system. The bubble traps also needed to be primed with fluid prior to start of system.

Perfusion Program: Each piezo pump was pre-calibrated to the channel geometry and tubing to flow at a rate necessary for 0.5 dyne*cm^{-2} shear stress by

monitoring weight change on a scale. A linear regression was derived from the graph to a set volumetric flow per unit time, in this case, 120.

Maintenance: Every other day, cells were fed with 0.5 % AgALI, gelled at room temperature, while a constant perfusion of fluid was kept in the flow hood. Notably, cell culture wells from a single condition could be removed temporarily for microscopy without disturbing other experiments. As needed, bubble traps were re-primed with fluid.

Figure 6.2. Ultrasonic Piezo Pump Setup

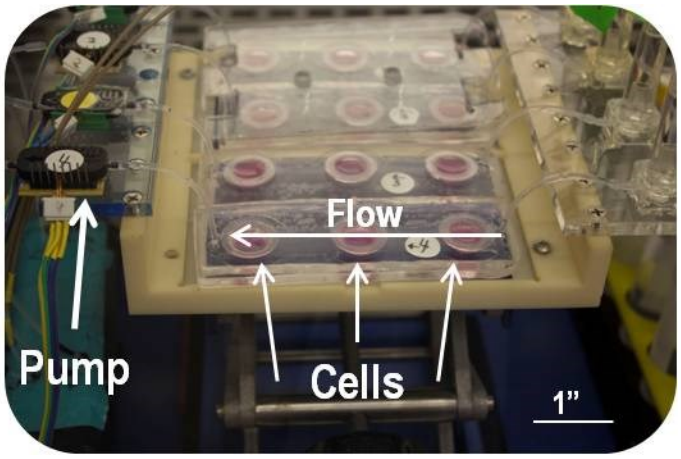

The system recycled fluid shear media in sterile manner in an incubator and kept physiologic conditions constant (5% CO_2, 37°C, 95% RH).

CHAPTER 7: SUPPLEMENTAL DATA FROM ENTRAINMENT EXPERIMENTS

Table 7.1. Summary of Entrained MCT Findings for Post-ciliogenesis Perfusion Studies

Codes , replicate	WxH	Flow rate	Time Perfusion	Dynamic Viscosity, 37 °C	Shear stress, Dyne/cm^2	Perfusion Type	Final Result	MC Direction 90 = along fluid flow
4,2	0.008" to 0.010" x 0.405"	0.125 ml/min	6 hours	0.692 cP	0.203 to 0.13	PBS, Syringe pump	Temporary unidirectional entrainment of Well differentiated cultures for 1 day	90 deg
1,3	0.008" to 0.010" x 0.405"	0.130 ml/min	6 hours	0.692 cP	0.21 to 0.135	PBS, UPP	Temporary unidirectional entrainment of Well differentiated cultures for 1 day	90 deg
2,3	0.008" to 0.010" x 0.405"	0.130 ml/min	3 days	0.692 cP	0.21 to 0.135	PBS, UPP	Temporary unidirectional entrainment of Well differentiated cultures for 1 day	90 deg
2,3	0.008" to 0.010" x 0.405"	0.130 ml/min	7 days	0.692 cP	0.21 to 0.135	PBS, UPP	Temporary unidirectional entrainment of Well differentiated cultures for several days but only in recovery period	Variable, 90 deg

4,3	0.008" to 0.010" x 0.405"	0.130 ml/min	3 days	1.07 cP	0.33 to 0.21	PFC, UPP	No Unidirectional Entrainment	Variable
1,3	0.008" to 0.010" x 0.405"	0.130 ml/min	3 days shear prior to ciliation; 5 day recovery	0.692 cP	0.21 to 0.135	PBS, UPP	Permanent Entrainment along direction of fluid flow for a few days, then became variable	90 deg
2,3	0.020" x 0.405"	2 ml/min	3 days	0.69 cP	0.52	KRB, UPP	Temporary Entrainment perpendicular to fluid flow; PCP images taken, Control - Duty cycle 1 min on 1 min off Experiment - Continuous flow	180 deg
1,4	0.010" x 0.405"	0.3 mL/min	9 hours	0.69 cP	0.52	PBS,UPP	Temporary Entrainment perpendicular to flow; continuous flow (2), Two controls - static fluid (1), unchanged; non-sheared (1), unchanged;	180 deg

CHAPTER 8: GLT SUPPLEMENTAL DATA

Table 8.1. Airflow mucus transport Dimensions, Flow Rates, Wall Stress[5]

	Open LPM (Closed)				
Adjusted Flow rate by Needle Valve	0.6 (0.5)	1 (0.8)	3 (2.5)	15 (8)	35 (35)
Old Chamber: CA = 0.021 in^2	0.62 m/s	1 m/s	3.7 m/s	18.5 m/s	43.2 m/s
New chamber CA = 0.031 in^2	0.42 m/s	0.67 m/s	2.1 m/s	5.9 m/s	29 m/s
Wall shear stress (dyne/cm^2), new, no slip	0.58	0.97	2.9	14.5	33.9
Wall shear stress (Pa), new, no slip	0.058	0.097	.29	1.45	3.39

Table 9.1: CA - cross section area, the old chamber design was utilized for mainly GLT studies. The new chamber is used for cough clearance studies.

[5] Wall shear stress assumes laminar flow for 0.2 s window of time in chamber. The constitutive equation used is on page 21.

Figure 8.1. Pressure drop across a culture during different airflow rates

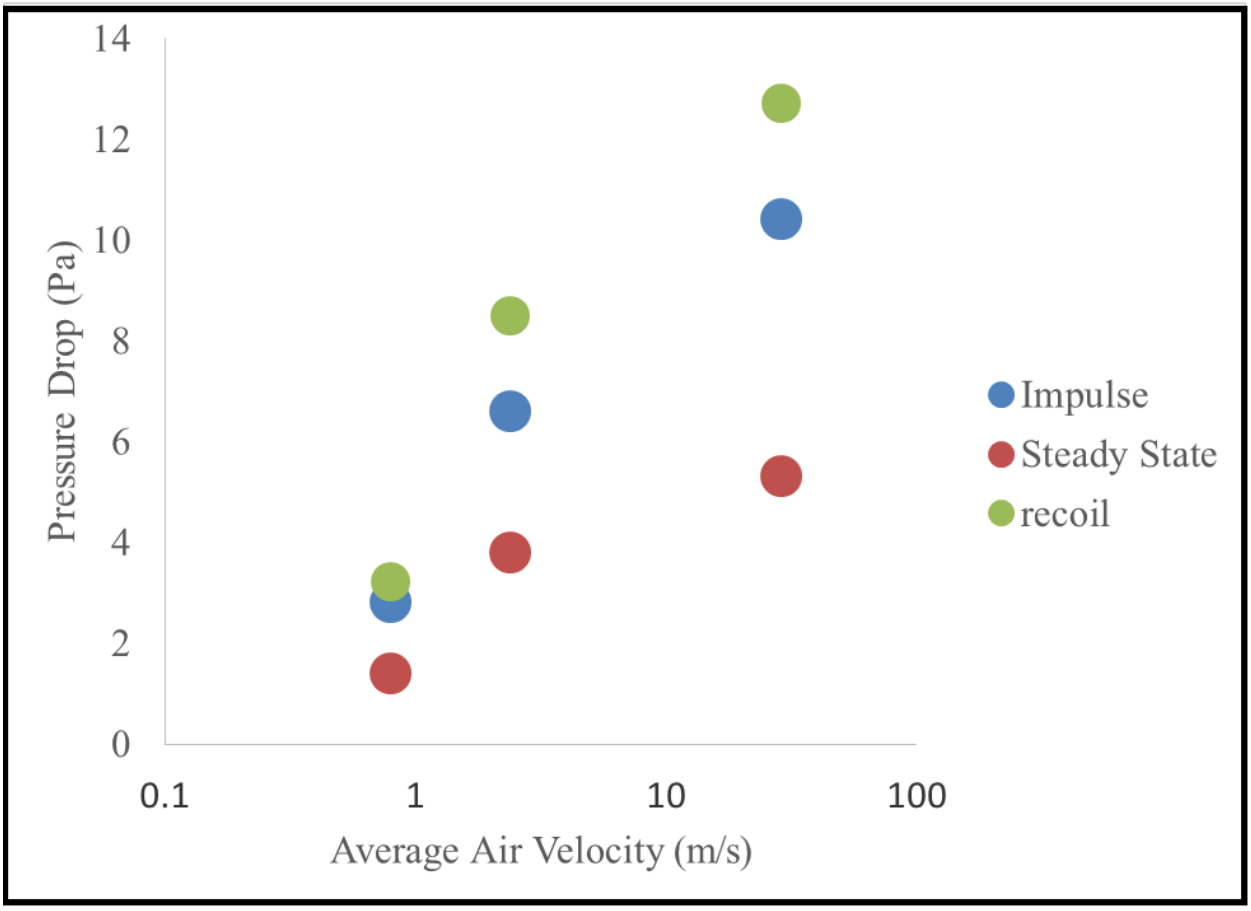

The peak cough pressure was around 12 Pa which equated to about 0.12 Pa of shear stress along the culture according to the equation for wall shear stress in a capillary rheometer (see below).[77]

The relationship between wall shear stress and the pressure drop was given by the following:

$$\tau_{wall} = \frac{Height}{2\left(1+\frac{Height}{Width}\right)} \frac{\Delta Pressure}{\Delta x} \qquad (1)$$

Relationship between Rheology and GLT metrics

Upon influx of laminar, humid airflow across surface of mucus layer, fluorescent tracers (surrogates for describing mucus transport) were temporarily entrained by the airflow. Each fluorescent tracer transported along or against the airflow depending on its initial trajectory. For every GLT air pulse, each bead showed a similar radial trajectory given in following figure.

Figure 8.2. Trajectory of Mucus during a single GLT pulse

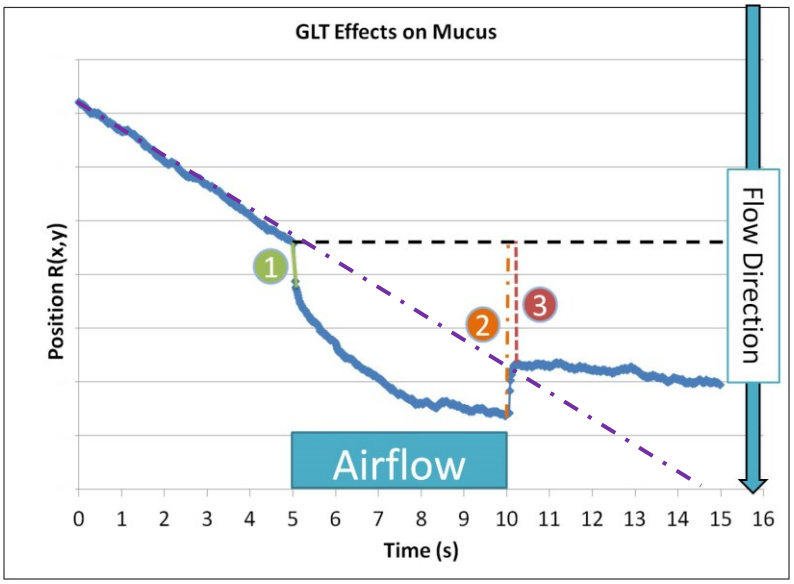

A sample trace showed different metrics involved in the analysis of a GLT experiment. After a period of 0.2 to 5 seconds of rest, airflow crossed over culture for another period of time (from 0.2 to 5 seconds) and when airflow is turned off, mucus recoiled to a steady state regime. The steady state and initial velocities varied greatly.

In Figure 8.2, mucus was cleared by an air puff that lasted for 5 seconds. The purple line was a theoretical line to show if the puff did not happen and the mucus continued to flow from the initial velocity. In this example, the air puff did not displace mucus very much as the blue trace intersected the purple trend-line. This failure of ineffective breath

clearance occurred when both elastic modulus of mucus and mucus solids concentrations were increased. This example trace came from a dataset with mucus solids concentration of about 8% mucus solids. However, the overall net displacement (Figure 8.2, circle 2) due to airflow placed the particle just above the purple line. The creep and recovery behavior of mucus highlighted above showed similarity in a model called Burgers Model which combined both Maxwell and Voight models for elastic creep and recovery for viscoelastic materials. [109] A single bead trajectory revealed three different metrics: 1) Instantaneous velocity, which was related to airflow-mediated clearance rate (μm/s), 2) Overall Displacement relative to starting position, which described the yielding nature of mucus at varying concentrations, and 3) Percent Loss which related to efficiency of the elastic recoil properties of mucus. In one pulse, the bead transport characterized the viscoelastic properties of mucus.

Figure 8.3. GLT Relationship to Burgers Model

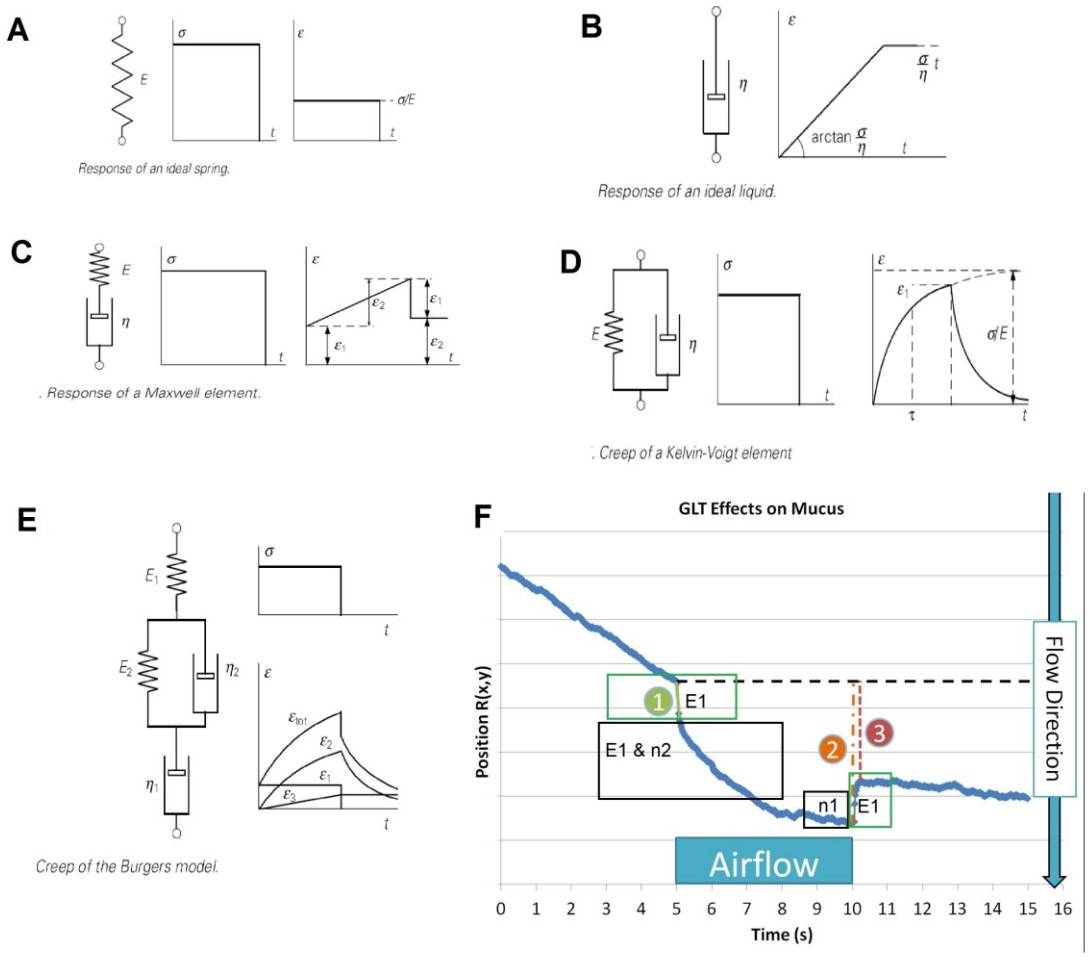

Pictorials were taken from [109,110]. A) *Component 1: Linear Spring*. This spring represented an elastic solid creep behavior where the strain was proportional to the stress and relaxed immediately after removal of stress. B) *Component 2: Linear Viscous Dashpot*. This dashpot denoted the creep behavior of a viscous liquid where the strain rate was proportional to the stress applied. C) *Maxwell Model*. Under constant stress, a linear spring in series with a dashpot showed an instantaneous deformation and a slow steady creep and did not recover fully. D) *Kelvin-Voight Model*. Under constant stress, a spring and dashpot in parallel with each other yielded an exponential creep and exponential recovery type of deformation. E) *Burgers Model*. This model combined three elements, a linear spring in series with a Voight element, and in series with a dashpot. F) *Burgers Model and GLT relationship*. Boxes highlighted regions where the Burgers and GLT models merged to yield a model to predict the viscoelastic properties of mucus during a GLT experiment.

CHAPTER 9: TUBULAR BIOREACTOR PROTOCOL

There were many boundary effects near the walls of the GLT chamber design which may cause erroneous data. Therefore, a system to culture *in vitro* human bronchial epithelial (HBE) cells in a cylindrical tube bioreactor was developed. With this system, *in vitro* experiments were anticipated to be performed to investigate air flow velocities necessary for clearing a mucus plug. The control over geometry, mucus concentration and air flow velocities provided versatile tools for analyzing mucus transport.

Figure 9.1. An *in vitro* Bronchiole Concept

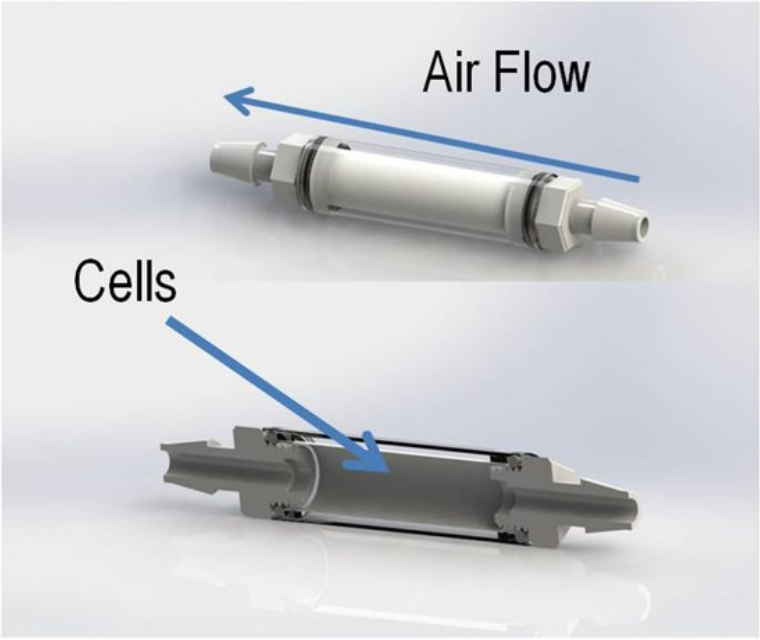

In the concept pictured, in Figure 9.1, housed a porous, hydrophilic ePTFE membrane (40 μm thick), which was a substrate to seed HBE cells. The ePTFE

membrane was kept taut on opposite ends by radial compression by O-rings seated on threaded Luer ends— a similar mechanism found using PTFE pipe thread tape. The membrane was bound within a capillary glass tube (about 1 cm ID). An interstitial narrow cavity between the glass tube and ePTFE membrane allowed for filling of basolateral ALI media. Inlet and outlet glass tube ports were molded into a glass chamber (not shown). A stent-like mesh was made of a strong adhesive (3M, #1522). The ePTFE membrane became optically translucent when in contact with fluid; thus, this model was suitable for epi-fluorescence microscopy and bright-field microscopy described in Chapter 3 and 4. A minimal, safe optical working distance for the interface was kept within 1 mm. An accurate CFD model with two phase flow is was developed to characterize the optimal seeding area for delivering shear forces induced by laminar airflow.

Prior Art

The hydrophilic ePTFE membrane had been used widely in tissue culture research as it was incorporated readily in Millicell™ circular filter supports. According to a histology specialist, this ePTFE membrane had a similar consistency and integrity as de novo skin tissue, and had a high probability of a multilayered HBE cell model (verbal communication, Kimberly Burns). The production of tubular bioreactors for airway cellular growth was not new and had been developed by Dr. Barbara Grubb here at the CF Center; however, the maintenance of the artificial bronchioles were cumbersome and thus this methodology was abandoned (verbal discussion with Dr. Barbara Grubb). Grubb, B. *et al*. utilized a biofiber matrix to support airway cells that were not transparent so microscopy applications were not possible. However, they found

absorption characteristics to be significantly greater in bronchial cells than in tracheal epithelial cells on conventional inserts.[111] Histological sections showed morphology similar to cultures grown on conventional filter support structures. The tubular biofiber matrix (see Figure 9.2) was kept submerged in a large quantity of culture media in a petri dish.[112] The tubular design improved this aspect as the media chamber needed less than a milliliter of culture medium; thus, the technique decreased maintenance costs.

Figure 9.2. Initial Tubular Bioreactor

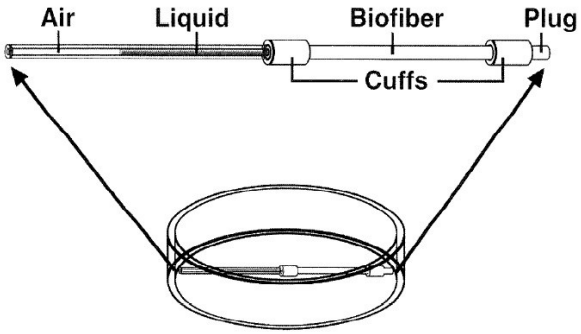

A port for air and liquid perfusion was made and silicone cuffs were used to keep tubular biofiber rigid. The tube was placed in a vat of culture medium.[111]

In another application published by Ghaedi, M., *et al*. a tubular, rotating bioreactor was made with the same Biopore™ membrane for growing induced pluripotent stem cells programmed to differentiate in to alveolar type II cells which is very difficult to culture *in vitro* (see Figure 9.3).[113] Interestingly, the alveolar cells were seeded onto the membrane and the PVDF filter remained as an additional sterile control. The cultures were housed in a rotating cylindrical bioreactor. As the bioreactor rotated, an aliquot of culture medium was perfused at 50 % duty cycle, meaning the cultures were flooded with media half the time and the other half for aspiration.[113] These

methods outlined in this article helped in creating confluent HBE cells and formed in to a tube for airflow induced plug flow studies. In their design, they left a seam between the edges of the ePTFE membrane and further techniques were needed to create a seam along the ePTFE membrane in the tubular bioreactor so that plug flow was continuous.

Figure 9.3. Rotating Tubular Bioreactor for Biopore™ Membrane

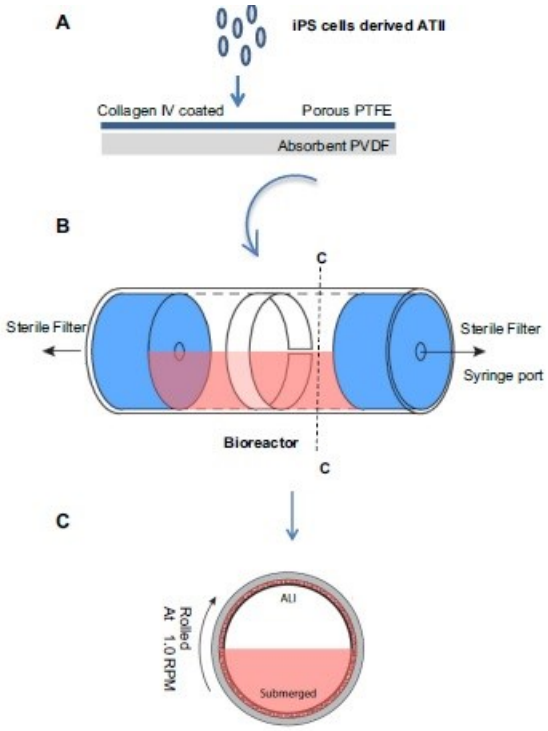

A) IPS derived alveolar type II cells seeded on to PTFE top layer. B) Pictorial of rotating bioreactor with sterile filter end caps. The end caps connected to freely rotating stopcocks which allow for air and fluid perfusion. C) A 50 percent duty cycle perfusion allowed cultures to absorb culture medium as well as retain oxygen and CO_2.[113]

Tubular Bioreactor for Airway Epithelial Cells

Several prototypes of the initial concept have been made using a variety of techniques. An experimental protocol was yet to be derived due to the complexity of trying to create a seamless tube with the ePTFE membrane. A high concentration gel like methylcellulose, gelatin or mussel adhesive protein (Cat. MAP-O4012, ACRO

Biosystems) was used as a biocompatible adhesive to bond the edges of the membrane together to form a seam. A CO_2 laser was also employed to laser weld ePTFE together. Mucus transport was entrained unidirectionally by perfusion of fluid flow described and by bubbling culture medium up the tube which was a similar technique found in air-lift bioreactors to allow for uptake of oxygen and nutrients simultaneously.[114]

The design criteria for the *in vitro* bronchiole were as follows:

- Reproducibility: Approximately a hundred chambers had to be made with limited variance in geometry for validation and acceptance by standard research and development practices.
- Modularity: The user should be able to take the membrane out for mucus solids or histological measurements with ease. A mucus sample dispensed within the chamber for plug flow experiments.
- Sterility: All components was autoclaved, treated by UV or Ethylene oxide prior to experiment (excluding Biopore™ membrane)
- Geometry: The inner diameter ranged from 0.25 to 1 cm to represent bronchiole geometries. The fluid dynamics was derived from equations related to Poiseuille flow; whereas, previous chambers the fluid dynamics needed to be modelled with simulation software to investigate boundary conditions.

Tubular Bioreactor Preliminary results

A single tubular reactor experiment was performed in which five tubular grafts were cultured with passaged HBE cell cultures along with a conventional Millicell as a control (see an example in Figure 9.4). On week three, these artificial tubular grafts were imaged using an epi-fluorescent microscope to evaluate mucus transport speed and direction, and they were sectioned for histology (see Figure 9.5).

Figure 9.4. Tubular Bioreactor Prototype

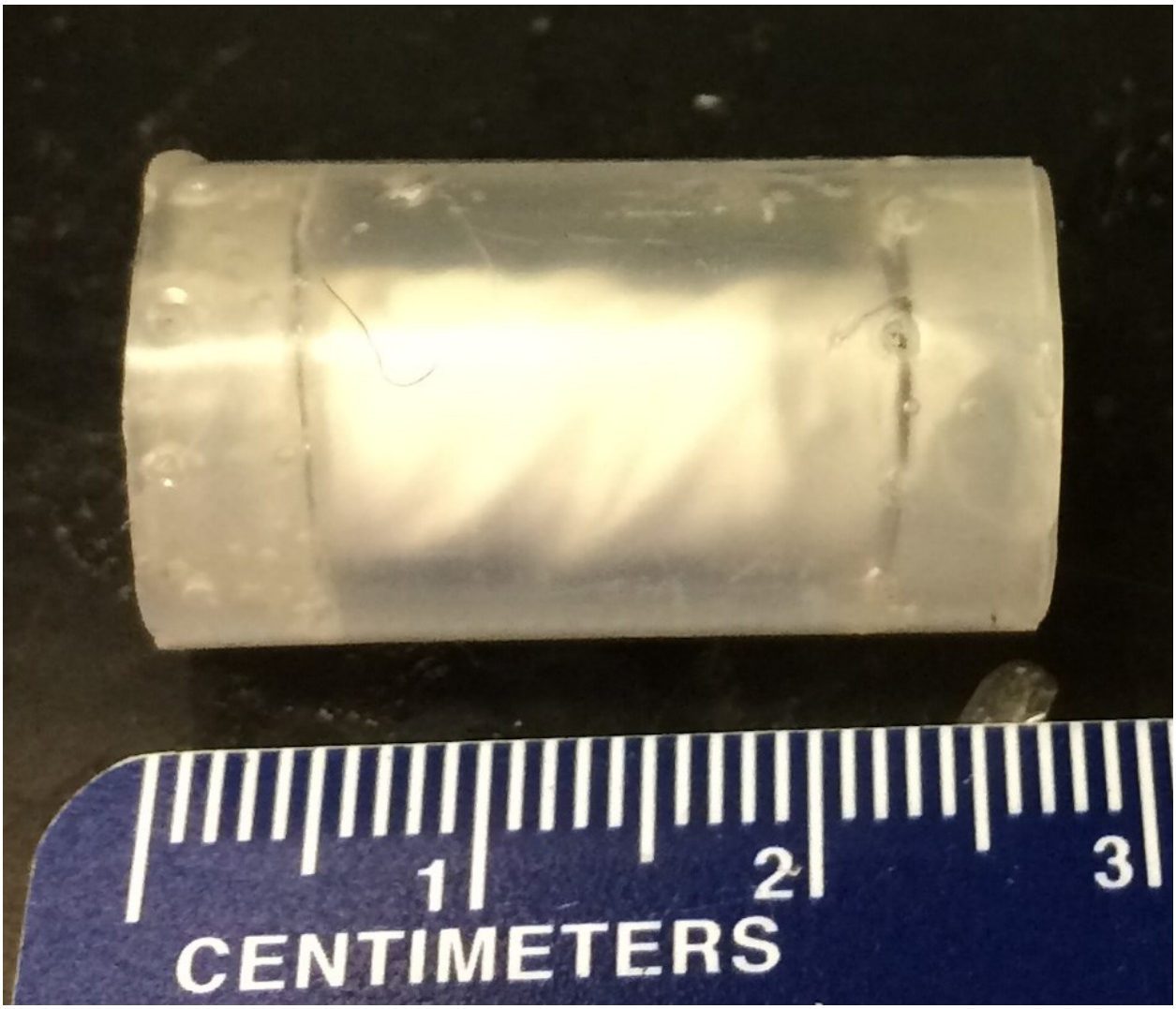

Tubular Bioreactor Prototype. Two inner PDMS cuffs provided radial seal between the inner white tubular graft and the outer PET cover. About one milliliter of media was delivered around the white tubular graft.

Figure 9.5. Histological Section of Tubular Graft

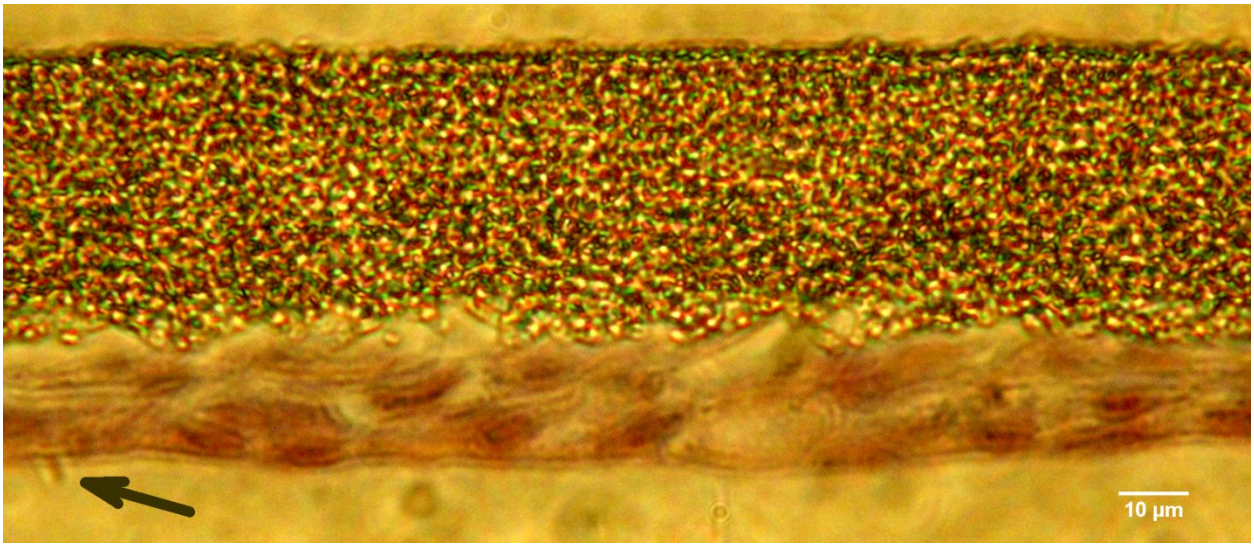

In a tubular graft, a bi-layer of HBE cells was visible on Millipore ePTFE membrane and ciliated cells were visible (arrow).

The tubular bioreactor system had several key components: 1) an artificial stent made from using a medical, biocompatible adhesive, a laser cutter and origami techniques (see Figure 9.6), 2) a plastic PET tube made from a centrifuge tube to house the tubular graft, 3) PDMS cuffs allowed for media exchange and provided a radial seal, 4) a syringe port for media exchange (see Figure 9.7) and 5) a rotating platform to help collagen coat , seed cells, and entrain mucus transport in to tubular graft (Figure 9.8). The ePTFE surface and the tubular bioreactor were functionalized for collagen treatment[115] and sterilized simultaneously through the use of oxygen plasma (Harrick Plasma, Inc) for several minutes.

Figure 9.6. Tubular Graft without Filter backing

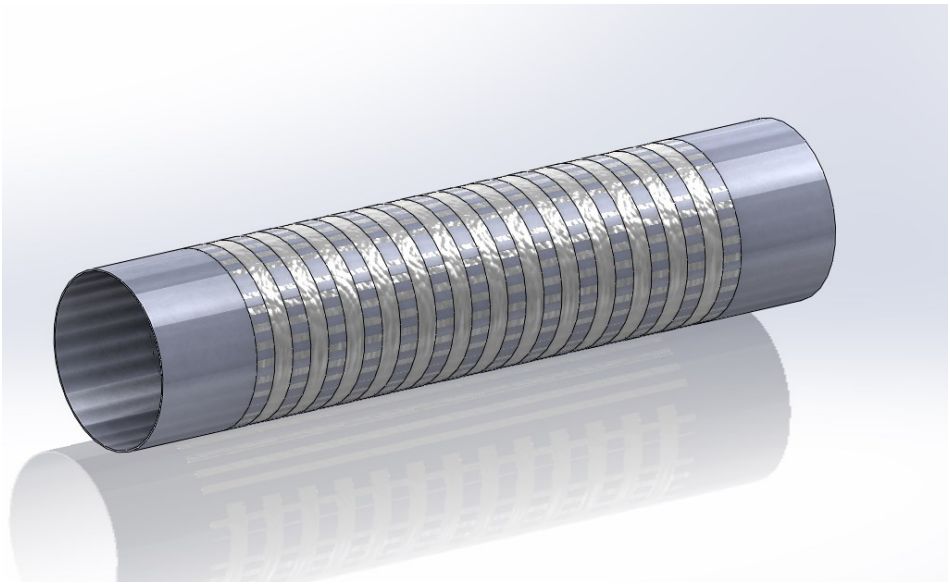

Figure 9.7. Syringe Port for Media Exchange

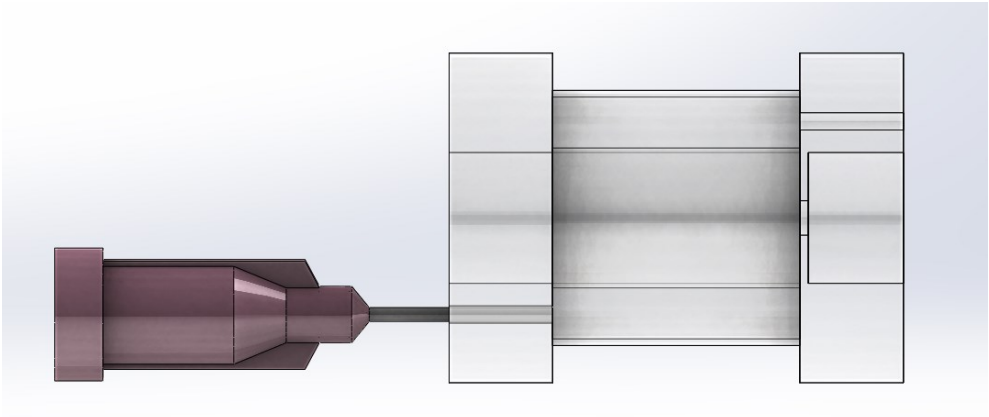

The artificial stent made of double-sided adhesive was the bridge that supported the ePTFE membrane on which cultures were seeded and an additional ePTFE membrane backing provided extra sterility and stability. The design of the stent incorporated eight vertical "tracks" when laid flat on a table. Once rolled in to a tube, the vertical tracks became a continuous ring. Once bridged, the grafts did have a seam and mucus pooled at the seam since there was no avenue for proper drainage. The epi-fluorescence videos showed that mucus transport was unidirectional in the middle of the

track but flowed in the opposite direction along the boundaries of the stent. Potentially there were 8 linear or ring-like mucus tracks within a tube.

Figure 9.8. Tubular Bioreactor Assembly

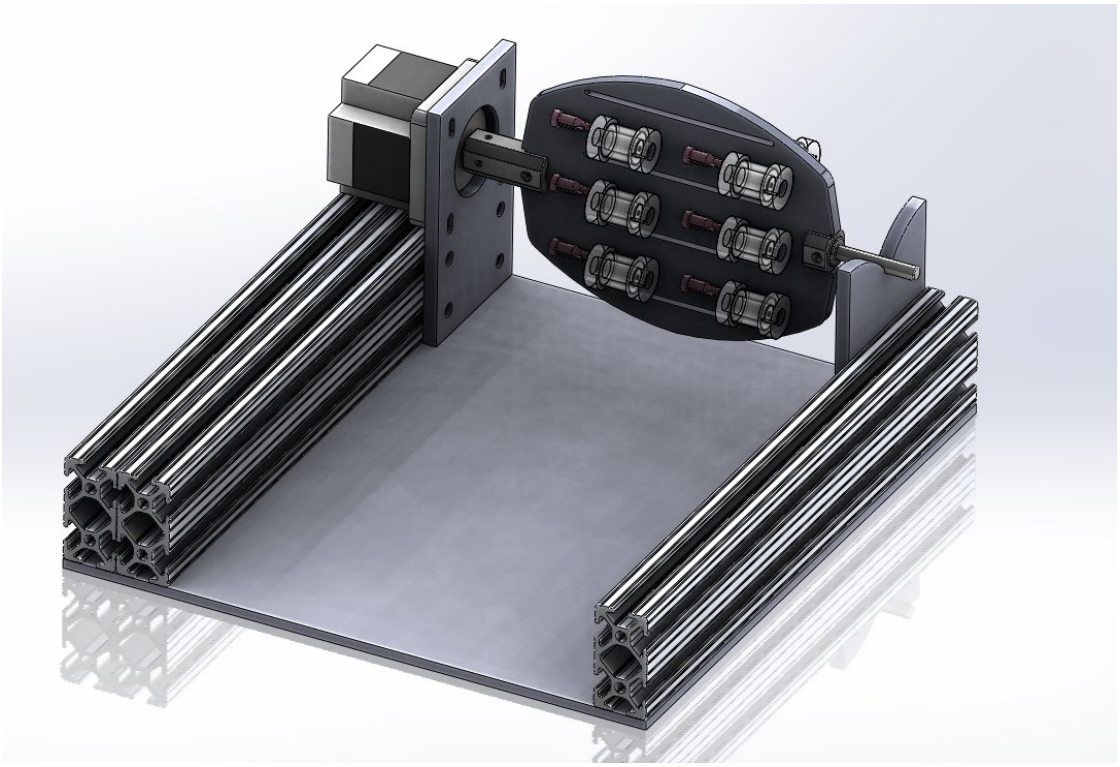

A single assembly housed two rotating systems, which could carry about twelve tubular bioreactors. This assembly was mounted inside an incubator. The tubular bioreactors were harnessed to the rotating platform using zip-ties. The motor rotated at a speed of 15 revolutions per minute for initial cell seeding and slowed to 5 RPM for cell growth.

Future Directions

Future efforts are required to redesign the stents such that these tracks run horizontal instead of vertical so that mucus transport can be imaged with the tube intact. Additionally, the backing has to be made from the same membrane material and a clear polystyrene tube can be used to provide better visibility of the culture during imaging.

The opaque PVDF filter made it impossible to see the culture, so the grafts had to be cut and laid down, cultures facing down flat on a petri dish to observe mucus transport.

Future Application: HBE Cells in a weightless environment

Weightlessness was the absence of contact or normal forces on a body such as the force due to gravity and a body's mass. The experience of sliding along the seat in car due to a sharp turn is because of a non-gravitational force- called centripetal force. Centripetal force acted to move a body in a uniform circular motion along a circular path. A rotating bioreactor moved the tubular graft around in a circle while placing apical and basolateral media during the first two weeks of cell seeding and proliferation (Figure 9.9A). The outcome of this experiment allowed the HBE cultures to transport mucus in the direction of overall circular motion by the end of the third week. In this experiment, however, the axis of the tubular graft would be placed directly along the center axis of the stepper motor such that the ciliated culture moves with a constant speed uniformly in a circle (Figure 9.9B).

Figure 9.9. Weightlessness Application

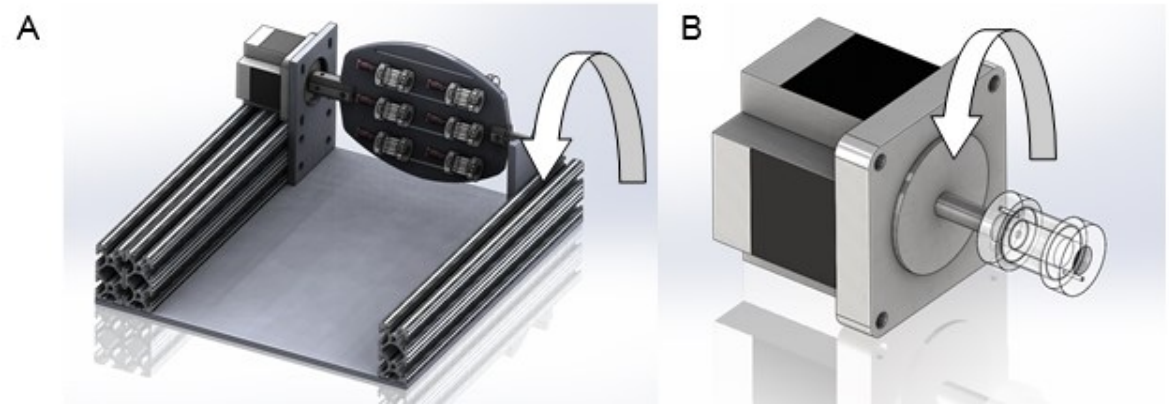

Slight modification for original rotating bioreactor (A) to address "weightlessness" attribute (B) using centripetal acceleration

All grafts would be evaluated for percent ciliation, cilia beat frequency, and mucus transport before and after centripetal acceleration

Experiment - tubular graft cultures will have following conditions:

After 4 weeks of static incubation

Cultures would be rotated at a constant 20 revolutions per minute with about 1 mL apical media to provide shear stress for entrainment. Control cultures would run with similar parameters with basolateral media only allowing mucus to rotate centripetally. Parallel control cultures would be on a tilter and a unidirectional perfusion system to show the difference between centripetal perfusion, a gentle rocking perfusion and unidirectional perfusion.

Interestingly, the adhesive nature of mucus would dominate in the system but this would depend on the thickness and rheological properties. After mucus, the centripetal force was the greatest at applying force on to the cell culture. In Table 9.1, this system has several magnitudes of forces acting on the HBE cultures.

Table 9.1. Magnitude of forces in the system.

Type of Force	Magnitude (dynes)
Centripetal force (20 rpm, diameter = 1 in)[6]	0.5
Phasic apical fluid shear stress on cultures[7]	0.003
Mucus adhesive tack force (~1.7 mN for 2% solids)[8]	170
Airflow shear stress[9]	0.00006
Force generated by outer dynein arm[39]	0.00002

Computation Fluid dynamic models:

These parameters were used in the CFD models of humidified air travelling through chamber at different initial velocities using Solidworks™ Flow Simulation 2010:

Temp: 37 °C
Pressure: 101325 Pa (parameter used for outlet pressure)
Wall Temperature: 37 °C
Humidity: 100%
Roughness: 0.5 microns
Diameter: 8 mm
Mach inlet: 0.0015 (parameter used for inlet condition)
Mesh size: Very fine (level =8, highest)
Fluid cells: 12,000 to 18,000
Assumption is Laminar and Turbulent flow.
Mach number = velocity of air / speed of sound (1 atm, 37 °C, 100% RH)
Mach #, Low Q = 0.5 / 354 = 0.0015
Mach #, High Q = 12 / 354 = 0.034

Reynolds number (Re) $= \frac{D_h \rho \bar{v}}{\eta} = \frac{0.008m * 1.14 \frac{kg}{m^3} * 1 \frac{m}{s}}{1.9E-5\ Pa*s} = 480$

[6] Fc = mass * (velocity)^2/radius
[7] phasic shear stress =(viscosity*angular velocity*radius*liquid height)/acceleration time [64]
[8] Unpublished data from personal experiment
[9] Viscosity of air at 37 °C is about 0.02 centipoise

Figure 9.10. Simple Tube CFD results

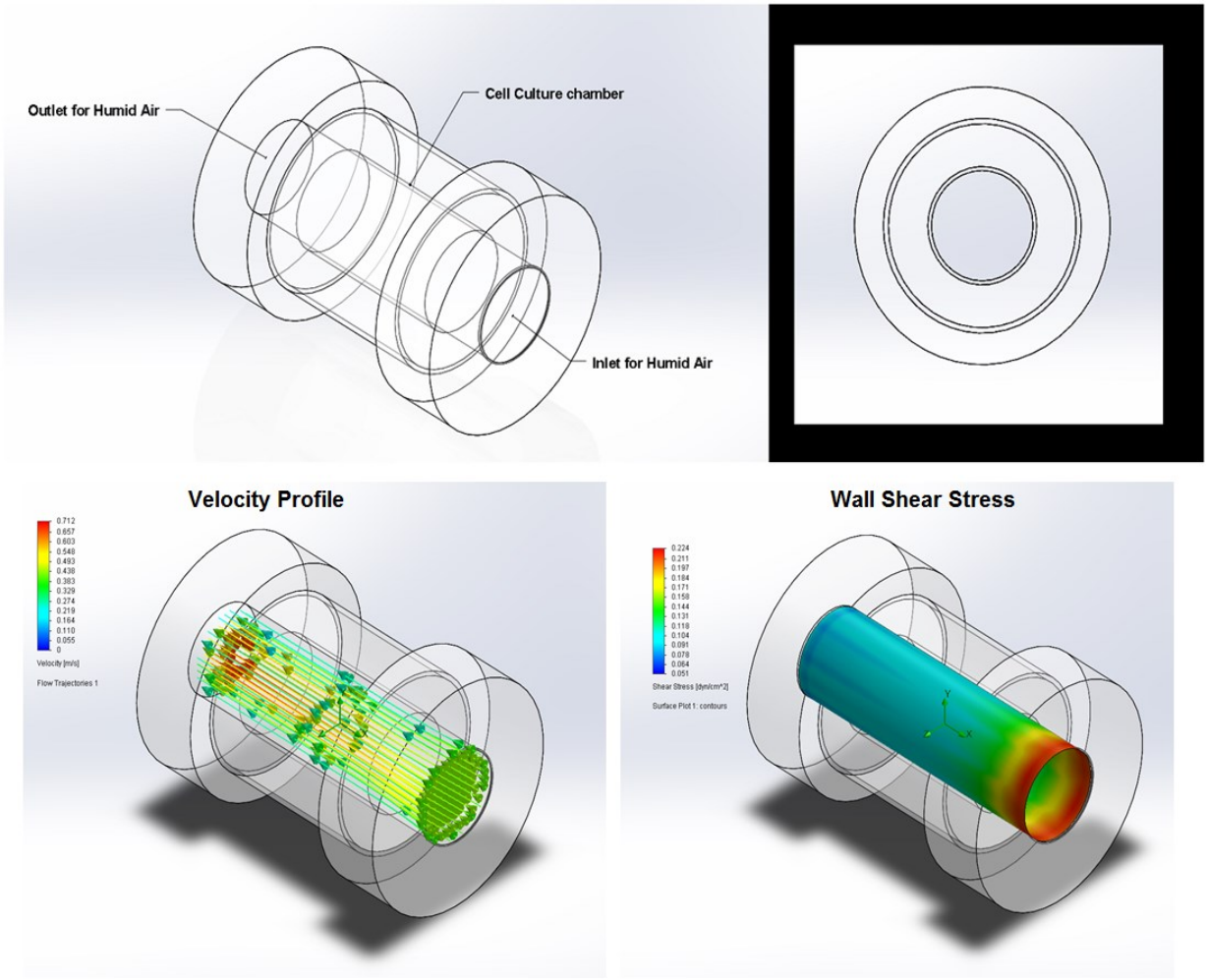

The average velocity in the tube from CFD analysis was 0.42 m/s with an initial velocity of 1 m/s. The wall shear stress ranges from 0.06 to 0.12 dyne/cm^2. The simple tube with a seam feature showed little or no difference with the results presented. Re = 202

Shear stress imparted along the walls of the chamber is important because the following figure shows the magnitude of shear stress imparted along the inner surface of the lungs during a breath depending upon the generation of bronchi (Figure 10)[64]. A shear stress of 0.12 dyne/cm^2 from this model would be typical for bronchi near alveolar cells.

Figure 9.11. Perturbation 1- High flow results with a seam

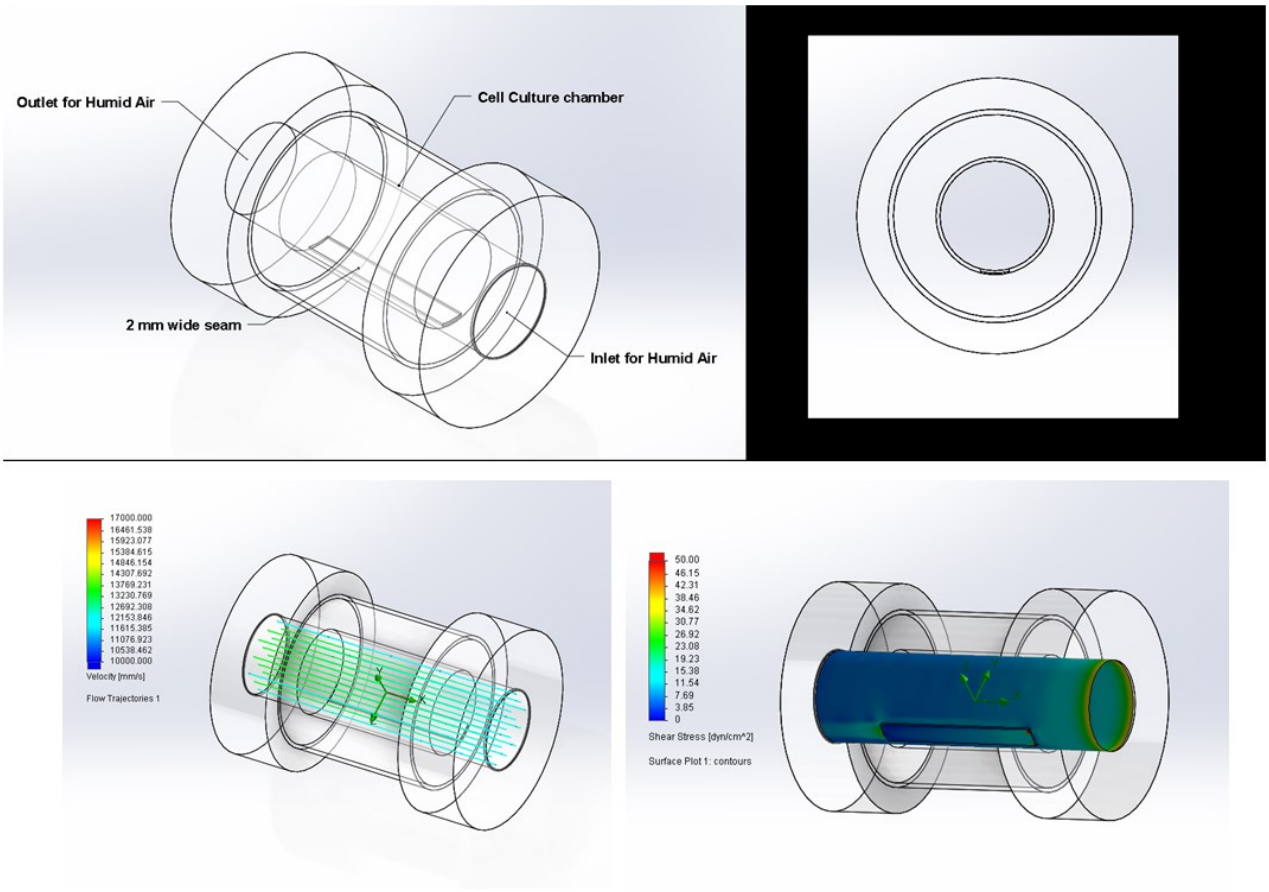

A seam feature was incorporated at the bottom of the model. Initial airflow rate was set to 12 m/s, which is typical for cough-like velocities. The average velocity and wall shear stress was 12.2 m/s and 7 dyne/cm^2. For comparison, the amount of wall shear stress imparted by blood flow in endothelial vessels is about 25 dyne/cm^2.[116]. Interestingly, near the beginning of the seam drop off point, any sharp corners experienced as much as 50 dyne/cm^2 shear stress but for a short distance. The integration of a wide seam feature caused plowing effects in mucus along the sharp edge of the material- boundary effects are predicted in this model. Re = 5856

Figure 9.12. Perturbation 2: Vertical Valley Analysis.

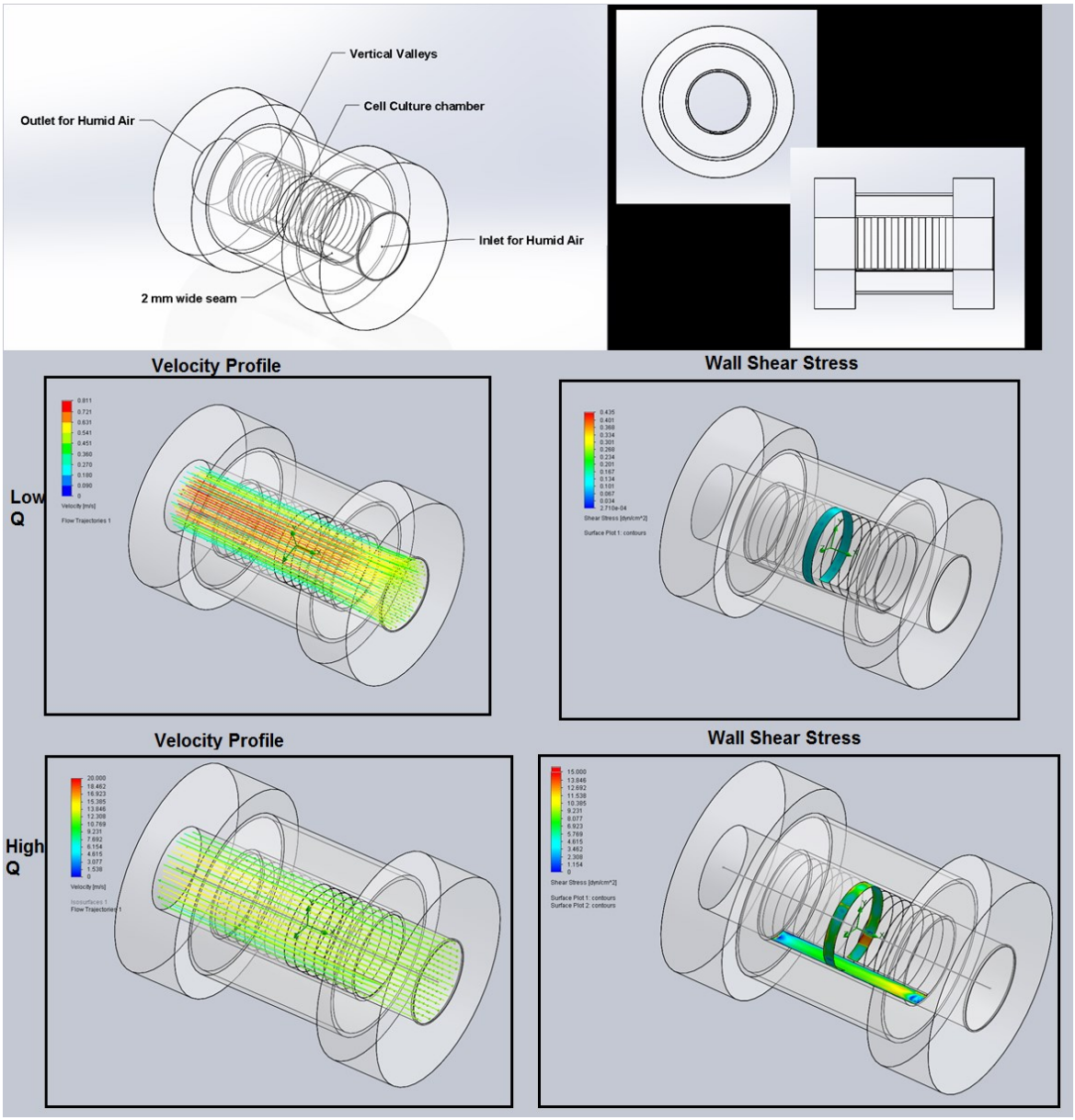

This CFD model incorporated both a seam and an array of valleys made by adhesive stent within the membrane due to compression and adhesion of the adhesive material. The average velocity, wall shear stress and Reynolds for low flow were 0.48 m/s, 0.08 dyne/cm^2, 230 respectively. Interestingly, in the high air flow, the average velocity also matched the initial velocity 11.7 m/s (Re = 5616) but the wall shear stress in the valley was highly variable between 8 and 15 dyne/cm^2. The stress spike happened to be near the seam feature of the model, which also showed some variability in stress along the length of the bronchiole.

Figure 9.13. Perturbation 3: Horizontal Valley Analysis.

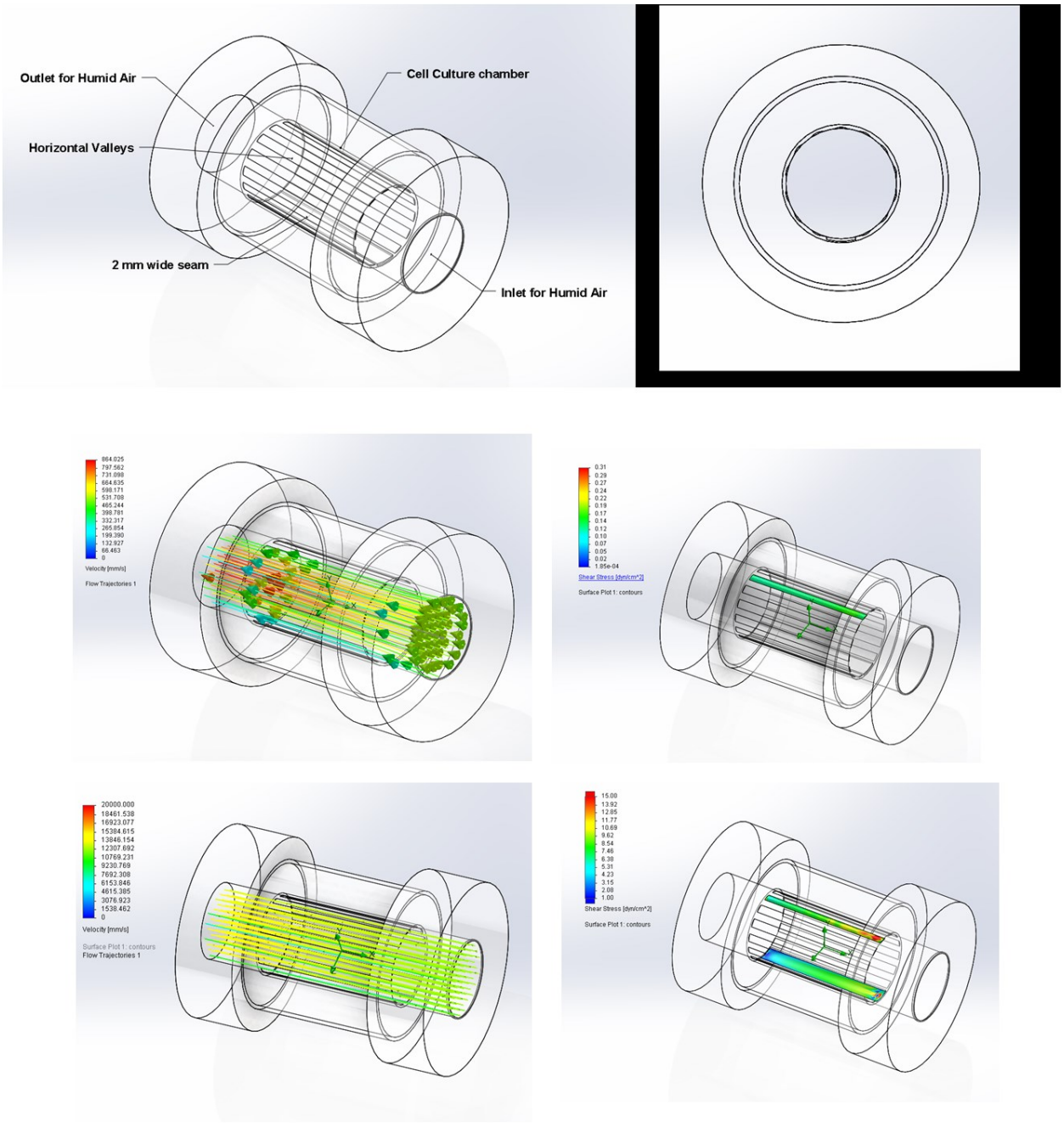

This CFD model incorporated both a seam and an array of valleys made by adhesive stent within the membrane due to compression and adhesion of the adhesive material. Here, the idea was that the majority of cultures transport mucus along the axis of the tube rather than around a ring mentioned previously. The average velocity and wall shear stress for low flow was 0.52 m/s (Re = 280) and 0.17 dyne/cm^2. The slight change in geometry for the cells also slightly changed the effective wall shear stress. Interestingly, in the high air flow, the average velocity also matched the initial velocity

12.5 m/s (Re = 6000) but the wall shear stress in the valley was highly variable between 8 and 15 dyne/cm^2, which showed some consistency near the end of the tube. The stress spike happened to be near entrance of the tube; this spike was expected to be related to the coefficient of discharge.

APPENDIX 2: ANALYSIS OF DATA

Adapted from (http://www.nasa.gov)

"The nitrogen in our DNA, the calcium in our teeth, the iron in our blood, the carbon in our apple pies were made in the interiors of collapsing stars. We are made of star-stuff." – Carl Sagan, *Cosmos*

CHAPTER 10: ALGORITHMS FOR EVALUATING MUCUS ENTRAINMENT

Selection of driven transport

Multiple thresholding algorithms were employed to evaluate mucus transport from the analysis of trajectories of ~1μm carboxylated, fluorescent beads, which acted as a surrogate to describe mucus transport. The first threshold filtered trajectories that lasted for at least half of the time lapse video. The second threshold looked at the curvature of mean-square displacement curves on a log-log plot. The third threshold teased out trajectories that showed linear transport rather than circular transport. Lastly, to remove inherent drift, the final net displacement threshold selected particles that moved at least twice their diameter during the video.

Mean-Square Displacement Theory

Particles driven by cilia-mediated flow were identified by assessing mucus transport velocity and directionality. These particles were 1 micron and carboxylated that stick to mucus/proteins in the mucus layer or are buoyant in a solution of PBS. Sometimes, these particles adhered to the tips of cilia on ciliated cells and did not show net transport. On other occasions, there were particles that show drift or showed no movement as they are stuck to a surface or they are locked within the mucus polymer mesh network. Some particles vibrated inherently showing Brownian or random motion. These aspects of transport of particles in mucus were discriminated by the use of mean-

squared displacement (MSD) curves. The alpha or exponent to the MSD power curve signified three modes of transport:

$$MSD = D_{fBm} * t^{alpha}$$

$$D \text{ (diffusion coefficient, function of dynamic viscosity)} = \eta_{Bm} T / 6\pi\eta\varphi$$

If alpha was 0, then the particles were stationary and did not move on long timescales- Brownian motion.

If alpha was near 1, then the particles were moving by diffusion.

If alpha was greater than 1 and close to 2, then the particles were driven by mucus transport.

The main caveat to the analysis was that the video needed to have enough frames (>1000) to assess MSD. If there were too few frames, then the accuracy diminished because there were too few windows or tau timescales. Since the videos lasted for approximately 30 seconds, the MSD curve depended on the number of total frames of the video. Nikon's Elements software accurately accounted for the timeline by accounting for the both the exposure of the image and acquisition time between frames (verbal communication with Dr. Jacob Sawyer, Nikon, Inc.). Another caveat was that one had to ensure this analysis was performed on particles that lasted throughout the video- missing tracks or gaps did not yield accurate results for MSD calculations. This code isolated particles in a population (>=100) that were valid within the timeframe of the experiment (30 to 500 s).

In MATLAB, a power series fit model extrapolated the coefficients D and alpha with a confidence interval of 95%. The windowing scheme was adjusted to include all frames.

Figure 10.1. Example of MSD Curves

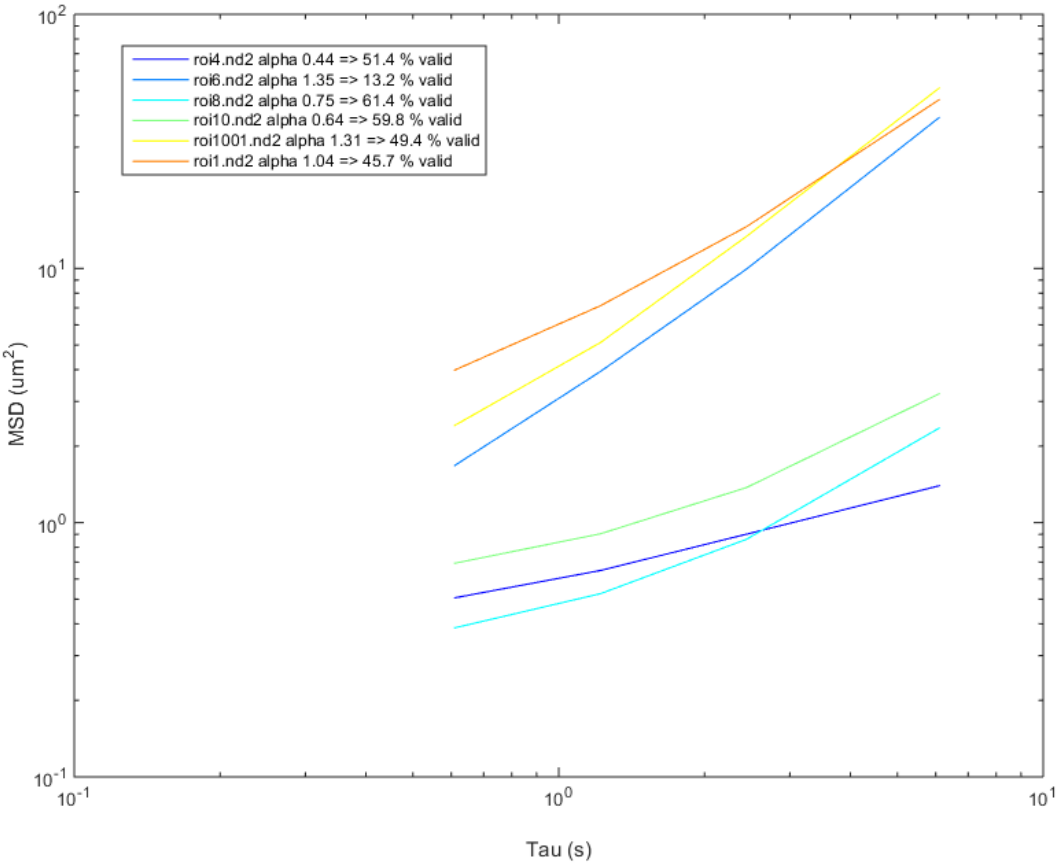

Averaged MSD curves from multiple ROIs from a drip perfusion experiment showed variable transport characteristics in one culture sample after 1 week of perfusion. Only valid trajectories were analyzed and evaluated as a percentage of the total population of recorded tracks.

Exclusion of Non-linear Transport

Using circular statistics from Figure 2.12, random or circular trajectories showed a broad distribution of angles during the movement. Linear or entrained forms of transport, including drift, delineated a tight distribution of angles, which represented a net direction of mucus transport. In circular statistics, the strength of the distribution of angles was derived from the resultant number: R = 1, no variance in angle distribution, and R = 0, highly variable in angle distribution. In the code, a threshold greater than 0.5 was used to select trajectories that showed net transport along a particular direction.

Figure 10.2. Example of Random Motion of Particle in Mucus

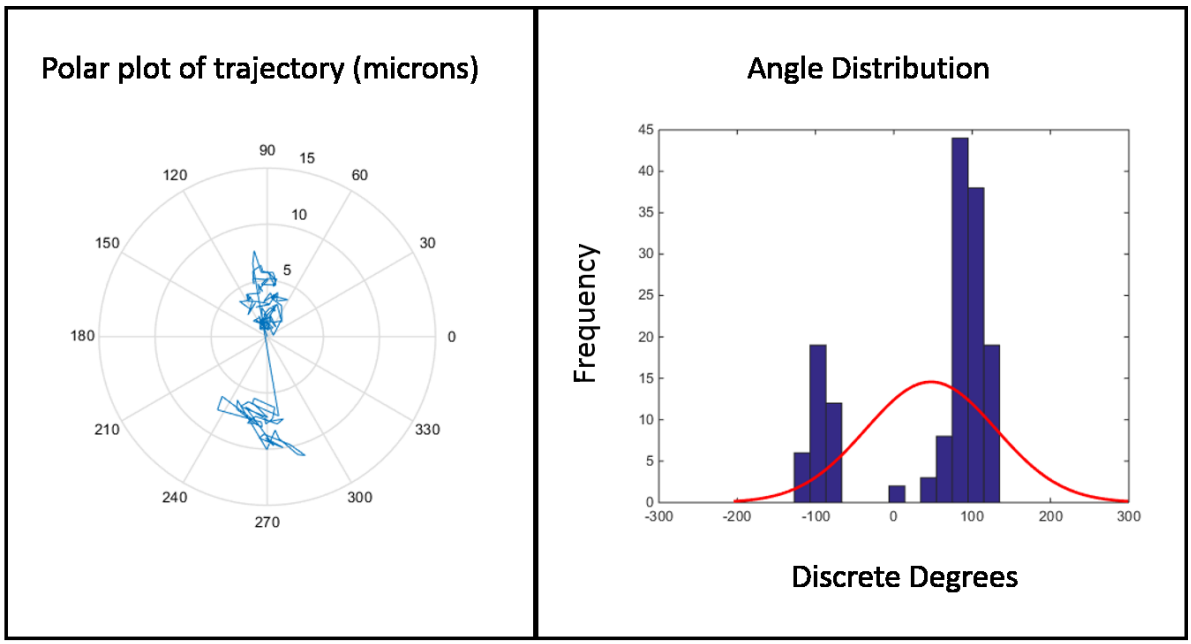

Figure 10.3. Example of Linear Motion of Particles in Mucus

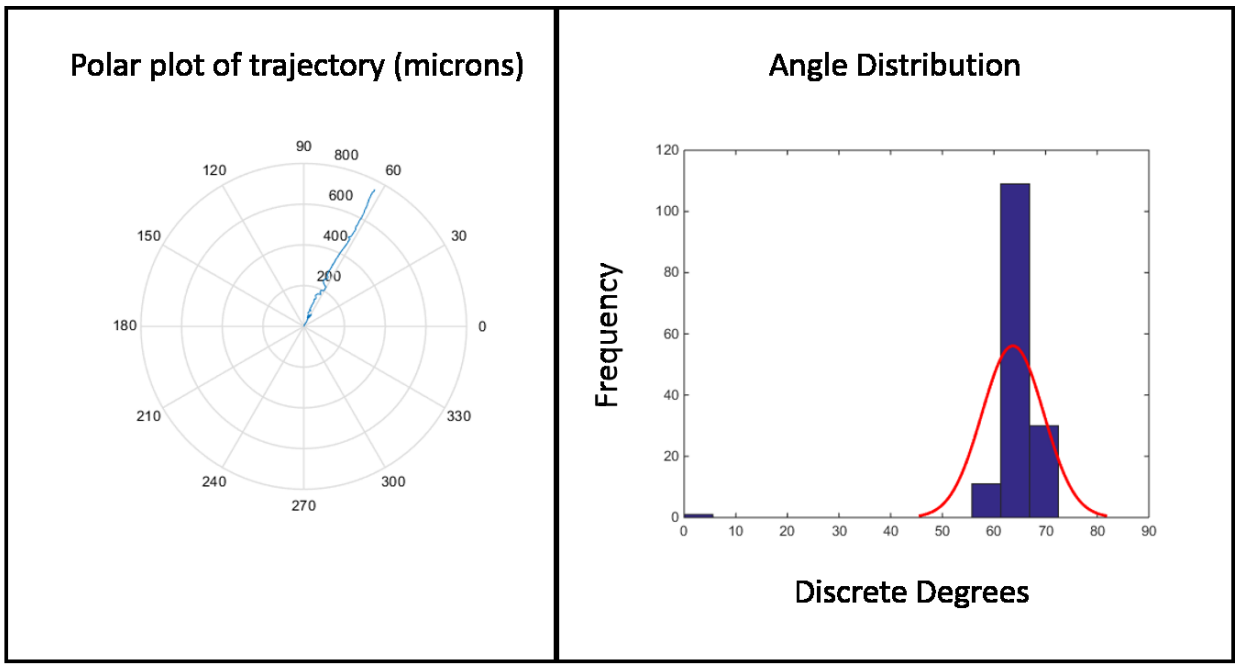

Calculation of Percent Ciliation

Percent ciliation was derived from analyzing videos using MATLAB fast Fourier transform software made by Dr. Peter Koenig and Dr. Christian Buj from the University of Lübeck. A Gaussian distribution was derived from the histogram output to determine the mean cilia beat frequency and percent ciliation. The example image showed a heat map of a culture and the corresponding histogram showed the distribution of pixels in different frequency ranges. Videos were taken with a 120 fps CMOS camera (Flea3) and/or 50 fps CCD camera (Photometrics, Coolsnap2).

Figure 10.4. Percent Ciliation and Cilia Beat Frequency Analysis

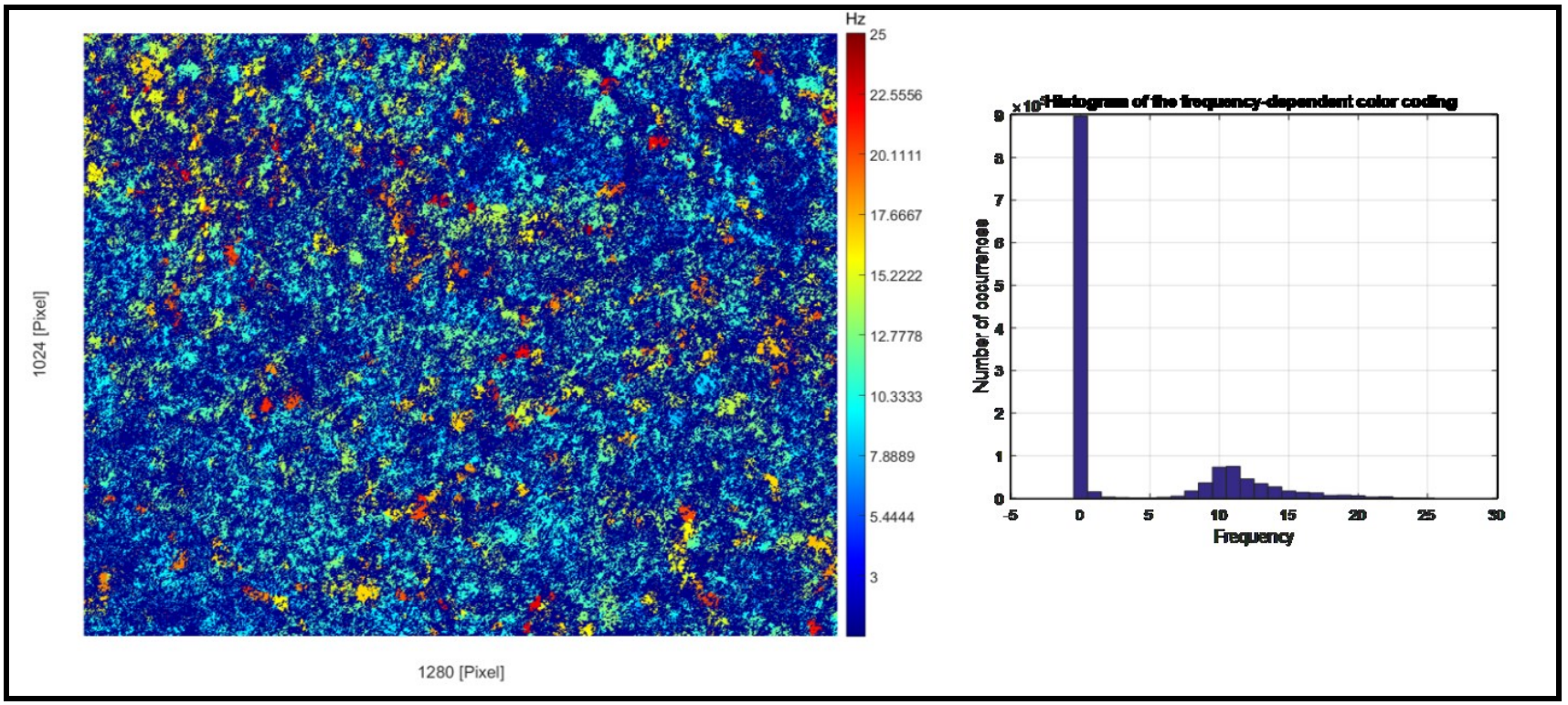

The panel to the left showed the heat map of the distribution of pixels that vibrated at frequencies between 0 (noise) to 25 Hz. The right panel showed the histogram distribution of the heat map. From the histogram, the low frequency noise was taken out and a Gaussian distribution was fitted around the rest of the histogram. The mean cilia beat frequency was reported as 11 ±1.8 Hz and the area was 25 percent ciliated around that distribution of frequencies.

Figure 10.5. AnalyseGUI vs. SAVA Evaluation

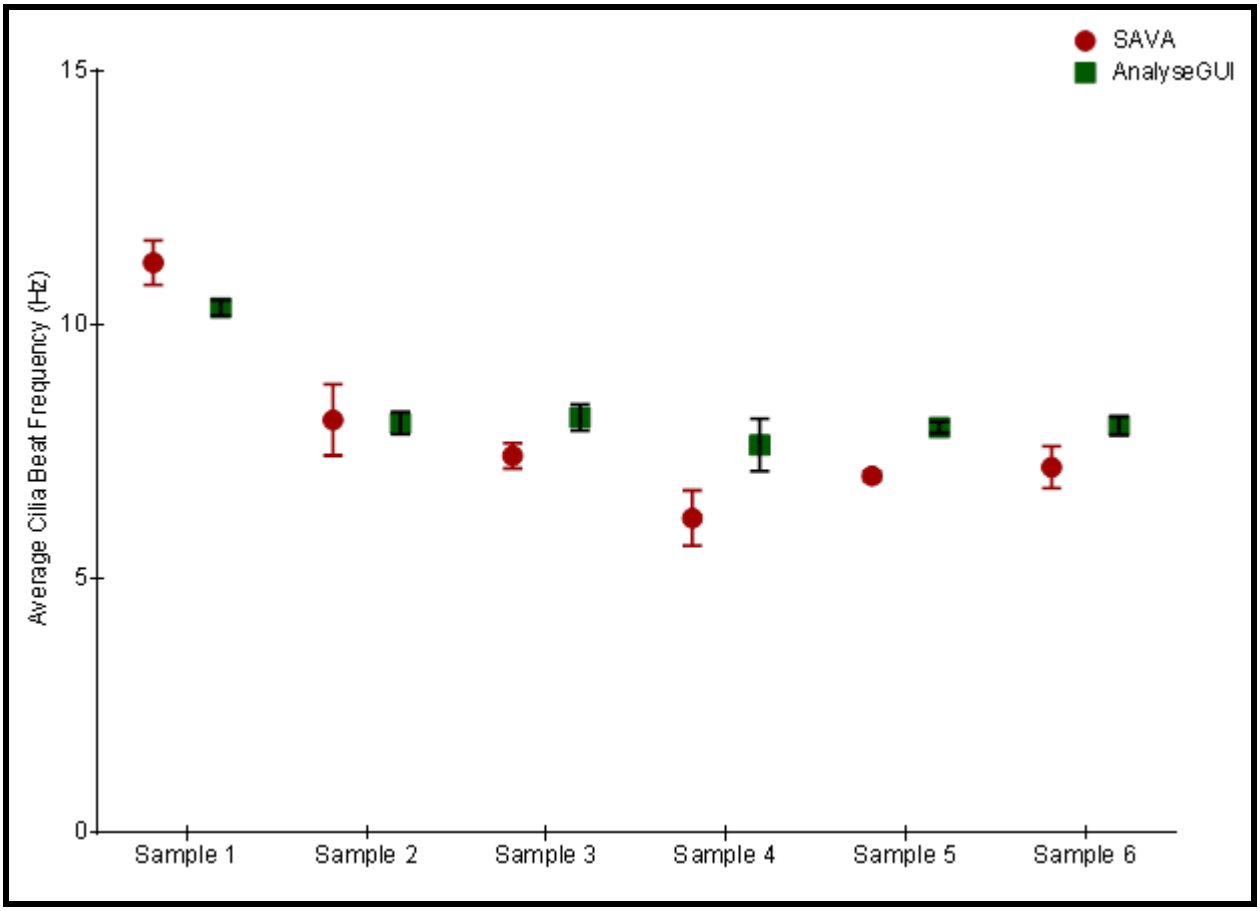

Across a number of samples, the German software, AnalyseGUI, yielded comparable results for average cilia beat frequency against the standard software in the field (SAVA) while the ROI pixel area and frequency range were kept the same.[117]

CHAPTER 11: ALGORITHM FOR EVALUATING AIR FLOW-MEDIATED MUCUS TRANSPORT

Calculation of Airflow-mediated velocities

In a gas-liquid transport and cough clearance experiment, the fiducial's radial trajectory or displacement was expressed as a function of both x and y pixels given in the following:

$$\boldsymbol{R(x,y)} = \sqrt{\left(\Delta \boldsymbol{x_{px}}\right)^2 + \left(\Delta \boldsymbol{y_{px}}\right)^2} \qquad (1)$$

The radial displacement versus time plots helped to determine the window in which the instantaneous velocities occur due to airflow shear force. A linear regression model was made through the tracer's trajectory (R, t) in this window to get the peak airflow-mediated clearance rate $v_{instant}$. Additionally, the R^2 value from the linear regression was also tabulated as a threshold in the calculations. If a particle were to swirl in a circle or curve when the airflow crosses over, then the R^2- value from linear regression will be below 0.5 and thus these aberrant trajectories were thrown out from the further analysis. The unit vector (equation 2) was derived by knowing the start (0, 0) and end points (x, y) of the particle within a time frame. The main utility of a unit vector was to preserve the direction of mucus trajectory and to compare against the direction of the airflow. The final value of GLT-mediated velocity was derived by subtracting the initial velocity due to cilia-mediated clearance from the instantaneous velocity due to air in vector algebra

notation to preserve both magnitude (derived from linear regression models) and direction (derived from unit vectors) (equation 4).

Unit Vector:

$$\hat{u}_{(x\_end,y\_end)} = \frac{R(x_{end},y_{end})*e^{i\theta}}{\|R(x_{end},y_{end})*e^{i\theta}\|} \quad (2)$$

Mean Direction:

$$\theta = \arctan\left(\frac{y_{end}}{x_{end}}\right) \quad (3)$$

Airflow-mediated Mucus Transport:

$$\overrightarrow{v_{GLT}} = \|v_{instantaneous}\|\hat{u}_{instantaneous} - \|v_{initial}\|\hat{u}_{initial} \quad (4)$$

Reported Clearance Rate:

$$v_{GLT} = \|\overrightarrow{v_{GLT}}\| \quad (5)$$

The final reported value for GLT -mediated clearance rate was derived from equation 5 and multiplied by a conversion factor for microns per second. Similar calculations were made for recoil velocities and for net displacements.

REFERENCES

1. Clauss, M. A., Fronius, M., Clauss, W. G. & Althaus, M. Why Do We have to Move Fluid to be Able to Breathe? *Front. Physiol.* **3,** 1–9 (2012).
2. *Toxicology of the Lung*. (Philadelphia,, PA: Taylor and Francis, 1999).
3. Livraghi, A. & Randell, S. H. Cystic fibrosis and other respiratory diseases of impaired mucus clearance. *Toxicol. Pathol.* **35,** 116–129 (2007).
4. Boucher, R. C. Cystic fibrosis: a disease of vulnerability to airway surface dehydration. *Trends Mol. Med.* (2007).
5. Farmer Stephen G., 1954- & Hay Douglas W. P., 1956-. *The airway epithelium : physiology, pathophysiology, and pharmacology / edited by Stephen G. Farmer, Douglas W.P. Hay*. (New York : M. Dekker, 1991).
6. Verdugo, P. Supramolecular Dynamics of Mucus. *Cold Spring Harb. Perspect. Med.* **2,** a009597–a009597 (2012).
7. Hoegger, M. J. *et al.* Impaired mucus detachment disrupts mucociliary transport in a piglet model of cystic fibrosis. *Science (80-.).* **345,** 818–22 (2014).
8. Yuan, S. *et al.* Oxidation Increases Mucin Polymer Cross-Links To Stiffen Airway Mucus Gels. *Sci Transl Med* **7,** 1–19 (2015).
9. Hill, D. B. *et al.* A biophysical basis for mucus solids concentration as a candidate biomarker for airways disease. *PLoS One* **9,** 1–11 (2014).
10. Kirkham, S., Sheehan, J. K., Knight, D., Richardson, P. S. & Thornton, D. J. Heterogeneity of airways mucus: variations in the amounts and glycoforms of the major oligomeric mucins MUC5AC and MUC5B. *Biochem. J.* **361,** 537–546 (2002).
11. Hovenberg, H. W., Davies, J. R. & Carlstedt, I. Different mucins are produced by the surface epithelium and the submucosa in human trachea: identification of MUC5AC as a major mucin from the goblet cells. *Biochem. J.* **318 (Pt 1,** 319–324 (1996).
12. Sheehan, J. K. *et al.* Physical characterization of the MUC5AC mucin: a highly oligomeric glycoprotein whether isolated from cell culture or in vivo from respiratory mucous secretions. *Biochem. J.* **347 Pt 1,** 37–44 (2000).
13. Kesimer, M., Makhov, A. M., Griffith, J. D., Verdugo, P. & Sheehan, J. K. Unpacking a gel-forming mucin: a view of MUC5B organization after granular release. *Am. J. Physiol. Cell. Mol. Mol. Physiol.* **298,** L15–22 (2010).
14. Henke, M. O., Renner, A., Huber, R. M., Seeds, M. C. & Rubin, B. K. MUC5AC and MUC5B mucins are decreased in cystic fibrosis airway secretions. *Am. J. Respir. Cell Mol. Biol.* **31,** 86–91 (2004).
15. Hayashi, T., Ishii, A., Nakai, S. & Hasegawa, K. Ultrastructure of goblet-cell

metaplasia from Clara cell in the allergic asthmatic airway inflammation in a mouse model of asthma in vivo. *Virchows Arch.* **444,** 66–73 (2004).

16. Gardiner, M. B. The importance of being Cilia. *HHMI Bulletin* 33–64 (2005).
17. Waters, C. M., Sporn, P. H. S., Liu, M. & Fredberg, J. J. Cellular biomechanics in the lung. *Am. J. Physiol. Lung Cell. Mol. Physiol.* **283,** L503–9 (2002).
18. Sleigh, M. A. *et al.* The propulsion of mucus by cilia. *Am. Rev. Respir. Dis.* **137,** 726–741 (1988).
19. Mitran, S. M. Metachronal wave formation in a model of pulmonary cilia. *Comput. {&} Struct.* (2007).
20. Gueron, S., Levit-Gurevich, K., Liron, N. & Blum, J. J. Cilia internal mechanism and metachronal coordination as the result of hydrodynamical coupling. in *Proceedings of the National Academy of Sciences* **94,** 6001–6006 (National Acad Sciences, 1997).
21. Wanner, A., Salathe, M. & Riordan, T. G. O. State of the Art Mucociliary Clearance in the Airways. 18–23
22. Sleigh, M. A., Blake, J. R. & Llron, N. State of Art The Propulsion of Mucus by Cilia.
23. Boucher, R. C. Airway surface dehydration in cystic fibrosis: pathogenesis and therapy. *Annu. Rev. Med.* **58,** 157–70 (2007).
24. Button, B. *et al.* A Periciliary Brush Promotes the Lung Health by Separating the Mucus Layer from Airway Epithelia. *Science (80-.).* **337,** 937–941 (2012).
25. Mall, M., Grubb, B. R., Harkema, J. R., O'Neal, W. K. & Boucher, R. C. Increased airway epithelial Na+ absorption produces cystic fibrosis-like lung disease in mice. *Nat. Med.* **10,** 487–493 (2004).
26. Boucher, R. C. Evidence for airway surface dehydration as the initiating event in CF airway disease. *J. Intern. Med.* **261,** 5–16 (2007).
27. Kalhoff, H. Mild dehydration: a risk factor of broncho-pulmonary disorders? *Eur. J. Clin. Nutr.* **57,** S81–S87 (2003).
28. Rubin, B. K. Secretion properties, clearance, and therapy in airway disease.
29. Matsui, H. *et al.* A physical linkage between cystic fibrosis airway surface dehydration and Pseudomonas aeruginosa biofilms. *Proc. Natl. Acad. Sci. U. S. A.* **103,** 18131–18136 (2006).
30. W, K. Cystic Fibrosis: Everything you need to know. (2003).
31. Bhogaraju, S., Engel, B. D. & Lorentzen, E. Intraflagellar transport complex structure and cargo interactions. *Cilia* **2,** 10 (2013).
32. Nauli, S. M. *et al.* Endothelial cilia are fluid shear sensors that regulate calcium signaling and nitric oxide production through polycystin-1. *Circulation* **117,** 1161–1171 (2008).

33. Hierck, B. P. *et al.* Primary cilia sensitize endothelial cells for fluid shear stress. *Dev. Dyn.* **237,** 725–735 (2008).

34. Praetorius, H. A. & Spring, K. R. A physiological view of the primary cilium. *Annu. Rev. Physiol.* **67,** 515–529 (2005).

35. Whitfield, J. F. The neuronal primary cilium---an extrasynaptic signaling device. *Cell. Signal.* (2004).

36. Wheatley, D. N. Landmarks in the first hundred years of primary (9+0) cilium research. *Cell Biol. Int.* **29,** 333–339 (2005).

37. Satir, P. & Christensen, S. T. Overview of structure and function of mammalian cilia. *Annu. Rev. Physiol.* **69,** 377–400 (2007).

38. Gilula, N. B. & Satir, P. The ciliary necklace. A ciliary membrane specialization. *J. Cell Biol.* **53,** 494–509 (1972).

39. Salathe, M. *Cilia and mucus : from development to respiratory defense*. (M. Dekker, 2001).

40. Sloboda, R. D. *Primary Cilia*. (Elsevier Inc., 2009).

41. Marshall, W. F. & Nonaka, S. Cilia: Tuning in to the cell's antenna. *Curr. Biol.* **16,** R604–R614 (2006).

42. Abdul-Majeed, S. Regulation of Shear Stress by mechanosensory primary cilia. (University of Toledo, 2011).

43. Moyer, J. H. *et al.* Candidate gene associated with a mutation causing recessive polycystic kidney disease in mice. *Science* **264,** 1329–1333 (1994).

44. SOROKIN, S. P. Reconstructions of Centriole Formation and Ciliogenesis in Mammalian Lungs. *J. Cell Sci.* **3,** 207–230 (1968).

45. Jain, R. *et al.* Temporal Relationship between Primary and Motile Ciliogenesis in Airway Epithelial Cells. *Am. J. Respir. Cell Mol. Biol.* **43,** 731–739 (2010).

46. Shah, A. S., Ben-Shahar, Y., Moninger, T. O., Kline, J. N. & Welsh, M. J. Motile cilia of human airway epithelia are chemosensory. *Science* **325,** 1131–4 (2009).

47. Trieu, D. *et al.* A microfluidic device to apply shear stresses to polarizing ciliated airway epithelium using air flow A microfluidic device to apply shear stresses to polarizing ciliated airway epithelium using air flow. **064104,** (2014).

48. Jo&euml *et al.* Transcriptional control of genes involved in ciliogenesis: a first step in making cilia. *Biol. Cell* **102,** 499–513 (2010).

49. Fulcher, M. L., Gabriel, S., Burns, K. A., Yankaskas, J. R. & Randell, S. H. Well-differentiated human airway epithelial cell cultures. *Methods Mol. Med.* **107,** 183–206 (2005).

50. Button, B., Okada, S. F., Frederick, C. B., Thelin, W. R. & Boucher, R. C. Mechanosensitive ATP release maintains proper mucus hydration of airways. *Sci. Signal.* **6,** ra46 (2013).

51. Robertson, H. T. & Buxton, R. B. Imaging for lung physiology: what do we wish we could measure? *J. Appl. Physiol.* **113,** 317–27 (2012).

52. Sidhaye, K. V *et al.* Shear stress regulates aquaporin-5 and airway epithelial barrier function. in *Proceedings of the National Academy of Sciences* **105,** 3345–3350 (2008).

53. Tarran, R. *et al.* Normal and cystic fibrosis airway surface liquid homeostasis. The effects of phasic shear stress and viral infections. *J Biol Chem* **280,** 35751–35759 (2005).

54. Mitchell, B., Jacobs, R., Li, J., Chien, S. & Kintner, C. A positive feedback mechanism governs the polarity and motion of motile cilia. *Nature* **447,** 97–101 (2007).

55. Delaere, P. R. *et al.* Mucociliary clearance following segmental tracheal reversal. *Laryngoscope* **106,** 450–456 (1996).

56. Soleas, J. P., Paz, A., Marcus, P., McGuigan, A. & Waddell, T. K. Engineering airway epithelium. *J. Biomed. Biotechnol.* **2012,** 982971 (2012).

57. Button, B. & VanHook, A. M. Science Signaling Podcast: 11 June 2013. *Sci. Signal.* **6,** pc15 (2013).

58. Malek, a M. & Izumo, S. Mechanism of endothelial cell shape change and cytoskeletal remodeling in response to fluid shear stress. *J. Cell Sci.* **109 (Pt 4,** 713–26 (1996).

59. Chien, S. Mechanotransduction and endothelial cell homeostasis : the wisdom of the cell. *Am. J. Physiol. Hear. Circ. Physiol.* **292,** (2007).

60. Tarran, R., Button, B. & Boucher, R. C. Regulation of normal and cystic fibrosis airway surface liquid volume by phasic shear stress. *Annu. Rev. Physiol.* **68,** 543–561 (2006).

61. Sears, P. R., Yin, W.-N. & Ostrowski, L. E. Continuous Mucociliary Transport by Primary Human Airway Epithelial Cells in vitro. *Am. J. Physiol. - Lung Cell. Mol. Physiol.* ajplung.00024.2015 (2015). doi:10.1152/ajplung.00024.2015

62. Fiddes, L. K. *et al.* A circular cross-section PDMS microfluidics system for replication of cardiovascular flow conditions. *Biomaterials* **31,** 3459–3464 (2010).

63. Chung, S. H. & Min, J. Morphological investigations of cells that adhered to the irregular patterned polydimethylsiloxane (PDMS) surface without reagents. *Ultramicroscopy* **109,** 861–867 (2009).

64. Tarran, R., Button, B. & Boucher, R. C. in *Annual Review of Physiology* **68,** 543–561 (2006).

65. Lehmler, H.-J. Perfluorocarbon compounds as vehicles for pulmonary drug delivery. *Expert Opin. Drug Deliv.* **4,** 247–262 (2007).

66. Das, a & Niven, R. Use of perfluorocarbon (fluorinert) to enhance reporter gene expression following intratracheal instillation into the lungs of Balb/c mice:

implications for nebulized delivery of plasmids. *J. Pharm. Sci.* **90,** 1336–1344 (2001).

67. Tarran, R., Grubb, B. R., Gatzy, J. T., Davis, C. W. & Boucher, R. C. The relative roles of passive surface forces and active ion transport in the modulation of airway surface liquid volume and composition. *J. Gen. Physiol.* **118,** 223–236 (2001).

68. Matsui, H. *et al.* Evidence for periciliary liquid layer depletion, not abnormal ion composition, in the pathogenesis of cystic fibrosis airways disease. *Cell* **95,** 1005–1015 (1998).

69. Gaillard, D. a, Lallement, a V, Petit, a F. & Puchelle, E. S. In vivo ciliogenesis in human fetal tracheal epithelium. *Am. J. Anat.* **185,** 415–28 (1989).

70. Mitrovski, S. M. & Nuzzo, R. G. An electrochemically driven poly(dimethylsiloxane) microfluidic actuator: oxygen sensing and programmable flows and pH gradients. *Lab Chip* **5,** 634–645 (2005).

71. Yang, L.-J. Y. L.-J. & Kao, A.-F. K. A.-F. Gas permeation in PDMS monitored by on-site pressure sensors. *Nano/Micro Eng. Mol. Syst. (NEMS), 2010 5th IEEE Int. Conf.* (2010). doi:10.1109/NEMS.2010.5592233

72. Tarran, R., Trout, L., Donaldson, S. H. & Boucher, R. C. Soluble mediators, not cilia, determine airway surface liquid volume in normal and cystic fibrosis superficial airway epithelia. *J. Gen. Physiol.* **127,** 591–604 (2006).

73. Frangos, J. a, Engineering, D. of, McIntire, L. V & Eskin, S. G. Shear stress induced stimulation of mammalian cell metabolism. *Biotechnol. Bioeng.* **32,** 1053–1060 (1988).

74. Carpenter, J., Superfine, R. & Washburn, S. Clearing Things Up : A Vertical Mucus Clearance Assay to Investigate Rheological and Biochemical Parameters Governing Mucociliary Clearance . Approved by. (2013).

75. Worthington, E. N. & Tarran, R. in *Jama* **302,** 77–92 (2011).

76. Ando, J. *Shear Stress and Shear Rates for ibidi µ-Slides*. *ibidi* **58 Suppl 1,** (2000).

77. Macosko, C. W. & Larson, R. G. *Rheology: principles, measurements, and applications*. (VCH New York, 1994).

78. Liu, Y., So, R. M. C. & Zhang, C. H. Modeling the bifurcating flow in a human lung airway. *J. Biomech.* **35,** 465–473 (2002).

79. Grotberg, J. B. Repiratory fluid mechanics and transport processes. *Annu. Rev. Biomed. Eng.* **3,** 421–457 (2001).

80. Bermbach, S. *et al.* Mechanisms of cilia-driven transport in the airways in the absence of mucus. *Am. J. Respir. Cell Mol. Biol.* **51,** 56–67 (2014).

81. Gaillard, D. a *et al.* In vivo ciliogenesis in human fetal tracheal epithelium. *Am. J. Anat.* **185,** 415–28 (1989).

82. Vladar, E. K., Antic, D. & Axelrod, J. D. Planar cell polarity signaling: the developing cell's compass. *Cold Spring Harb. Perspect. Biol.* **1,** a002964 (2009).

83. Vladar, E. K., Bayly, R. D., Sangoram, A. M., Scott, M. P. & Axelrod, J. D. Microtubules enable the planar cell polarity of airway cilia. *Curr. Biol.* **22,** 2203–2212 (2012).

84. Stubbs, J. L., Vladar, E. K., Axelrod, J. D. & Kintner, C. Multicilin promotes centriole assembly and ciliogenesis during multiciliate cell differentiation. *Nat. Cell Biol.* **14,** 1–33 (2012).

85. Guirao, B. *et al.* Coupling between hydrodynamic forces and planar cell polarity orients mammalian motile cilia. *Nat. Cell Biol.* **12,** 341–50 (2010).

86. Button, B., Yoder, B., Frederick, C. B., Lalush, D. & Grubb, B. R. Quantitation of Mucus Clearance in Conscious and Anesthetized Mice by Radionuclide Scintigraphy. *Pediatr. Pulmonol.* **44,** 281–282 (2009).

87. Schroter, R. C. & Sudlow, M. F. The prediction of pressure drop and variation of resistance within the human bronchial airways' t. j. 387–405 (1970).

88. Kendrick, A. H. Airway clearance techniques in cystic fibrosis: physiology, devices and the future. *J. R. Soc. Med.* **100 Suppl ,** 3–23 (2007).

89. Cai, L. Structure and function of airway surface layer of the human lungs & mobility of probe particles in complex fluids. (University of North Carolina- Chapel Hill, 2012). at <http://dc.lib.unc.edu/cdm/singleitem/collection/etd/id/4333/rec/5>

90. Anderson, W. H. *et al.* The Relationship of Mucus Concentration (Hydration) to Mucus Osmotic Pressure and Transport in Chronic Bronchitis. *Am. J. Respir. Crit. Care Med.* 1–38 (2015). doi:10.1164/rccm.201412-2230OC

91. Matsui, H., Davis, C. W., Tarran, R. & Boucher, R. C. Osmotic water permeabilities of cultured, well-differentiated normal and cystic fibrosis airway epithelia. *J. Clin. Invest.* **105,** 1419–27 (2000).

92. Kim, C. S., Rodriguez, C. R., Eldridge, M. a & Sackner, M. a. Criteria for mucus transport in the airways by two-phase gas-liquid flow mechanism. *J. Appl. Physiol.* **60,** 901–7 (1986).

93. Kim, C. S., Iglesias, A. J. & Sackner, M. A. Mucus clearance by two-phase gas-liquid flow mechanism: asymmetric periodic flow model. *J. Appl. Physiol.* **62,** 959–971 (1987).

94. Hu, Y. *et al.* A microfluidic model to study fluid dynamics of mucus plug rupture in small lung airways. *Biomicrofluidics* **9,** 044119 (2015).

95. Norton, M. M., Robinson, R. J. & Weinstein, S. J. Model of ciliary clearance and the role of mucus rheology. *Phys. Rev. E* **83,** 011921 (2011).

96. Kim, C. S. *et al.* Criteria for mucus transport in the airways by two-phase gas-liquid flow mechanism. *J. Appl. Physiol.* **60,** 901–7 (1986).

97. Gupta, J. K., Lin, C.-H. & Chen, Q. Flow dynamics and characterization of a

cough. *Indoor Air* **19,** 517–25 (2009).

98. Wu, D., Tawhai, M. H., Hoffman, E. a. & Lin, C.-L. A Numerical Study of Heat and Water Vapor Transfer in MDCT-Based Human Airway Models. *Ann. Biomed. Eng.* **42,** 2117–2131 (2014).

99. Kim, C. S., Iglesias, a J. & Sackner, M. a. Mucus clearance by two-phase gas-liquid flow mechanism: asymmetric periodic flow model. *J. Appl. Physiol.* **62,** 959–71 (1987).

100. King, M., Brock, G. & Lundell, C. Clearance of mucus by simulated cough. *J. Appl. Physiol.* **58,** 1776–82 (1985).

101. Mitran, S. M. A numerical model of viscoelastic layer entrainment by airflow in cough. *AIP Conf. Proc.* **1027,** 603–605 (2008).

102. Mitran, S. Continuum-kinetic-microscopic model of lung clearance due to core-annular fluid entrainment. *J. Comput. Phys.* **244,** 193–211 (2013).

103. Leith, D. E. *et al.* in *Handbook of Physiology - The Respiratory System III* 315–336

104. Gravish, N. *et al.* Rate-dependent frictional adhesion in natural and synthetic gecko setae. *J. R. Soc. Interface* **7,** 259–269 (2010).

105. Mahadevan, L., Daniel, S. & Chaudhury, M. K. Biomimetic ratcheting motion of a soft, slender, sessile gel. *Proc. Natl. Acad. Sci. U. S. A.* **101,** 23–26 (2004).

106. Button B, B. R. Role of mechanical stress in regulating airway surface hydration and mucus clearance rates. *Respir. Physiol. Neurobiol.* **163,** 189–201 (2008).

107. Zamankhan, P., Helenbrook, B. T., Takayama, S. & Grotberg, J. B. Steady motion of Bingham liquid plugs in two-dimensional channels. *J. Fluid Mech.* **705,** 258–279 (2012).

108. Fulcher, M. L., Gabriel, S., Burns, K. a, Yankaskas, J. R. & Randell, S. H. Well-differentiated human airway epithelial cell cultures. *Methods Mol. Med.* **107,** 183–206 (2005).

109. Findley, W. & Davis, F. *Creep and Relaxation of Nonlinear Viscoelastic Materials*. (North-Holland Pub. Co.). at <http://www.barnesandnoble.com/w/creep-and-relaxation-of-nonlinear-viscoelastic-materials-william-n-findley/1003283169?ean=9780486145174>

110. Mainardi, F. Creep , Relaxation and Viscosity Properties for Basic Fractional Models in Rheology. **193,** 133–160 (2010).

111. Grubb, B. R., Schiretz, F. R. & Boucher, R. C. Volume transport across tracheal and bronchial airway epithelia in a tubular culture system. *Am. J. Physiol.* **273,** C21–9 (1997).

112. Grubb, B. R., Schiretz, F. R. & Boucher, R. C. Volume Transport across tracheal and bronchial airway epithelia in a tubular culture system. *AJP Cell Physiol.* **273,** C21–C29

113. Ghaedi, M. *et al.* Alveolar epithelial differentiation of human induced pluripotent stem cells in a rotating bioreactor. *Biomaterials* **35,** 699–710 (2014).

114. Merchuk, C. Why use air-lift bioreactors. *Trends Biotechnol.* **8,** 66–71 (1990).

115. Li, Y.-H. & Huang, Y.-D. The study of collagen immobilization on polyurethane by oxygen plasma treatment to enhance cell adhesion and growth. *Surf. Coatings Technol.* **201,** 5124–5127 (2007).

116. Mofrad, M. *Cytoskeletal mechanics models and measurements*. (Cambridge University Press, 2006).

117. Sisson, J. H., Stoner, J. A., Ammons, B. A. & Wyatt, T. A. All-digital image capture and whole-field analysis of ciliary beat frequency. *J. Microsc.* **211,** 103–111 (2003).

118. Adams, D. *The Hitchhiker's guide to the galaxy*. (Harmony Books, 1980).